CZECH UNIVERSITY OF LIFE SCIENCES PRAGUE

Faculty of Tropical AgriSciences

Department of Animal Science and Food Processing

DETECTING LARGE UNGULATES IN THE MIDDLE EAST AND AFRICA USING UAV ACQUIRED IMAGERY AND ANALYSIS

Ph.D. Dissertation thesis

Prague 2022

Author: Meyer Etienne de Kock, MSc.

Supervisor: prof. RNDr. Pavla Hejcmanová, Ph.D.

Co-supervisor: doc. Ing. Karolína Brandlová, Ph.D.

CZECH UNIVERSITY OF LIFE SCIENCES PRAGUE

Faculty of Tropical AgriSciences

Ph.D. THESIS ASSIGNMENT

Meyer Etienne De Kock, MSc.

Agricultural Specialization
Tropical Agrobiology and Bioresource Management

Thesis title

Detecting Large Ungulates in the Middle East and Africa using UAV Acquired Imagery and Analysis

---

Objectives of thesis

The thesis aims to provide an insight into the detection processes of large ungulates in the arid regions of the Middle East and Africa by using UAV-acquired imagery and computer-based analysis for semi- and automated detection and feature extraction. Specific objectives are:

1) To provide an overview of the current trends in UAV-based ungulate monitoring and the ethical aspects to be considered when deploying UAVs as a data capture tool.

2) To provide an insight into the semi and automated detection of large ungulates using computing techniques, especially semi-automated detection using object-based image analysis (»OBIA).

3) To test the application of zoometric data extraction and modelling from UAV acquired imagery.

Methodology

The methods will consist in:

1) Systematic literature review on UAV applications and ethical considerations

when using UAVs in wildlife monitoring, and a synthesis of own experience from a series of monitoring across Africa and Middle East;

2) Testing the various methods of UAVs-acquired data processing on the model species of Arabian oryx (Oryx leucoryx) free-ranging within the Dubai Desert Conservation Reserve in the UAS and in captive conditions. This includes the verification of UAV acquired zoometric, feature extraction, and animal coat refection data with reintroduced populations and in the spectral reflection laboratory.

The proposed extent of the thesis

80 – 100 pp.

Keywords

Animal ecology; Dron ecology; mammals; remote sensing; UAV;

Recommended information sources

Berteška T, Ruzgienė B. 2013. Photogrammetric mapping based on UAV imagery. Geodesy and Cartography 39:158-163.

De Kock ME, Gallacher D. 2016. From drone data to decisions: Turning images into ecological answers — innovation Arabia 2016.

Dennis C. Duro SEF, Monique G. Dubé. 2012. A comparison of pixel-based and object-based image analysis with selected machine learning algorithms for the classification of agricultural landscapes using SPOT-5 HRG imagery. Remote Sensing of Environment 118:259–272.

Gonzalez LF, Montes GA, Puig E, Johnson S, Mengersen K, Gaston KJ. 2016. Unmanned Aerial Vehicles (UAVs) and artificial intelligence revolutionizing wildlife monitoring and conservation. Sensors 16:97.

LeCun Y, Bengio Y, Hinton G. 2015. Deep learning. Nature 521:436.

Rey N, Volpi M, Joost S, Tuia D. 2017. Detecting animals in African Savanna with UAVs and the crowds. Remote Sensing of Environment 200:341-351.

Expected date

2021/2022 (summer) – FTA – State Doctoral Examinations

The Dissertation Thesis Supervisor

prof. RNDr. Pavla Hejcmanová, Ph.D.

Supervising department

Department of Animal Science and Food Processing

Advisor of thesis

doc. Ing. Karolína Brandlová, Ph.D.

Electronic approval: 24. 6. 2022

Mgr. Barbora Černá Bolfíková, Ph.D.

Head of department

Electronic approval: 24. 6. 2022

prof. RNDr. Pavla Hejcmanová, Ph.D.

Chairperson of the field of study board

Electronic approval: 27. 6. 2022

prof. dr. ir. Patrick Van Damme

Dean

Prague on 12. 07. 2022

ABSTRACT

Uncrewed Aerial Vehicles (UAVs) are becoming a popular data acquisition tool for animal detection and monitoring in conservation management. Advances in the sensory capabilities of UAV platforms are driving customised detection models which have specific data requirements. UAV-based monitoring of ungulates is relatively new and has undergone limited research on the application of this method, its shortcomings and the effect on species and the environment compared to more traditional, well research and established monitoring methods. Therefore, the limited research justifies the focus of this research field and the contribution to the development of generalised best practices that focus on data acquisition standardisation traded off against minimised environmental disturbance.

This thesis had three main goals. Firstly, I aimed to provide an overview of recent UAV-based ungulate monitoring techniques including ethical considerations given to possible environmental disturbance. The gaps in these processes were identified and solutions were explored. Secondly, the semi-automated detection of reintroduced Arabian Oryx (*O. leucoryx)* was tested, using the spectral signature of the species' coat as input for an object-based image analysis (OBIA) rule set to identify adult *O. leucoryx*, applied in UAV acquired imagery. Our method uses the lab-measured spectral reflection of hair sample values, collected from captive *O. leucoryx* as input for an OBIA ruleset to identify adult *O. leucoryx* from UAV survey imagery using semi-automated supervised classification. Using species spectral reflectance signature to identify re-introduced *O. leucoryx* and extract location data using a non-invasive UAV-based tool is a novel method with enormous application possibilities. Coat refection species-specific signatures can be developed for a range of species and customised to autodetect and classify the species from remote sensing data. Lastly, the zoometric and feature extraction of *O. leucoryx* data using data acquired from a captive population for comparison with reintroduced populations monitored by UAVs were assessed. Highly accurate scaled and geo-rectified imagery derived from UAV surveys allowed precise morphometric measurements of the oryx. The scaled top view imagery, combined with baseline data from known sex, age, weight, and pregnancy status of captive individuals were used to develop predictive models. A bracketed index developed from the predictive models showed high accuracy for predicting the age group ≤ 16 months, animals with a weight >80 kg, and pregnancy. The pregnancy prediction decision tree model performed with a 91.7% accuracy. The polynomial weight predictive model performed well with relatively high accuracy when using the total top view surface measurement. The accuracy of the age prediction model reduces as the age of the animal exceeds 16 months. Photogrammetrically processed UAV acquired imagery can yield valuable zoometric data, feature extraction and modelling. It is a tool with a practical application for field biologists that can assist in the decision-making process for species conservation management.

Keywords: Aerial imagery; Antelope conservation; Drone; Large mammal monitoring; Photogrammetry; Wildlife management; Zoometric measurements

Declaration of integrity

I, Meyer Etienne de Kock, hereby declare that I have developed and written the enclosed PhD thesis entitled "Detecting Large Ungulates in the Middle East and Africa using UAV Acquired Imagery and Analysis" completely presenting my own research work, independently and in collaboration with co-authors in the respective articles related to this thesis. Any thoughts from others or literal quotations are clearly marked, and all the sources have been quoted and acknowledged using complete references under the professional guidance of Prof. RNDr. Pavla Hejcmanová, PhD and Doc. Ing. Karolína Brandlová, PhD. I state that the work has not been submitted for any other degree to this or any other university within and outside Czechia.

In Prague, July 2022

MSc. Meyer E de Kock

Acknowledgements

Contents

List of tables

List of figures

List of the abbreviations used in the thesis

AI	Artificial Intelligence
AOI	Area of Interest
AGL	Above Ground Level
B/H	Base to Height ratio
DDCR	Dubai Desert Conservation Reserve
DEM	Digital Elevation Model
EAZA	European Association of Zoos and Aquaria
FCS	Flight Control System
GCP	Ground Control Points
GPS	Global Positioning System
GSCAO	The General Secretariat for the Conservation of the Arabian Oryx
IUCN	International Union for Conservation of Nature
NDPI	Normalised Drone Print Index
MCDA	Multi-Criteria Decision Analysis
OBIA	Object-based Image Analysis
PAAT	Positional Accuracy Assessment Tool
PBIA	Pixel-based Image Analysis
SfM	Sstructure from Motion
TL	Total Length
UAV	Uncrewed Aerial Vehicles
UAE	United Arab Emirates
UTM	Universal Transverse Mercator
VLOS	Visual Line of Sight
VTOL	Vertical Take-off and Landing
WGS84	World Geodetic System

1. Introduction

Uncrewed Aerial Vehicles (UAVs) or commonly referred to as Drones have become an attractive tool for conservation and wildlife managers. The reasons may include an unprecedented progress in technologies development in the last decade and the rapid growth in the market with UAVs, becoming more affordable and more user-friendly. UAVs are equipped with high-resolution cameras that are capable of generating large volume of data that requires significant computing power to analyse to provide information for decision-making processes in species and environmental management.

Surveying species to obtain accurate population estimates is a necessary but challenging task that requires a considerable investment of time and resources. Traditional ground-based monitoring techniques, such as camera traps and surveys performed on foot, are known to be resource-intensive, potentially inaccurate and imprecise, and difficult to validate (Gonzalez et al. 2016). For conservation purposes, it is important to collect consistent and reliable information about species distribution and diversity to develop plans for species protection and sustainable use (Riede 2000). Remote sensing is generally regarded to be able to contribute to this aim, mainly by its ability to provide continuous spatial information (Leyequien et al. 2007). Recent developments in UAVs have great promise as a scientific monitoring tool nevertheless only when combined with appropriate sensors, established sampling protocols, and statistical analysis (JONES IV et al. 2006). The rapid growth in the use of UAV imagery for environmental monitoring (Laliberte et al. 2010; Gonzalez et al. 2016; Rey et al. 2017) and the availability of off-the-shelf UAV units, make this an attractive option for environmental researchers. Researchers face a trade-off between the performance of the materials, the logistics and the investment, which explains why mainly small UASs are used (Linchant et al. 2015c). A range of options, techniques and settings are reviewed in real-world scenarios to give the environmental researcher, responsible for large mammal monitoring, a reference guide for the best application.

UAV's environmental monitoring adoption by the conservation sector has lagged behind the resources sector, such that many technological possibilities remain untapped. Applying low-altitude aerial imagery to conservation requires the merging of three skill sets: ecological knowledge, operating of UAV hardware, and data interpretation (De Kock & Gallacher 2016).

Ungulates, and their population demographics in particular, are often good indicators of ecosystem function (McMahon et al. 2021; Ito et al. 2022). They are a good target animal group for UAV-based monitoring as they are easily identified, can be counted using automated methods and respond predictably to environmental change (Zhou et al. 2021; Rahman et al. 2022).

Researchers are confronted with a range of questions in the development of an applied methodology where UAVs are used; this can include the appropriate altitude, the use of video or photographs, direct piloting or programmed piloting; to name a few. Selecting the incorrect application may result in the loss of data quality or unusable data. The UAV's applied methodology is typically tailored to the research and monitoring question. The thesis focuses on off-the-shelf UAVs, single and multi-router units and in some commonly used, third-party accessories and software additions.

1.1. Aims of the thesis

This thesis aimed to provide insight into the detection processes of large ungulates in the arid regions of the Middle East and Africa by using UAV-acquired imagery and computer-based analysis for semi- and automated detection and feature extraction. The thesis aimed to investigate this topic as subdivided into the following main themes:

1) Provide an overview of the current trends in UAV-based ungulate monitoring and the ethical aspects to be considered when deploying UAVs as a data capture tool.
   a. The first objective was to identify gaps in the standardisation of the methods through a systematic review which focused on the methods used, including the UAV platform and sensors, the flight plan, species of interest, and the type of data extracted. A specific focus was paid to a synthesis of ethical considerations before using UAV monitoring techniques that include disturbance of the target species' natural behaviour and the disturbance of secondary species as a result of UAV survey 'bycatch' which describes the environmental disturbance.
   b. The second objective was to contribute to the need for common approaches to guide the standardisation of methods and ethical considerations by reflecting on our research. Here, we summarised data from six years of UAV ungulate surveys in a conservation management capacity and presented a case study on one of the largest antelope species. Specifically, we tested the effect of height of a surveying UAV on the visual disturbance behaviour of the Western Derby eland (*Taurotragus derbianus derbianus*). We culminated this into a discussion about best practices and a summary of considerations to inform future practical applications of UAVs as a survey tool.
2) Provide insight into the semi and automated detection of large ungulates using computing techniques, especially semi-automated detection using object-based image analysis (OBIA).
   a. The first objective was to investigate the application of animal coat spectral reflection to identify individual adult Arabian oryx (*O. leucoryx*) using lab-measured reflectance of coat samples as an input for a semi-automated supervised classification using the colour values as an input for the OBIA ruleset.
   b. The conversion process of lab measured Commission Internationale de l'Eclairage (CIE) Lab colour values to a compatible digital computer-based colour (sRGB) environment was investigated. We tested the performance of the OBIA image extraction ruleset on a range of data sets acquired by UAV based image-capture survey of a protected area housing re-introduced *O. leucoryx*.
3) Test the application of zoometric data extraction and modelling from UAV acquired imagery;
   a. The objective was to examine the accuracy of species-specific zoometric measurements acquired by a non-invasive extraction from photogrammetrically processed drone-based imagery.
   b. The second objective was to test the predictive value of UAV-acquired post-processed imagery to classify the herd structure in terms of age groups, including offspring identification, sex, and pregnancy status of *O. leucoryx* (n=43) in a protected area with the purpose to assist in the decision-making process for conservation management of the species.

2. Literature review

2.1 Uncrewed Aerial Vehicles

Monitoring animals in their natural environment are of critical importance because of recognised global declines in biodiversity (Jewell 2013). The value of aerial surveys in wildlife monitoring is well known (Linchant et al. 2015b), while the cost, safety and logistics usually limit the use of manned aircraft in this field of monitoring free-living animals in their environment. In the early 2000s, some of the first assessments on using UAVs with imagery capture equipment for use in wildlife monitoring and surveying were done (Jones IV et al. 2006). Since this time, the use of UAVs across a range of ecosystems and to address a variety of scientific objectives has increased. A larger range of species was surveyed using UAVs in a range of environments and sensor types (Watts et al. 2010; Anderson & Gaston 2013; Groom et al. 2013; Linchant et al. 2018b). UAV monitoring is not limited to the identification of species. Zoometric measurements, for instance, can reveal additional information about the species that may include insight into the species' age structure (de Kock et al. 2021b), growth rates (Christiansen et al. 2018), sex ratios, body condition (Krause et al. 2017) and behaviour (Torres et al. 2018).

UAV technology has shown great potential as a scientific monitoring tool. According to Jones et al. (2006), however, only when combined with appropriate sensors, established sampling protocols, and statistical analysis will this technology be fully utilised. The rapid growth in the use of UAV-acquired imagery for environmental monitoring (Laliberte et al. 2010; Gonzalez et al. 2016; Rey et al. 2017), and the availability of off-the-shelf UAV units, make UAV-based environmental monitoring an attractive option for researchers. UAV environmental monitoring adoption by the conservation sector has lagged behind the technology sector, such that many technological possibilities remain under-utilised. Applying low-altitude aerial imagery to conservation requires the merging of three skill sets: ecological knowledge, operating of UAV hardware, and data interpretation (De Kock & Gallacher 2016).

2.1.1 Do UAV hardware and flight parameters matter?

During the selection process of optimising the UAV capability for the best data acquisition system (*Table 1*), decisions must be made on the hardware (UAV and sensors) and applied methods to be used. These decisions are usually derived from the research question that dictates data standards, data type and resolution. Secondary factors include available finances, accessibility, availability of the UAV platform, area to be covered, site location, legal restrictions, operational requirements in the form of training needed and site-specific environmental conditions. Lastly, pre-flight and operational planning that, among others, include the ethical considerations for each flight operation.

Therefore, we identified the diversity of approaches, the range and the most frequent values of individual technical parameters applied in the UAV-based monitoring of ungulates (*Table 1*).

Table 1: An overview of UAV platform, sensor and flight operation parameters and considerations

Categories	UAV flight setup considerations			
UAV Platforms	Multi-Rotors	Fixed Wings	Vertical take-off and landing (VTOL)	Custom
UAV Size (Weight)	250g - 25000g	1000g - 25000g	1000g - 25000g	1000g - >2500g
Flight Time (approximate maximum flight time per battery)	22 min - < 30 min	30 min - 120 min	30 min - 120 min	15 min - 120 min
Sensors	Imagery and Lidar	Imagery and Lidar	Imagery, Lidar and Radio frequency equipment related to animal tracking	Custom
Type of flight	Piloted: Visual line of sight Piloted: Beyond visual line of sight Piloted: First Person View Autonomised flights	Piloted: Visual line of sight Piloted: Beyond visual line of sight Piloted: First Person View Autonomised flights	Piloted: Visual line of sight Piloted: Beyond visual line of sight Piloted: First Person View Autonomised flights	Piloted: Visual line of sight Piloted: Beyond visual line of sight Piloted: First Person View Autonomised flights
Monitoring techniques	Targeted individuals Census or survey Combination flights Custom	Targeted individuals Census or survey Combination flights Custom	Targeted individuals Census or survey Combination flights Custom	Targeted individuals Census or survey Combination flights Custom
Species	Single Target species Multiple species Environmental monitoring	Single Target species Multiple species Environmental monitoring	Single Target species Multiple species Environmental monitoring	Single Target species Multiple species Environmental monitoring
Flight considerations	Launce distance	Flight altitude	Approach path	Airspeed
Ethical Considerations	UAV disturbance during the flight	UAV survey bycatch	Environmental impact	

In this perspective, there is a requirement for synthesis on the factors that govern the influence of UAVs on ungulate behaviour to better inform the application of UAVs for ungulate research. Several case studies have demonstrated the effectiveness of the technique, but few make mention of the impact of the approach on the species under study. A review, therefore, needs to consider the impact on the target species, but also on the survey 'bycatch', taking into account

the effects on the entire ecosystem. The trends and best practices need to be identified so that the field ecologist has a holistic picture of the required considerations for UAV-based surveys.

2.2 UAVs used for wildlife survey and monitoring

Accurate population estimates and an understanding of the ecology and behaviour of animals are cornerstones for effective wildlife conservation and management. These can be obtained from species monitoring and surveys which are challenging tasks that require considerable investment of time and resources. Traditional ground-based monitoring techniques, such as camera traps and surveys performed on foot, are resource-intensive, demanding to design, potentially inaccurate and imprecise, and difficult to validate (Gonzalez & Johnson 2017). However, for conservation initiatives that rely on adaptive management, it is essential to collect consistent and reliable data about species distribution, demographics and diversity (Mulero-Pazmany et al. 2015; Petso et al. 2021) to develop species protection and sustainable use strategies (Riede 2000). These required data can be reliably obtained from various remote sensing platforms (Leyequien et al. 2007), especially UAVs (Hodgson et al. 2016; Mangewa et al. 2019). Their use for data collection inevitably translates to the quality of information and clarifying the methods and standardisation of technical parameters for data collection are important for wildlife management and conservation practitioners (Buters et al. 2019).

The application of UAVs is rapidly advancing and proving its worth as a promising monitoring tool, with substantial reductions in size and increases in sensory capabilities and flight times (Allan et al. 2018). The use of UAV-based surveys in the conservation sector has lagged behind that of the commercial sector and many avenues remain where UAV-based approaches can aid in conservation efforts (Christie et al. 2016). First attempts at ecological UAV surveys used specialised, often custom-built UAVs, which required the consolidation of three skill sets: ecological knowledge, safely operating UAV hardware, and data processing and interpretation (De Kock & Gallacher 2016). Advances in automated flight software and UAV platform and software designs have closed the gap between UAV hardware, piloting and data acquisition specialisations, and even very low-cost UAVs can now easily be used for ecological mapping and monitoring (Myburgh et al. 2021). Rapid growth in the use of UAV imagery for environmental monitoring (Laliberte et al. 2010; Gonzalez et al. 2016; Rey et al. 2017) and the availability of off-the-shelf UAV units, make this an attractive option for conservation-based species research and monitoring (Castellanos-Galindo et al. 2019; Mangewa et al. 2019). Researchers face a trade-off between the performance of the UAV and sensors, the logistics and the capital investment, which explains why mainly small UAVs are used in wildlife monitoring (Linchant et al. 2015c; Myburgh et al. 2021). Regardless of the size or price tag, UAVs functionally remain merely flying platforms unless combined with the appropriate sensors, sampling protocols and statistical analyses (JONES IV et al. 2006).

Although multi-rotor UAV surveys are capable of covering areas of up to 2km^2 on a single charge (Pradeep et al. 2018), fixed-winged UAVs are capable of covering areas at a large reserve scale within feasible time scales (>10km^2) (Su et al. 2018). At these scales, entire populations of large body-sized mammals can be surveyed, depending on the species and environment. Ungulates are a good target animal group for UAV-based monitoring as they are easily identified, can be counted using automated methods and respond predictably to environmental change (Zhou et al. 2021; Rahman et al. 2022).

Flight plans for ungulate survey missions are planned for maximum detection of wildlife in their natural environment, often tailored to a species of interest. This requires a range of, inclusive of limiting the impact of the UAV on the species of interest (Andrews 2014; Linchant et al. 2015c; Hodgson & Koh 2016).

Although UAVs present a considerably more capable platform for ungulate population research, disturbance and negative effects have been demonstrated and linked to UAV-based wildlife monitoring (Mulero-Pázmány et al. 2017). Disturbance in ungulates is usually identified as a physical reaction to the presence of the UAV that will ultimately manifest into a fight or flight response. The strength of the reaction depends on the perception of the risk, which naturally relates mostly, but not exclusively to a risk of predation. Potentially life-threatening situations for ungulates include the proximity to human settlements, hunting activities (Tarakini et al. 2014; Yamashita et al. 2018), tourism, i.e. visitors in their natural environment (Malo et al. 2011), or flying objects, such as helicopters in which the negative effect of such strong disturbance may persist long after the disturbance (Brambilla & Brivio 2018). Anthropogenic disturbances create trade-offs between avoiding perceived risk and other fitness-enhancing activities similarly to natural predator risk situations (Frid & Dill 2002; Stankowich 2008) and therefore should not be neglected in considerations. In regard to UAVs, research about effects of UAV disturbance is rare, for instance, research on bears showed UAVs to have a limited behavioural, but measurable physiological (stress) response (Ditmer et al. 2015). The research of the effects of UAV disturbance particularly on ungulates is largely insufficient (Mulero-Pázmány et al. 2017). Although here, disturbance is typically related to the species of interest, the UAV platform and the flight plan/characteristics. In the public domain, popular video streaming platforms (e.g. YouTube) have been used to elucidate evidence of disturbance on a range of taxa as a result of UAV flights (Rebolo-Ifrán et al. 2019). However, in the context of using UAVs for ungulate research, this sort of data remains scattered throughout the literature, making it difficult for the field biologist to assess and interpret.

2.3 UAV-acquired data processing

Most data-processing in the context of this thesis refers to UAV-acquired imagery and embedded information that include sensor setting and GPS location data. Post-processing of these imagery datasets is computer-based. Firstly the use of photogrammetry software (Berteška & Ruzgienė 2013) to stitch single images into a geo-rectified dataset. The secondly is semi- or automated object detection process using different types of software to analyse imagery data. This includes traditional Geographical Information System (GIS) based software and data classification tools (Dennis C. Duro 2012) and a relatively new method (LeCun et al. 2015) using custom computer learning algorithms (Gonzalez et al. 2016).

2.3.1 Photogrammetry and drone imagery

Photogrammetry data from drone imagery are becoming a popular tool for low altitude high-resolution large-scale mapping tools (Colomina & Molina 2014). The ability to extract photogrammetry data from images needs an adequate overlap of images from the same area. Front and side overlap are necessary for photogrammetry software that utilise structure from motion (SfM) process to estimate the three-dimensional information from two-dimensional imagery data (Fabris & Pesci 2005), this process and location data from images make it possible

to extract scaled three-dimensional data of landscapes (Butler et al. 1998) and objects (Colomina & Molina 2014). Figure 1 shows overlapping images in sequence and resulting extraction of 3-dimensional data.
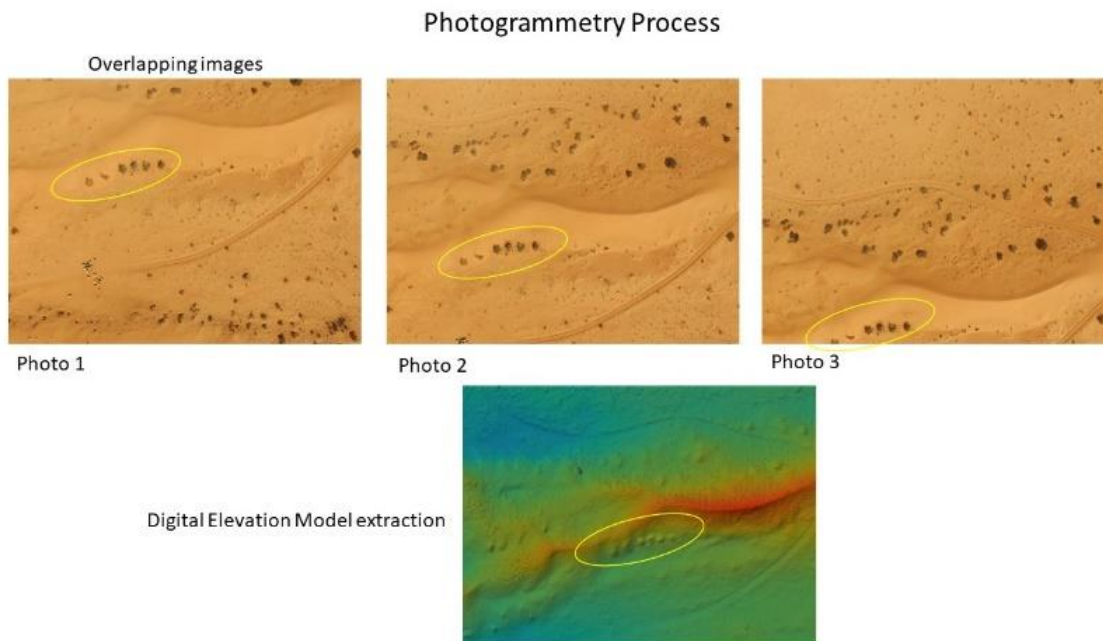
Figure 1: Overlapping images and the photogrammetry process to extract Digital Elevation Models (DEMs)

2.3.2 Model species

During the research and development process, it is common practice to select a species with a high success probability for a proof of concept. Because of the high visibility across a generally uniform environment. The *O. leucoryx* are well represented and accessible in re-introduced and captive populations this highly visible was chosen as a model species. The UAV-generated imagery and data analysis focuses on the detection and feature extraction of the *O. leucoryx*. However, a range of detection and feature extraction methods was used on a range of large ungulates in different habitats to test these hypophyses.

Species monitoring is essential for conservation-based population management (Riede 2000). Following successful breeding internationally and within the range states of the *O. leucoryx*, the pressure to change from captive to semi and fully free-living population as efforts increased to restore the historical distribution of the species. The first reintroduction of the 'world herd' occurred in Oman in 1982 followed by additional re-enforcement of this re-introduced herd (Spalton et al. 1999).

Historically, during post-release monitoring of *O. leucoryx*, the low-density distribution of these re-introduced animals results in a population size estimate with low accuracy (Zafar-Ul Islam 2011). Ground-based monitoring of *O. leucoryx* in a technical difficult desert terrain may have an additional negative impact on the low accuracy of population estimates (Islam 2008). Recent studies proved the use of UAVs to monitor the *O. leucoryx* can be a valuable tool for field

biologists (de Kock et al. 2021b). Because of the large amount of imagery collected during a UAV survey the need arises for an automated process to identify the species of interest (Corcoran et al. 2021).

2.3.3 Imagery data extraction

The relatively new concept of using geotagged imagery as a primary source of data for wildlife monitoring presents a range of questions in this field (Leyequien et al. 2007; De Kock 2015). Firstly, data processing to images with accurate location data, filtering a large amount of data and data extraction (Cai & Liu 2013; Rey et al. 2017). Adoption of technology requires broad expertise in ecology, drone hardware, and data interpretation, usually by a very small team or even an individual. Typically, an ecologist will first understand hardware, and only later develop the skills for interpretation (De Kock & Gallacher 2016).

Data extraction can be done on raw images or processed loose-standing images to a unified single orthophoto mosaic data set. The analysis can follow a manual (Rey et al. 2017) or automated (Groom et al. 2013) process. The automated process usually consists of a supervised classification (De Kock 2015) or unsupervised classification (Singleton et al. 2010).

Automated detection of wildlife from UAV-acquired imagery is dominated by the development of object detectors that are trained using convolutional neural networks (Kellenberger et al. 2017) and other variations of computer learning (Zheng et al. 2021; Tuia et al. 2022). The development of computer-learned object detectors usually involves the labelling of the object of interest in a large number of images. These labelled objects are divided into test and train datasets that are used to train the detection model through computer learning software (Pathak et al. 2018). A large number of samples are needed to train the model efficiently. Low numbers of examples can be improved with data augmentation that can include mirroring, shifting and rotations. However, a low number of training examples can lead to overfitting (Kellenberger et al. 2017).

An alternative when a large amount of imagery is not available of the species of interest to affectively train an object detector using deep learning is using extracted colour, texture and size values from biological samples to be used in object-based image analysis (OBIA) detection. This can be done by extracting the colour information from hair samples using reflective spectrometry. These colour values are used as inputs for the OBIA ruleset to perform a semi-automated supervised classification.

2.3.4 Manual classification

The manual classification of the object within UAV-acquired imagery is tedious and time-consuming. This method, on the other hand, is easy to deploy with limited training needed, compared with often complicated software algorithms used in automated classification. In the scope of wildlife survey: The analysis requires a human to look at each image or video identifying the species of interest. The large data set that can be generated in a relatively small time and human error are both drawbacks of using this method. However, it is proven to be a successful data analysis method if used correctly (Rey et al. 2017).

2.3.5 Supervised classification

Supervised classification use input from the user to guide the classification process. The user specifies the perimeters of the classification manually, but the classification is automated. This method usually results in a higher accuracy compared to unsupervised classifications. Supervised classification of UAV imagery in censuses of species is proven with a high amount of accuracy (Groom et al. 2013).

Supervised classification can be subdivided into two categories; pixel-based, and object-based. Pixel-based classification relies solely on the reflectance values of the included imagery colour bands, no ancillary data is used in the classification process. OBIA classification group pixel with similarities as an input from the user together as an object (Cai & Liu 2013). OBIA in classifying objects in imagery related to environmental studies are used with success (Laliberte et al. 2010; De Kock 2015), the process, however, requires technical knowledge of GIS-based classification software.

The use of reflective spectrometry, applied to remote sensing analysis is relatively a comen practice (Herold et al. 2004). However, uncommon when used as an input for wildlife detection from imagery. With the advances in UAV sensors, the use of survey-acquired imagery is more frequently applied in wildlife identification and management (Linchant et al. 2015b; Hodgson et al. 2016; Gonzalez & Johnson 2017). In conservation management where the monitoring is using UAV imagery, there is usually the need for the automatic detection of individuals or a specific species (Chabot 2009; Maire et al. 2015). Without automation, this process of a person looking at each image is time-consuming and labour intensive. However, applying OBIA to UAV-based acquired imagery to identify wildlife the detectability and limitations of this method need to be considered (de Kock et al. 2021). The use of lab measured coat reflection is a novel research area that requires the adjustment of processes to aline reflective spectrometry and OBIA. The conversion of data types generated by the reflective spectrometry analysis to be used in the digital environment of image analysis is a prerequisite.

Commission Internationale de l'Eclairage (CIE) defined the Lab colour space in 1976, where L indicates lightness, a is the red/green coordinate, and b is the yellow/blue coordinate. Converting CIE Lab to a digital red, green and blue (RGB) colour space that is visualised on digital monitors presents a range of challenges. With technology improving digital monitors, so do the sRGB colour space that is shown on digital monitors (Süsstrunk et al. 1999). From the sRGB standard (Stokes 1996) in 1996 with a relatively narrow gamut to the ITU-R BT.2020 with a wide gamut, usually used in ultra-high-definition monitors (Ryu et al. 2014). However, with the use of multiple digital platforms using sRGB colour space from UAV sensors, the photogrammetry software and the OBIA software need a standardised digital colour space for the data flow through these processes.

OBIA classifies groups of pixels with similarities as input from the user together as an object and was primarily developed for remote sensing data analysis where large data-set are relatively common (Dingle Robertson & King 2011; Cai & Liu 2013). This method of classifying objects in imagery related to environmental studies is used with success (Laliberte et al. 2010; De Kock 2015). OBIA use a ruleset that includes a range of user-defined conditions as an input from the user, to perform a semi-automated supervised classification (Yu et al. 2006). In this instance,

automated detection focuses on object detection of individual animals (Singleton et al. 2010) by using the input from lab-measured coat reflection values to target a specific species. When this analysis is applied to georectified orthophoto mosaic imagery, in addition to the objects identified, the process allows for a range of attribute information extraction e.g. location (X, Y and Z), size, height and colour values of the object. This additional information enriches the census data, opening the door for additional data mining and spatial analysis (Yu et al. 2006).

2.3.6 Automated classification

Automating the classification of the object in UAV imagery follows in most cases a GIS software approach. GIS techniques developed for use in Satellite imagery are widely used with processed imagery compatible with this platform.

2.3.7 Machine learning and artificial intelligence

Deep learning is a process describing computer-based learning that allows computational models that are composed of multiple processing layers to learn representations of data with numerous levels of abstraction (LeCun et al. 2015).

Recent developments in machine learning and artificial intelligence (AI) in wildlife monitoring and surveying (Gonzalez et al. 2016) open the door for future innovation in this field of computer-based data mining on UAV-acquired imagery. WildBook (Berger-Wolf et al. 2017), open-source software used by citizen conservation programs in a range of fields, is developed for species-specific research, identifying species or individual animals from imagery data set in an automated way. Other examples of using AI in data mining for wildlife conservation include shorebird extraction from UAV imagery (Groom et al. 2013).

2.4 More than species identification

The 'drone perspective' refers to the top view of the image where the horizontal sensor in relation to the environment or object. Processed UAV imagery data to a geo-reidentified orthophoto mosaic allow scaled imagery with relatively high accuracy. Consequently, if the object can be extracted from the processed dataset, this object will have embedded measurements that allow for the comparison with morphometric baseline measurements of the species. This new field in science has recently been explored in blue and grey whales (Burnett et al. 2018).
 If a baseline analysis of known sizes and lengths of the species of different sex and age exists, these data can be applied to the UAV imagery, and in theory, more information can be extracted. This method may include the identification of late pregnancy in females, age groups and individuals with unique morphometrics about the spatial resolution of the imagery.

2.4.1 Zoometric data extraction

Zoometric data derived from UAV-based wildlife surveys are attracting increasing attention because of the ability to collect data on the condition of individual animals. Surveying species to obtain accurate population estimates is a necessary but challenging task requiring a considerable

investment of time and resources. Traditional ground-based monitoring techniques, such as camera traps and surveys performed on foot, are resource-intensive, potentially inaccurate and imprecise, as well as being challenging to validate (Gonzalez et al. 2016). For conservation purposes, it is essential to collect consistent and reliable information about species distribution and abundance to develop plans for species protection and sustainable population management (Riede 2000). Remote sensing is generally regarded as being able to contribute to this aim, mainly through its ability to provide continuous spatial information (Leyequien et al. 2007). However, demographic parameters (e.g. age and sex structure) are needed for conservation decisions and appropriate management of animal populations. Previous studies show that the coefficient of variation of individual survey estimates of abundance often exceeded 50% (Seddon et al. 2003). Maximising the extraction of available data can assist in getting more information from limited field data and improve overall data quality.

Historically, aerial imagery from crewed aircraft and a manual system where field biologists document visual observations are an accepted method to estimate individual animal sizes (Koski et al. 2006). High-resolution, low-altitude UAVs can be used to determine the individual animal size, depending on the species and the survey environment (Watts et al. 2010). Advances in photogrammetry software and the use of low-altitude imagery from UAVs (Berteška & Ruzgienė 2013) have transformed the way data are handled in a digital environment; which has added a range of possibilities to individual animal morphometric analysis.
UAV monitoring is not limited to the identification of species. Extracting additional information can give further insight especially if enhanced by more nuanced perspectives of age structure, growth rates (Christiansen et al. 2018), sex ratios, reproductive status, body condition (Krause et al. 2017), and behaviour (Torres et al. 2018). This method provides the basis for rapidly and accurately measuring animal features from UAV data and fills a critical conservation need. Furthermore, this method is relatively non-invasive by nature (Horton et al. 2019) and usually allows monitoring of species that can be difficult to physically measure otherwise (Duro et al. 2007). The remote data collection, therefore, allows for the collection of critical monitoring data without the increased stress of capturing and handling the animals.

3 Methods

3.1 Study sites and animal species

The study was conducted altogether in eight countries (*Figure 2*), on 17 ungulate species, and a total of 121 flights, various UAV devices and types of flights were used (*Appendix 1*). Although there is no clear definition for the spatial reference for North Africa, the study focused mostly on the African continent north of 10-degree latitude. Particular study sites, namely Dubai Desert Conservation Reserve (UAE), are described in more detail later in the text where relevant to specific study.
 Investigated animal species predominantly included large ungulates from arid regions in Africa and the Middle East. Out of the 17 species that were surveyed, 11 are listed in the threatened category in the IUCN red list (IUCN 2021). Large ungulates refer to the total body weight of adult animals and in the context of this article; adult ungulates average weight of > = 50 kg. The most study species was *O. leucoryx* which is described in more detail later in the text where relevant to the specific study.
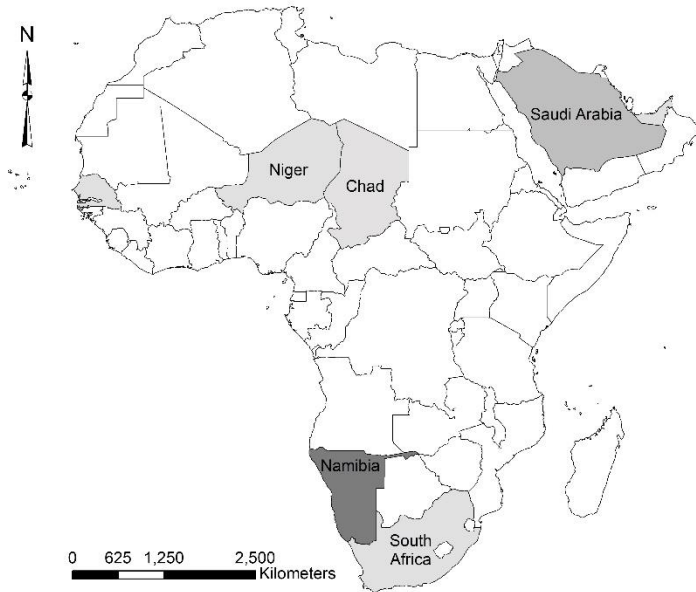
Figure 2: Study areas in Africa and the Middle East

3.2 Systematic review process

For the purpose of this review, we searched for scientific peer-reviewed papers using the Web of Science™ database on 2022/04/24. We used the timeframe from 2000/01/01 to 2022/04/24 and a topic search with the following Boolean operators: (((ALL=(Ungulates OR Wildlife OR Mammals)) AND ALL=(Drones OR UAV OR RPAS)) NOT ALL=(marine OR whale)) and only considered publications in the English language.

The Web of Science™ database search resulted in 428 identified publications which were imported into the review software package Covidence (Covidence 2022), where two duplications were removed and 428 studies were screened against title and abstracts. This screening process considered whether the title or abstract specifically included mention of ungulates and UAVs as a survey tool, where survey refers to any observation of the animals using UAVs. A total of 361 studies were excluded and 65 studies were assessed for the full-text review. Here, we included only those studies where a UAV survey/observation was the primary focus of the study so that details on the flight characteristics and specific species were available. During this process, an additional 29 studies were excluded, of which 14 studies were excluded because the study focused on UAV-acquired data analysis rather than specifically mentioning the methodology of UAV-based monitoring. In addition, nine studies did not specifically include a focus on ungulates, three were from a theoretical perspective, two did not focus on the use of UAVs and one was not written in English.

This process resulted in 36 studies included in the review. These studies then underwent a data extraction process (*Appendix 2*). The criteria for the data extraction focussed on the country and area, the species monitored, the UAV and the sensor/s used, the data collected, the flight details (including altitude, UAV launch location, flight speed and if the flight was automated or remotely piloted) and the ethical considerations made before flights, including disturbance to the species of interest, other animals and the environment.

The data extraction categories included the following:
- The ungulate species considered included odd- and even-toed ungulates and land-based Proboscidea.
- The country where the study was conducted.
- The UAV platform is categorised as multi-rotor, fixed-wing or vertical take-off and landing (VTOL) uncrewed aircraft. These were also divided into weight categories.
- The piloting/flight path of the UAV was divided into automated flights or remote piloted flights. In addition, if the flights were conducted for the purpose of census, flights were characterised as targeted (cantered around a specific point/target) or as transect (where the UAV was programmed to fly grids/patterns covering an area).
- Flight parameters were also extracted and these include the minimum and maximum altitude above ground level (AGL), as well as the minimum and maximum speed during the flight. The distance that the UAV was launched from the target species was also included.
- Ethical considerations were assessed using a "tick box" method where we ask the yes/no question: is disturbance/impact/effect mentioned in the article? If the answer to this was yes, we assessed whether any ethical considerations included only the target species, or whether other species were also mentioned.

3.2.1 Synthesis of six (2016-2022) years of UAV-based data acquisition for conservation-based monitoring: UAV platform, sensors and setups for UAV-based ungulate monitoring.

We summarised methodological approaches (*Table 2*) that we applied in our UAV-based ungulate monitoring, which included 121 flights in eight countries and 17 ungulate species (*Appendix 1*).

Table 2: Summary of UAV-based ungulate monitoring flight setups in our research

Region	No
Africa	87
Asia	6
Middle East	28
Species	
Wild	96
Domestic	2
Wild & Domestic (Single flight)	23
Type	
Census	94
Targeted	27
UAV size	
250g – 1000g	18
1000g – 1500g	64
>1500 g	39
Flights	
Automated	83
Piloted	38

Most studies were primarily conducted for population demographic surveys as an adaptive management tool or as baseline data to inform species conservation initiatives on endangered ungulates. Out of the 17 species that were surveyed, 11 are listed in the threatened category, in the IUCN red list (IUCN 2021) and for those species, these flights contributed toward population management strategies in an official capacity. This data set is also unique in that it spans the development period of UAV-based surveys, serving as an informative dataset on the capabilities and ease of use of this emerging technology. We utilised five types of multi-rotors and fixed-wing UAVs, with AGL UAV flight heights ranging from 40-120 m.

3.2.1 Defining disturbance levels: a case study on the Western Derby eland

The disturbance study was done on the Western Derby eland (*Taurotragus derbianus derbianus*) in Bandia Reserve (Senegal). We used two types of multi-rotor UAVs: DJI (Da-Jiang Innovations Science and Technology Co., Ltd.) Phantom 3 Pro and DJI Phantom 4 Pro. All flights were launched > 200m away from the target. A dedicated UAV operator piloted the UAV manually, and an observer observed the target with 10 x 42 binoculars (Steiner, Germany). The disturbance was quantified into four categories: *(I)* No disturbance detected, *(II)* animal exhibited alert behaviour (i.e., ears pointed in direction of UAV), *(III)* animal/s walking away from approaching UAV and *(IV)* animal/s running away from approaching UAV.

A total of ten flights, per UAV type, were conducted on groups of at least three individuals. All flights started and ended at the launch position. The UAV was launched and its AGL was increased to 120m (the maximum allowed flight height in many regions) vertically above the take-off location. Hereafter, the UAV was flown horizontally at 120m AGL above the target species (*Figure 3*). The UAV was kept hovering over the target for one minute before descending at <1.0m.s^{-1} (to avoid excessive propeller noise during stabilisation) to the following flight levels: 100 m, 75 m,

50 m and 25 m. If any reaction was observed during the transition from one altitude to the next, the AGL altitude was recorded for that disturbance event. The UAV was stationary at each flight level for one minute in which any reaction was recorded. The highest-ranking reactions of any individual were recorded. If more than one reaction was observed, the highest scored disturbance was recorded. If the target showed a reaction as described for *III* and *IV,* the test was aborted and the UAV returned vertically to the 120 m flight level before being returned to the take-off location. All flights were conducted downwind of the target species groups to avoid the effects of olfactory detection and to reduce audible disturbances during take-off and approach of the UAV.
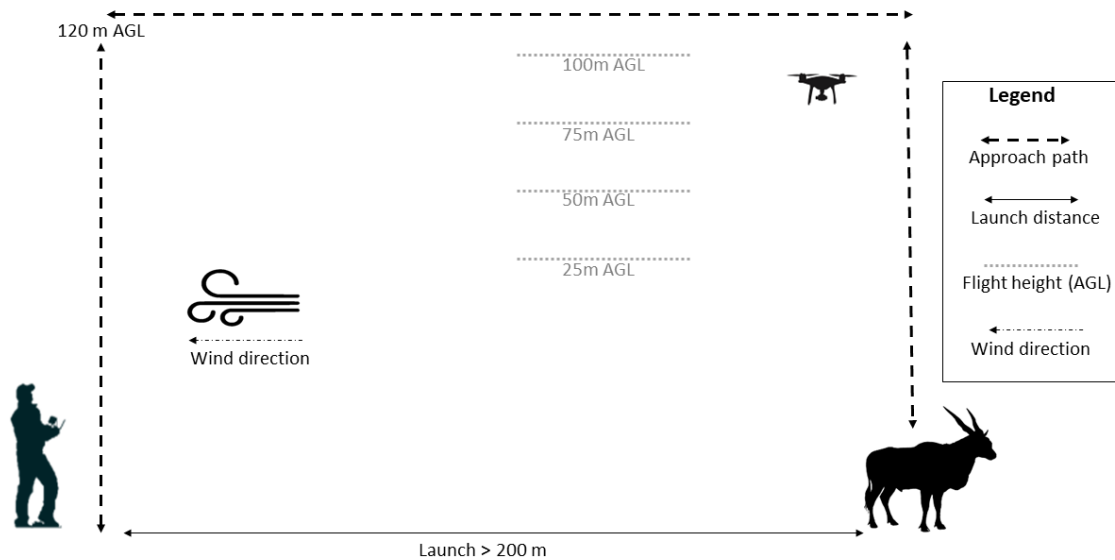
Figure 3: UAV flits to quantify disturbance

3.2.2 Statistical analyses of review and own data outputs

Analyses to visualise data were conducted in R (V 4.0.5) through the R Studios interface (V 1.31056). The R-markdown file on all statical analyses in R is available under the supplementary electronic material. The geom_boxplot as part of ggplot2 was used to visualise the data extracted from the article review and the data from our research. The boxplot shows the median of the plotted data as a line in the box, dividing the box into the lower and upper quartiles. The line extended past the box indicates the lowest to highest data value and the dots indicate data outliers.

A K-mean cluster analysis was used to visualise the data that was collected in categories that was represented a range, e.g. minimum or maximum altitude of the UAV. To compare the K-mean cluster centres from the minimum and maximum AGL flight altitude, the outlier of 800m (Su et al. 2018) was removed and two clusters and the centres were calculated.
We developed classification and regression trees using the CARET package (Kuhn 2019). Decision tree models developed from the data extracted from the review investigate if the minimum and maximum AGL altitude, and flight speed can predict when disturbances are detected. In addition, the minimum AGL altitude and UAV size were used in a model to predict detectable disturbance.

Using our data we modelled maximum altitude and flight time to predict the UAV type to be used (*Appendix 4*).

3.3 Semi-automated detection using object-based image analysis

3.3.1 Model animal species, study sites, and hair and image sampling

The *Oryx leuoryx is* classified in the genus *Oryx* and is the only within the genus with distribution out of Africa. Compared with the species within the *Oryx* genus, the overall size makes the *O. leucoryx* (*Figure 4A*) the smallest. This medium-sized desert-dwelling antelope historically ranged over the Arabian Peninsula and as far north as Syria (Tear et al. 1997). The *O. leucoryx* was declared extinct in 1972 (Henderson 1974) and through successful captive breeding programmes (Wilson & Price 1994; Hatwood 2017) the species was reintroduced (Daly 1988; Price 1989; Ostrowski et al. 1998; Simkins 2007; El Alqamy et al. 2008) to their historical range. Post-release monitoring was identified as a critical management action to manage the species in protected areas (Ostrowski et al. 1998; El Alqamy et al. 2008; Islam et al. 2011).

Hair samples from the study herd (n=50) were collected at Al Bustan Zoological Centre (lat 25.134944, long 55.881889), a conservation breeding centre, situated in Sharjah Emirate within the United Arab Emirates (UAE). The managed *O. leucoryx* population is housed as part of the regional captive conservation breeding programme of *O. leucoryx*. All individuals are handled yearly for routine veterinary checks that include: vaccinations, health checks, breeding access and separations, as per the best practice guidelines (De Kock 2018). Hair samples of *O. leucoryx* older than ten months, the weight of sample <3g per individual, were collected from the back of each animal during this management process. The age parameter was added because of the change of the calf 'sand' colour (called 'الطلا') before the calf transforms to the white adult colour, which usually happens from around 2.5 to 8 months old. The samples were collected from the full herd (N=61) excluding individuals < 10 months (N=11) of age. Each sample was stored separately and included attribute data of each individual that included the transponder identification number, age, sex and date of collection.

The outputs of hair sample analyses from the study herd were compared with datasets *(Table 3)* collected by UAV in the Dubai Desert Conservation Reserve (DDCR; lat 24.824789, long 55.657069). The DDCR is a 225km^2 protected area in the Dubai Emirate in the UAE that houses >800 reintroduced free-roaming *O. leucoryx* with the purpose of an *O. leucoryx* national and regional conservation plan.

Table 3: UAV Survey datasets summary

Survey Date	Animals identified	Time of day (UTM +4)	Lamination and conditions	Flight Time	Resolution	Sensor
4/03/2018	72	10:34 AM – 10:45 AM	Natural sunlight, No clouds	11m 23 s	3.94 cm/pixel	1/2.3" CMOS Lens 20mm f/2.8
18/03/2018	56	09:38 AM – 09:54 AM	Natural sunlight, No clouds	16m 54 s	3.98 cm/pixel	1/2.3" CMOS Lens 20mm f/2.8
14/10/2018	47	08:55 AM – 09:11 Am	Natural sunlight, Slight cloud cover	16m 34s	3.98 cm/pixel	1/2.3" CMOS Lens 20mm f/2.8

3.3.2 Reflect spectrometry

Hair samples of 50 individuals from the captive study herd of *O. leucoryx* were analysed with the Konica Minolta CM-5 spectrophotometer (Tokyo, Japan). The sample quantity per animal was specified by the permit not to exceed 3g of hair. The reflection was measured of each sample spread to cover the measurement window in a petri dish. The Konica Minolta CM-5 built-in petri dish calibration was activated for reflection analysis. Simulating daylight for digital analysis was considered, options include the D75 for 'North Sky Daylight, D65 'Average Daylight and D50 simulating 'Noon sky Daylight. D65 is a CIE standard illuminant that simulates mid-day daylight with a correlated colour temperature of 6504 K (Noboru and Robertson, 2005). The D65 best represents the high luminosity of a desert environment.

The spectrometer measures wavelengths of 360 nm to 740 nm with a standard deviation within 0.1% (400 nm to 740 nm). Each sample was measured three times with a slight adjustment of the sample to increase the variety of angles and the covering a more significant part of each sample during the analysis process. The data output was provided in a range of colour formats (CIE Lab, Hunters L, a, b; CIE XYZ) and wavelength-specific measurements.

3.3.3 Conversion of CIE Lab to digital RGB

Although there is a standardised colour space with a wide gamut, the relative narrow sRGB colour space resulted from the CIE Lab colour space conversion for inclusive digital representation was selected because the UAV sensor captured imagery in RGB format. The mean of the three readings of each sample was converted from CIE Lab to an RGB 8-bit digital value with a D65 setting. MATLAB (Natick 2019) was used as a platform for the conversion following command lab2rgb (Mathworks 2020).

The sRGB 8-bit converted colour values with the visualised colour in *Table 4,* show a colour value darker than expected when looking at the image of the *O. leucoryx* in *Figure 4A* as well as dominated light grey colours in *Figure 4* to the earth colours in *Table 3.* This colour difference occurred because the hair samples were not washed before the spectrometry analysis. This is because the aim was not to determine the colour composition of the *O. leucoryx's* coat, but to

see the colour in real-world conditions as seen by UAV-based surveys. This may allow for environmental colour pollution like desert sand trapped between the hair. Secondly, in *Figure 4 (C and D)* the colour gamut is split into individual colours that represent the black of the horns and face markings, environmental pollution like desert sand and dirt trapped in the coat as the sandy colour, and the overall light grey representing the majority of the *O. leucoryx's* body.

Table 4: CIA Lab converted colour range to sRGB 8-bit range with 65% daylight as a white point. The range of each colour band is shown as a minimum, maximum and mean value. The RGB colour is a combination of each value combination.

Brightness adjustment of sRGB

CIE Lab (D65)	L	a	b
Min	45.02	-0.29	2.74
Max	75.54	1.72	9.9
Mean	62.82	0.323	6.33
sRGB (8Bit)	R	G	B
Min	108	106	102
Max	197	184	168
Mean	157.45	151.39	140.83
Standard Deviation	14.89	13.96	14.80
sRGB (8Bit)	R +65	G + 65	B +65
Min	173	171	167
Max	255	250	233
Mean	222.45	216.39	205.83
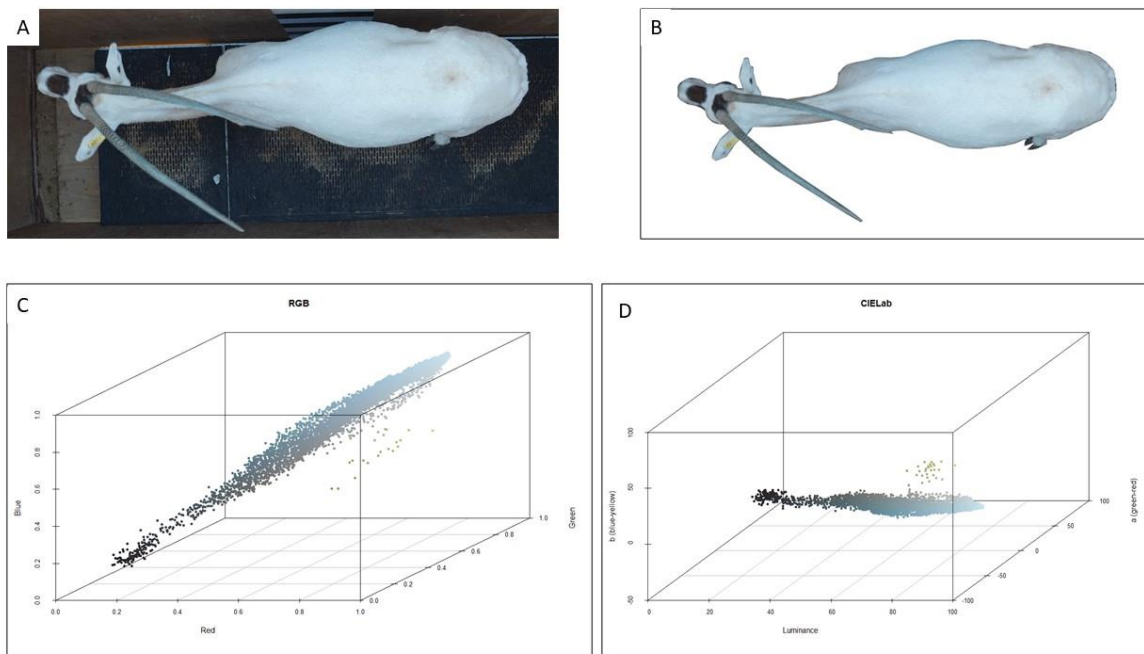
Figure 4: A: An adult O. leucoryx top view. B: The O. leucoryx top view where the background was removed. C: The sRGB gamut represents the O. leucoryx as seen in B. D: The CIE Lab gamut represents the O. leucoryx as seen in B.

The RGB gamut does not have a specific band for brightness if compared to CIE Lab where the 'b' represents the brightness band, in sRGB this 'brightness' is generally incorporated in the respective RGB values by a higher value to represent an increase in 'brightness', among others. Adjusting brightness in sRGB is a complex adjustment depending on the required field of application (Reinhard et al. 2002). The brightness adjustment was done using the Brightness modification of 8-bit sRGB values formula (Bezryadin et al. 2007) and resulted in the values shown in *Table 4*.

$$(R, G, B) = (r + M0, g + M0, b + M0)$$

Where 'r', 'g', 'b' values each respectively represent the 8-bit sRGB values.
Where 'R', 'G', 'B' represent the adjusted sRGB 8-bit colour band values adjusted for brightness (*Table 5*).
Were M0 represents the respective sRGB value for brightness adjustment.

3.3.4 UAV, sensors and control systems

During the data acquisition of the re-introduced *O. leucoryx* in the DDCR, the following UAV was used: the Ebee Plus (SenseFly, Switzerland) with a Canon S100 (Canon Inc., Japan) camera. The flight plan was developed in Pix4Dcapture (Ver 4.2.0) with a flight altitude of 90m AGL and picture intervals with a subsequent 80% side- and 80% front overlap, with an orthophoto mosaic resolution of 3.98cm/pixel. Three flights of the study herd over different time periods: 4 -, 18 March 2018 and 14 October 2018, were surveyed and processed.

3.3.5 Photogrammetric processing and data analysis

The UAV acquired images with location data captured during the flight and written in the Exif header file of each image with the required overlap needed for photogrammetric processing. This processing of imagery to a georectified orthophoto mosaic was done using DroneDeploy online processing services (www.dronedeploy.com).

The processed imagery was added to eCognition Developer$^©$ v.9 (Trimble, USA), an OBIA software (Blaschke 2010) where the data were analysed using a developed ruleset to extract adult *O. leucoryx* from the imagery using OBIA supervised classification. The 'Adult Arabian Oryx' ruleset, available under supplementary electronic material, provides details on the segmentation process, object identification, class assignment and the export of the data.
The OBIA ruleset starts with the segmentation analysis, two segmentation processes were used. Firstly, the multiresolution segmentation and secondly the spectral deference segmentations analysis. The process divided the orthophoto mosaic into well-defined objects, including the *O. leucoryx*. Both analyses weighted the sRGB colour bands the same. The input for object classification was the three colour bands, sRGB >= minimum values identified in *Table 3*. The objects that met the bigger or equal to the set minimum values were classified. The classified object was filtered using a minimum size requirement of >= 50 pixels (3.98 cm/pixel) to refine the results. This minimum size of 199cm^2 representing the 50 pixels is <10% of the drone footprint of adult *O. leucoryx* (de Kock et al. 2021b). This allows for noise reduction to still identify *O. leucoryx* if the animal is partly obstructed, for example, by vegetation, during the survey.

Lastly, the identified object was exported as a smoothed polygon shapefile (.shp) with added attribute values that include the mean of each colour band and the total brightness represented in the object and the number of pixels represented in each object. The extracted shapes were exported as a polygon shapefile that includes data on the number of pixels within the polygon. This analysis was completed for a total of three sample data sets taken from the UAV imagery sample data of the protected area, and each sample set exceeds 1 km^2 in size.

The digital measurements in a comma-separated file format were exported as a dataset in R v3.6.2 (R_Core_Team 2013). The dataset included all digital measurements as well as attribute data that included; the date, colour values, and the individual object size. The data structure was investigated and visualised using ggplot2 (Wickham 2016), colour-distance (Weller 2019) and colourspace (Ihaka et al. 2019) libraries.

The orthophoto mosaic imagery of each dataset and the OBIA vector files were added to ArcMap 10.7.1 (ESRI, Redlands, CA, USA) to visualise the results identified objects on the UAV-based orthophoto mosaics.

3.4 Zoometric measurements and modelling

3.4.1 Study species and sites

The *O. leucoryx* is a large-bodied arid-adapted antelope and the only member within its genus that ranges outside of Africa. Compared with other species within the *Oryx* genus, the overall size makes *O. leucoryx* the smallest. The historical range of this medium-sized desert-dwelling antelope covered the Arabian Peninsula and as far north as Syria (Harrison & Bates 1991). The species now occurs in a few reintroduced populations and many semi-captive populations in the Arabian Peninsula with substantially improved conservation status; yet most of the sites included in the 2011 assessment had to be fenced (Mallon & Price 2013), including our study site, the DDCR in the United Arab Emirates (UAE).

The present research incorporated information on three herds. The first referred to as the reference herd (n=10); these animals were marked and data were collected from both a fixed camera and a UAV to compare the two types of digital image collection methods. The second herd, referred to as the study herd (n=121), was used to collect baseline top view imagery data (*Appendix 3*) where measurements and known data like age, sex and weight were used to develop predictive models. The reference herd and study herd were both from managed captive populations. The third herd, referred to as the reintroduced herd, consisted of animals within the protected area. The study herd and the reference herd imagery were collected at Wadi al Safa Wildlife Centre (25.091200, 55.282360), the Arabian oryx conservation breeding centre, situated in the Emirate of Dubai, UAE (*Figure 5*). A large managed *O. leucoryx* population is housed as part of the regional captive *O. leucoryx* conservation breeding programme. All individuals are handled yearly (O'Donovan & Bailey 2006) for routine veterinary work, including vaccinations, health checks, and breeding access and separation, as per best practice guidelines (De Kock 2018). Individual animal baseline data including identifiers, weight, demographics and pregnancy status in females, were collected during this management process. Historically collected data like date of birth were referenced from the zoo-based database.
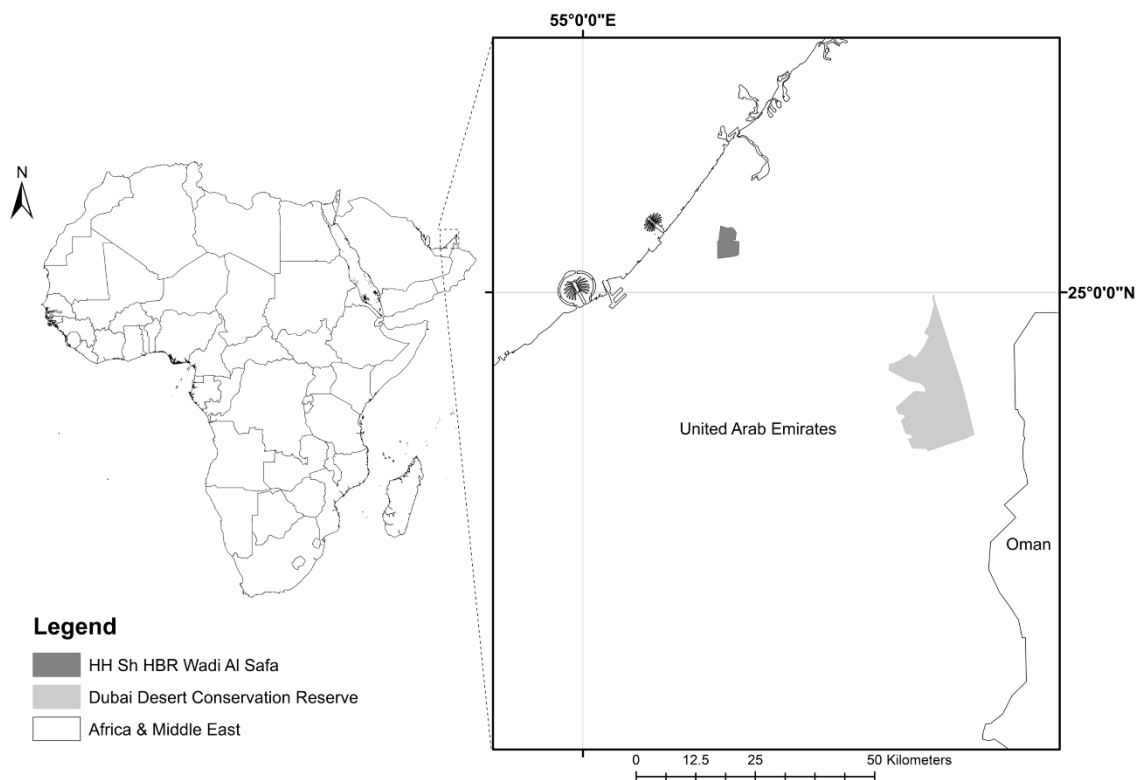
Figure 5: Arabian oryx conservation breeding centre, situated in the Emirate of Dubai, UAE

Field data collected from digital measurements on captive *O. leucoryx* of the 'study herd' were compared with data collected from the reintroduced herd by UAV, in the Dubai Desert Conservation Reserve (DDCR; 24.824789, 55.657069), a 225 km^2 protected area that is home to over 800 reintroduced *O. leucoryx* to conserve the species. To validate accuracy between the digital photo measurements and UAV imagery, the reference herd was measured using both techniques.

3.4.2 Validation image acquisition

As part of ongoing veterinary monitoring of captive and reintroduced oryx, both populations are captured annually, and routine measurements, such as weight, are collected. During this process, we also validated photogrammetry techniques using a remotely triggered camera affixed to the animal management area during captures. Digitised morphometric measurements of the species were obtained using scale and colour-rectified top view imagery where the sex, age, and weight of individual *O. leucoryx* were known, from the study herd (n=121) and reference herd (n=10). This imagery was acquired by a remotely triggered camera mounted within the animal management area.

To calibrate these images, we placed vertical and horizontal scale bars in the separation areas, where the oryx were temporarily held for veterinary procedures (*Figure 6*). The mounted scale bar was used as a point of calibration at the point of focus and permitted digital measurement of the total visible animal as seen from a top-view image; this image is referred to as the animal's 'drone print' where the animal is present in the aerial view of UAV derived imagery. Images of

27

the animals taken in the separation area were recorded with either a GoPro 3 (GoPro, USA) action camera or with a Sony QX1 (Sony Cameras, Japan) with a Sony E 20 mm f/2.8 lens, both set to maximum resolution.
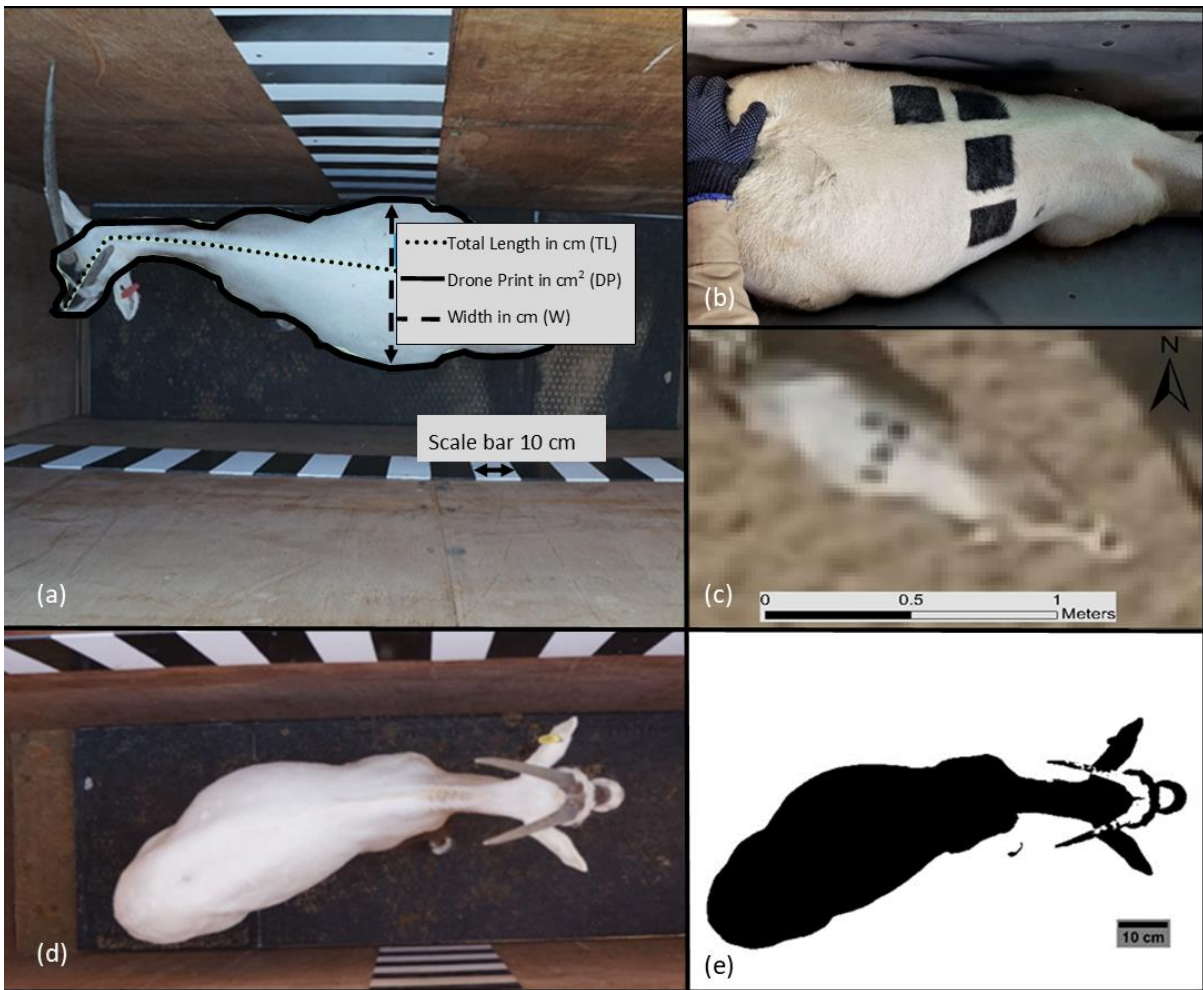
Figure 6: A - O. leucoryx top view image with digital measurement using KLONK software and scaled image. B - Temporary markers, used for animal identification during the accuracy assessment (n=10) of the reference herd from Wadi al Safa Wildlife Centre. Applied marks after baseline measurements. C - UAV processed image with a resolution of 2.5 cm/pixel from 100 m Above Ground Level (AGL) of the same animal after release. D - O. leucoryx top view image in the separation area. E - ImageJ, threshold object extraction for semi-automated measurements.

3.4.3 Digital zoometric measurements

To assess the accuracy of the digital measurements of the same individuals from a single scaled digital image and UAV acquired imagery processed, geo-rectified orthophoto mosaic, 10 animals of the reference herd were marked for individual identification using a non-toxic non-permanent coloured hairspray. A stencil with 12 squares in a grid of 4 x 3 (each square 7 cm x 7 cm) was cut into vinyl and placed on the back of the animals. Animals were marked consecutively as they were handled in a 'tamer' (Fauna Research, Red Hook, New York), an animal restraining system used for captive ungulate management, and released into their holding pen. The markers were added to allow accurate identification in the comparison of the digital measurements with geo-rectified UAV imagery.

A range of limitations that includes the available number of animals, managing stress levels and environmental conditions during the handling process, resulted in limited data. Because the animals were released into their enclosures as soon as possible after marking, some individuals were not visible during the subsequent UAV flight. With animal welfare as a prime concern, a second flight was not undertaken to avoid undue stress on the animals. As such, only six usable animal observations were utilised for the accuracy assessment.

Still images with reference scale of both the study and the reference herds were measured digitally. In the study herd, a total of 121 *O. leucoryx* were sampled (88 females and 33 males from the age of 1 month to 17 years). In the reference herd, ten animals were measured (5 males and 5 females ranging from 3-14 years). A total of three measurements of each animal was collected: 1. Total length from the base of the tail to tip of the nose (cm); 2. Overall 2-dimensional area of the top view (cm^2); 3. width, namely the fullest part of the animal (cm) perpendicular to the dorsal median plain. All measurements were made from scaled imagery in two dimensions.

Individual top view images were added to KLONK© Image Measurement Software Professional, Ver 16.1.1.4 (Image Measurement Corporation, Cheyenne, USA) for manual measurement and ImageJ©, Ver 1.52a (Laboratory for Optical and Computational Instrumentation, University of Wisconsin, USA), for semiautomated measurement using colour threshold analysis. The mounted scale bars in the separation area were used to rectify and scale the image on the focal length. Total body length (tip of the nose to base of the tail), and total visible area (top view perspective) were measured for the individual animals. In addition to the digital measurements of the scaled photos of the study-and reference herd, their sex, weight, age, and pregnancy status were recorded.

The reference herd (n=10) was measured twice in different software applications. These double measurements were taken to compare the relation between the manual digital scale imager measurements and the automated process resulted from the Object-Based Image Analysis (Bertelsen et al.). Firstly, similar to the study herd, the images were scaled and measured using the same techniques. Secondly, automated measurements were taken from OBIA results in the form of exported polygon files of the drone print of each identified animal, using measurement tools within ArcMap 10.7.1 (ESRI, Redlands, CA, USA). The second method was also applied to the reintroduced *O. leucoryx* oryx herd (*n=43*) within the DDCR, used to validate the effectiveness of the predictive pregnancy model.

3.4.4 UAVs, sensors and control systems

Aerial photographs were taken using a DJI Inspire 2 UAV (DJI, China) with a Zemusse X5S camera. Flight planning was carried out with DroneDeploy v.2.0.11 (DroneDeploy, USA) software set to a height of above ground level (AGL) of 100 m with a side-lap of 75% and front-lap of 85%, as recommended for the photogrammetry software. The maximum speed of the UAV was set to 15 m/s. To increase the total spatial accuracy of the photogrammetry model, ground control points (GCPs) were collected and added to the photogrammetry processing to provide validation points for subsequent distance-based measurements of imagery. A total of five GCPs in the pattern of four points in the corners and one in the centre (De Kock & Gallacher 2016) of the surveyed area were added to the photogrammetry input. Each GCP's geographical coordinates were acquired

with <15 cm, using a Trimble Geo 7x handheld GNSS (Trimble, UAV) system to improve the overall accuracy of the resulting orthophoto mosaic.

During data acquisition of the reintroduced O. *leucoryx* in the DDCR, an Ebee Plus UAV (SenseFly, Switzerland) with a Canon S100 (Canon Inc., Japan) camera was used. The flight plan was developed in Pix4Dcapture (Ver 4.2.0) with a flight altitude of 100 m AGL and picture intervals with a subsequent of 80% side- and 80% front overlap, with an orthophoto mosaic resolution of 4 cm/pixel.

3.4.5 Photogrammetric processing and analysis

The UAV acquired and geotagged images with the required overlap needed for photogrammetric processing were processed using DroneDeploy online processing services (www.dronedeploy.com). The processed imagery was added to eCognition Developer$^{©}$ v.9 (Trimble, USA) using an object-based image analysis (Bertelsen et al.) software (Blaschke 2010), where the data were analysed using a developed ruleset (De Kock 2015) to extract O. *leucoryx* from the imagery using OBIA supervised classification. The extracted shapes were exported as a polygon shapefile that included data on the number of pixels within the polygon. The extracted size perimeters and digital measurements of marked individuals were compared to determine the accuracy of the drone imagery and secondly imported to R v3.6.2 (R_Core_Team 2013) statistical software.

The three available measurements from the processed images - total length, width (W) and total area (drone print) - were extracted in a semiautomated way. The width was rejected because of the possibility of an increase or decrease in these measurements over a relatively short period. Therefore, in animals that become fatter or thinner, while maintaining the same or similar body length (such as in pregnancy where the drone print and width measurements will increase during pregnancy and decrease after birth), the total body length will be similar. Similarly, the body condition can be affected by environmental conditions like droughts where the abundance of food for the O. *leucoryx* are directly influenced. Normalising the drone print using the total length of the animal allowed the data to be indexed with a single value, the normalised drone print index (NDPI):

$$NDPI = \frac{(DP - TL)}{(DP + TL)}$$

The NDPI value range was 0-1, with DP (drone print) being the total top view of the animal (cm^2) and TL (total length) the distance from tip of the nose to base of the tail (cm). The NDPI values were categorised in a bracketed index that represents certain features. The application of the NDPI and the bracketed index on the DDCR dataset required the calculation of the NDPI in ArcMap. The OBIA extracted polygons representing individual animals were imported into ArcMap. Because the OBIA identified the objects from a raster image, the object boundary followed pixel boundaries, the OBIA data consisting of a polygon shapefile and attribute data including the total number of pixels within the polygon and the end-to-end length of the polygon at its widest measurement. These two attribute values presented the DP and the TL of each extracted animal. The imported OBIA attributes included the pixel size and the number of pixels represented in the polygon, both values were used to calculate the DP (in cm^2). The NDPI was calculated within ArcMap and added as an attribute value to the polygon shapefile.

Lastly, the selected range of the bracketing index was displayed to visualise the result in a geographical format.

3.4.6 Data analyses and model evaluation

The dataset of the reference herd was used to compare the physical animal zoometric measurements and the UAV-based photogrammetry processed imagery and digital measurements. The data sets from the study herd were used to develop predictive models. The dataset included all digital measurements as well as attribute data that included the date of birth, sex, weight, identification number, and pregnancy status for females.

The Drone Print data (DP) were normalised using the Total Length (TL) of the animals (*Equation 1*), resulting in a Normalised Drone Print Index (NDPI) ranging from 0-1. The NDPI was used as the basis for the bracketing index, where a specific range of data was bracketed to present particular features. The average, mean average, minimum, and maximum of each feature, within the index, were used as a guide to determine the best-suited bracket with the highest R^2 and include the most significant number of correlated data within the dataset.

A variety of models and model types were developed to investigate the best model fit focus on predictability. The inputs were used to develop the best fitting model to predict the age, weight, sex and pregnancy of individual O. *leucoryx.* The model types included linear regression, polynomial and predictive models. Computer learning decision trees were also employed using R and the Classification And Regression Training (CARET) package (Kuhn 2019).
The models included: the O. *leucoryx* weight predicting models; the two developed polynomial models using respectively the DP and NDP to predict weight; *O. leucoryx* age predictive linear and polynomial models using DP and NDP; O. leucoryx pregnancy prediction based on the decision-tree models, using the DP, NDP, TL and W; *O. leucoryx* sex prediction using the decision-tree, based on DP, NDP, TL and W data. During the polynomial model fit test, the Akaike Information Criterion (AIC) was used to evaluate potential overfitting because the data used to develop the model were also used to test the overall fit.

Where the predicted data were known, the model fit was tested on the additional imagery, otherwise, the data were split into test and training subsets, and the models were tested using the 'test' subset. The polynomial model fit was evaluated using the P-value, R-squared and where $(x)^2$ was used, the adjusted R-squared.

The pregnancy status of the O. *leucoryx* in the DDCR was monitored by the rangers using researcher-led visual observations that were developed by the DDCR management team. The criteria included a visual assessment of physical features as well as behaviour, captured by well-experienced rangers.

4. Results

4.1 Methods and ethical considerations for the monitoring of ungulates using UAVs: Systematic review synthesis

From the articles that were reviewed (n=36), most ungulates focussed UAV studies have been conducted in Africa (n=11) (Mulero-Pazmany et al. 2014; Lhoest et al. 2015; Hartmann et al. 2021) nine studies have been conducted in Europe (Witczuk et al. 2018; Roberts et al. 2020). The number of studies has more than doubled from 2020 (n=6) (Beaver et al. 2020; Fritsch & Downs 2020; Hu et al. 2020) to 2021 (n=13) (de Kock et al. 2021a; Fritsch et al. 2021; Obermoller et al. 2021).

4.1.1 UAV platforms and sensors

The most utilised UAV type were multi-rotors at 69% (n=25) and within this class, the 1000g-1500g weight class was the most popular at 48 % (n=12) of all multi-rotors (Inoue et al. 2019; Liang et al. 2020; Petso et al. 2021) and was utilised in a range of research applications. Fixed-wing UAVs accounted for only 28% of studies (n=10) (Mulero-Pazmany et al. 2015; Linchant et al. 2018a; Witczuk et al. 2018) but these generally covered larger areas (> 2.km2^2). VTOL UAVs were only used in 5.6% of cases (n=2) (Chretien et al. 2016; Bennitt et al. 2019) and these were also the most expensive or specialised platforms (Gu et al. 2017).

In total, mostly RGB imagery sensors were mounted on UAV platforms (75%; n=27). Thermal imagery sensors were present in 42% (n=15) of cases (Beaver et al. 2020; Kim et al. 2021) and 25% (n=9) of the research that we assessed used this in a combination with RGB imagery sensors (Christie et al. 2016; Preston et al. 2021; Rahman et al. 2022) either on the same UAV or a dedicated UAV platform. One study used a radio-tracking system (Roberts et al. 2020) and one did not use any sensor (Hahn et al. 2017).

4.1.2 Data acquisition platforms and characterisation

The data types that were collected included census (Cukor et al. 2019; Rahman et al. 2022), feature extraction (de Kock et al. 2021a; Ito et al. 2022) and behavioural monitoring (Maeda et al. 2021; Schroeder & Panebianco 2021) (*Figure 7*). The reviewed articles indicate a preference for the use of fixed-wing UAVs for focused ungulate censusing (Beaver et al. 2020; Hu et al. 2020; Roberts et al. 2020), while multi-rotor UAVs are widely utilised across all fields of study (Schiffman 2014; de Kock et al. 2021a; Kim et al. 2021; Petso et al. 2021).
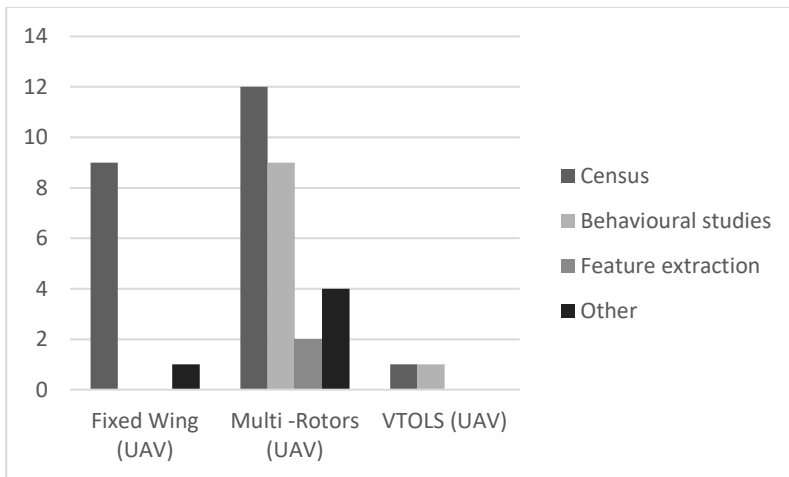
Figure 7: UAV type application in ungulate monitoring

Flights conducted for the purpose of an ungulate census are usually flown higher, faster and as automated flights when compared with targeted flights, which are more common in behavioural observations (*figure 8 and Appendix 4*).
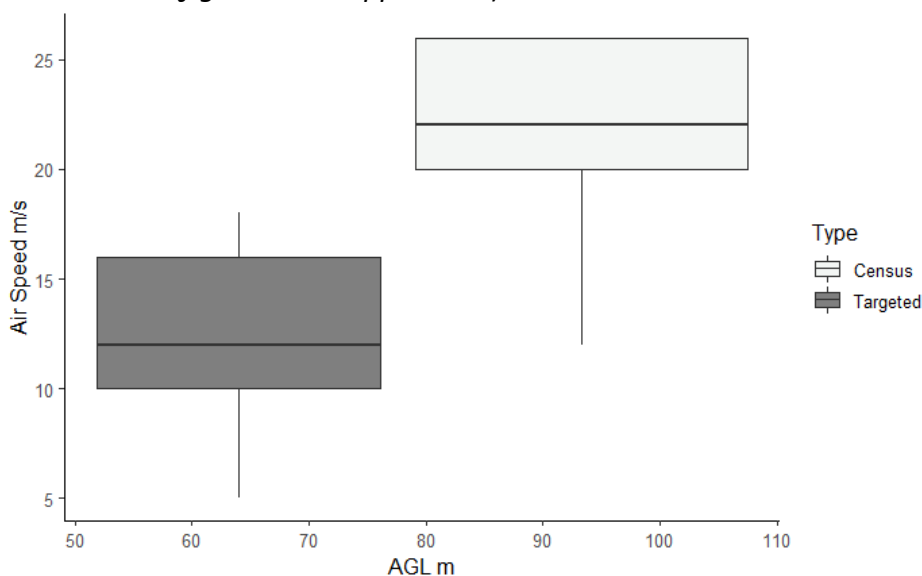
Figure 8: Type of UAV flights comparing airspeed and Above Ground Level (AGL) UAV flight height. The boxplot shows the airspeed median in m/s as a horizontal line, error lines indicate the min and max value.

4.1.3 Flight plans

Flight altitude
The flight altitude Above Ground Level (AGL) is mentioned as a range in AGL in most studies. The K-mean cluster centres were identified for both the minimum and maximum AGL and the K-mean centre for the lower AGL resulted in 57.88 m and the upper K-mean centre resulted in 104.66 m, with an outlier on both the minimum and maximum of 800 m which was removed from analysis (Su et al. 2018b).

AGL altitude for flights focused on censusing resulted in a mean of 61.23 m in the lower range (minimum AGL) and 104.23 m in the upper range (maximum AGL) with the mode of 100 m for both ranges. Compared to flights focused on behavioural studies where the AGL mean in the

lower range resulted in 40.71 m with a mode of 30 m. The AGL mean in the upper range resulted in 100 m with a mode of 50 m. The trend indicates a higher altitude for census-based UAV flights with a mean average of 85.11 m compared to flights focused on behavioural studies with a mean average of 76.18 m.

The trade-off between battery life and area under survey resulted in a generally higher AGL altitude for survey flights (Christie et al. 2016), which will allow more area to be surveyed with a mean average of the AGL range at 82.73 m when compared to piloted targeted flights with a mean average of the AGL range 70.36 m. Considering all flights combined, flights conducted over ungulate species on average are flown at 81.61 m AGL (*Figure 9*).
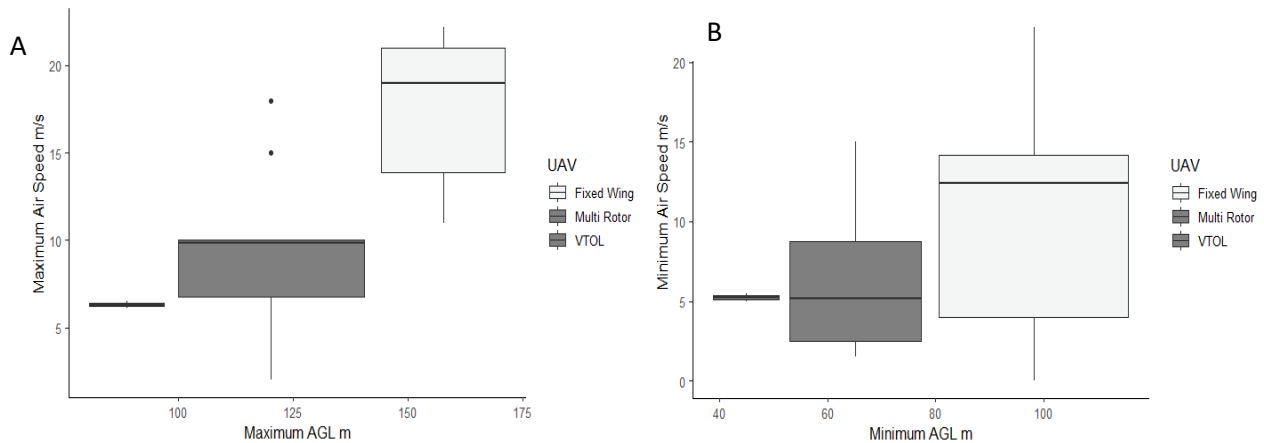
Figure 9: A: Minimum air speed and Above Ground Level (AGL) UAV flight height. B: Maximum air speed and AGL of different types of UAVs. The boxplot shows the maximum airspeed median (A), minimum airspeed median (B) as a vertical line, error lines indicate the m

4.1.4 Ethical considerations

Of the 36 papers that were considered, only 36% (N = 13) of the articles indicated ethical considerations made during the flight plan design that focused on multiple species (Hahn et al. 2017; Cukor et al. 2019; Hartmann et al. 2021) and 28%, (N = 10) of the article's ethical considerations focus on disturbance of the species of interest only (Obermoller et al. 2021; Zhou et al. 2021). In addition, 44% (N =16) of articles did not mention any ethical considerations or disturbance when developing the flight plan or during the flights (Linchant et al. 2015a; Inoue et al. 2019). The decision-tree models using the minimum and maximum AGL altitude, and minimum and maximum speed to predict disturbance were insignificant with an accuracy of 67% and p-value >0.05.

In the majority of the articles, even if ethical considerations were mentioned (Roberts et al. 2020; Fritsch et al. 2021) the disturbance was not quantified, and it was unclear what behaviour was interpreted as a disturbance. Limited articles (Bennitt et al. 2019; Zhou et al. 2021) quantify disturbance, and of these, both studies considered the launch distance and AGL altitude of the UAV as factors that will indicate disturbance in the form of a behavioural response from the species of interest. This behavioural response was classified as *(I)* any response and *(II)* evasive response (Bennitt et al., 2019).
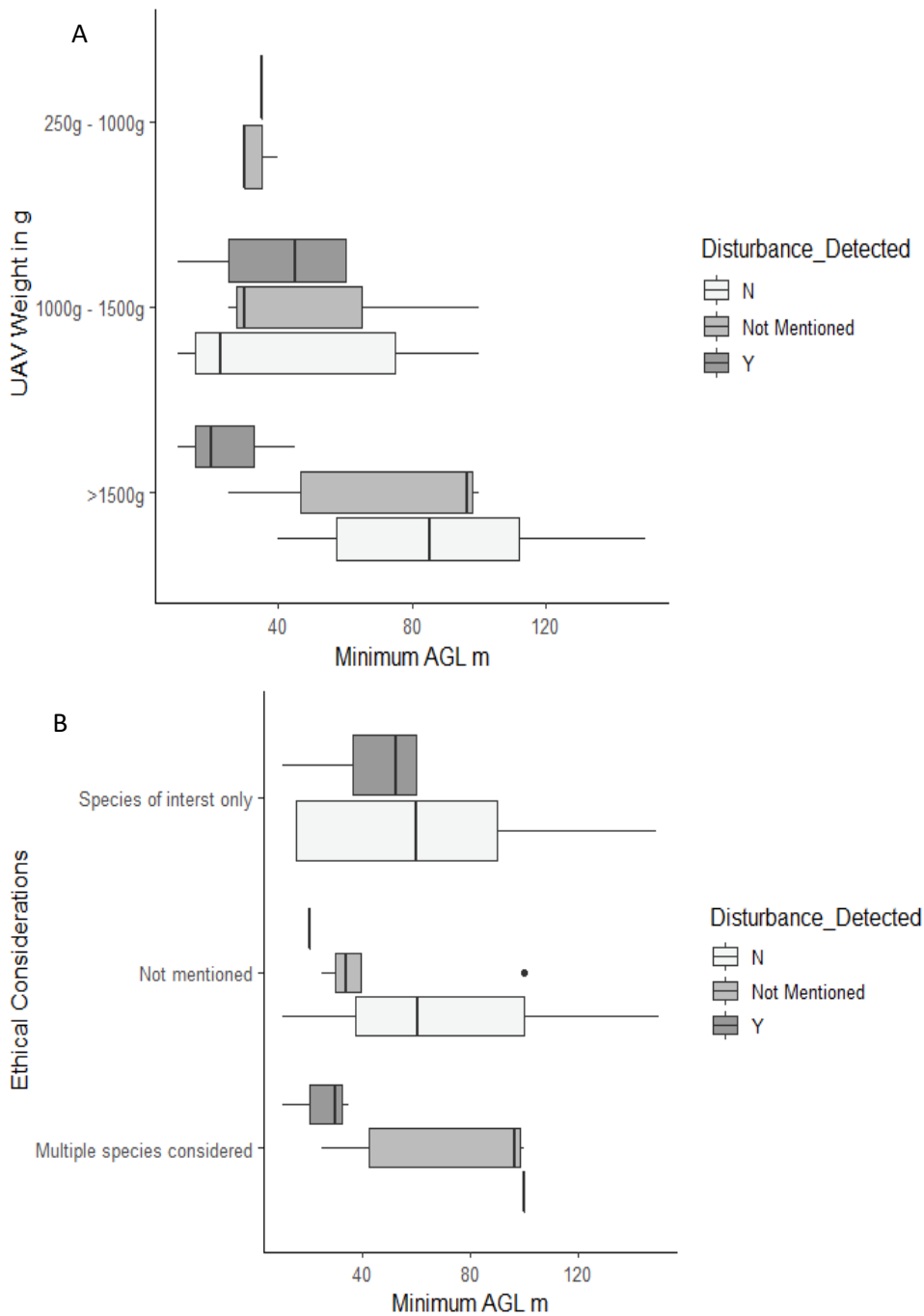
Figure 10: A: UAV weights and Minimum Above Ground Level (AGL) UAV flight height showing the level of disturbance and B: Ethical considerations made before flights and Minimum AGL UAV flights showing the level of disturbance. The boxplot shows the minimum AGL median in m as a vertical line, error lines indicate the min and max value, and the dots indicate outliers.

The UAV (*Figure 10 A*) size 1000g-1500g that was also used for 67% of the studies shows the highest level of disturbance. However, the skewed data set with over-representation of this weight class need to be considered in this context. Where disturbance was detected (*Figure 10 A & B*) regardless of weight classes, the analyses show no disturbance of flights > 60 m AGL. UAV size (*figure 11 A*), flight time over a target species (*Figure 11 B*) and the airspeed of the UAV, regardless of the flight type and UAV type; has less disturbance impact when compared to the AGL UAV flight height (*Figure 11 A-C*). The decision tree model using minimum altitude and UAV

size as an input to predict disturbance detected is not significant with an accuracy of 67% and a p-value >0.05.
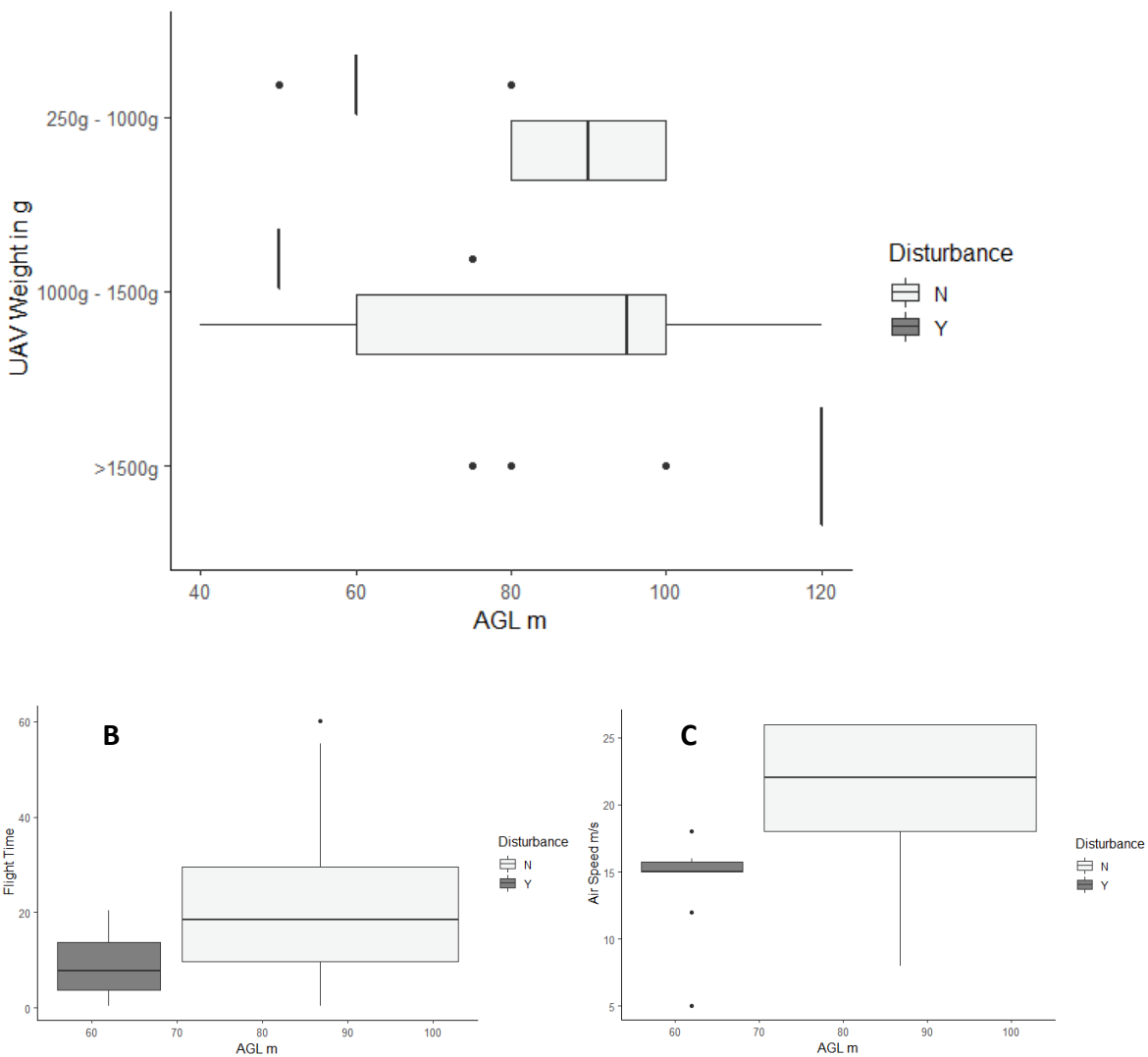
Figure 11: A: UAV size in weight classes and Above Ground Level (AGL) UAV flight height indicate if disturbances were observed. B: UAV flight time over the target species and AGL UAV flight height indicate if disturbances were observed. C: UAV airspeed over the target species and AGL UAV flight height indicate if disturbances were observed. The boxplot shows the AGL median in m (A), flight time median (B) and airspeed median in m/s (C) as a vertical line, error lines indicate the min and max value, and the dots indicate outliers.

4.1.5 A synthesis of six years (2016 -2022) of UAV-derived data from ungulate surveys for conservation.

We utilised five types of multi-rotor UAVs and fixed-wing UAV. With AGL flight height ranging from 40-120 m. During our surveys (*Appendix 4*), we found that the most appropriate UAV platform for ungulate surveys depends on the area under survey, the specific species and the survey requirements. Surveys on *Oryx dammah* (Chad), *Nanger dama* (Niger) in large reserves required the use of fixed-wing UAVs with longer flight time capabilities to cover the desired areas, whilst smaller areas could be covered by multirotor UAVs. The species detectability governed the combination of flight height and sensor resolution. For example, during automated detection model development approaches, lower flight heights were required for clearer images that increase detectability, especially for more cryptic species. The habitat also played a big role in the selection of the flight and sensor characteristics. For example, surveying the *Oryx leucoryx* could easily be done at 100 m AGL (de Kock et al. 2021b) as the habitat is relatively homogenous and open, and animals that have coat colour contrasting to the environment, could easily be detected in images from this altitude. This differed in other cases, e.g., brown-coated *Tragelaphus derbianus* (Senegal), where the tree cover induced detectability issues and flights had to be conducted at lower AGLs for clearer images.

4.1.6 Quantifying disturbance: a case study on the Western Derby eland.

The Western Derby Eland actively avoids UAVs when they are at or below 50 m AGL, and no active avoidance could be detected from approach flights at 120 m AGL to 50 m AGL (*Figure 12*). The DJI Phantom 3 Pro induced more disturbance at lower altitudes when compared to the DJI Phantom 4 Pro, and this UAV platform had noticeably more audible flight adjustment feedbacks during stable flight when compared to the Phantom 4 Pro, although not statistically significant when UAV height and type was used to predict disturbance with a model accuracy of 38% and p-value = >0.05. Differences could be detected in the induced disturbance between the two different types of UAVs at AGLs greater than 50 m.
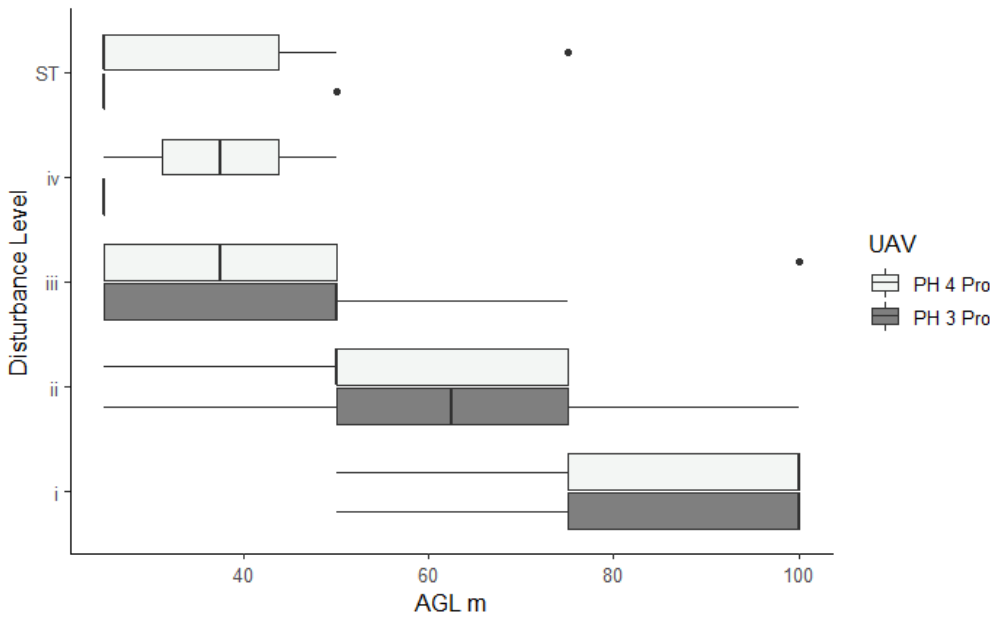
Figure 12: Summary of the reaction levels of disturbance of two types of UAVs on T. derbianus derbianus at a range of Above Ground Level (AGL) flight altitudes. The boxplot shows the AGL median in m as a vertical line in the box, error lines indicate the min and m.

4.2 Semi-automated detection of large ungulates

4.2.1 Object-Based Image Analysis

The results of the spectral data analysis (*Table 5*) and the visualisation (*Figure 13*) show the standard deviation and mean of each value in the CIE Lab and sRGB colour space of the adult O. *leucoryx* (n=50) analysed hair samples. The converted mean CIE Lab reflective spectrometry colour values of the hair samples of adult *O. leucoryx* to 8-bit sRGB resulted in a Red value of 157.450, Green value of 151.390 and Blue value of 140.832 without the brightness adjustment. These sRGB values were added as an equal or larger than the cut-off colour value where all the objects with a combination of all three colour values, equal or higher than the cut-off values and a minimum size permitter were added as the input of the OBIA ruleset identified adult *O. leucoryx.* The use of the sRGB values without the brightness adjustment was selected to allow the ruleset a wider range in identification when imagery is underexposed and because there is no upper limit set for the ruleset, this will allow a wider range of detection when images are overexposed.

The results of the three UAV imagery surveyed datasets of the protected area were re-introduced O. *leucoryx* after applying the 'Adult Arabian Oryx' ruleset as seen in *Figure 13*. The OBIA ruleset identified adult *O. leucoryx with a high degree of accuracy (Table 5), an average of 96.16% when applied to the* three datasets, therefore proving the potential to be a robust ruleset. The robustness needs additional testing on additional datasets on landscapes with a higher heterogeneity.
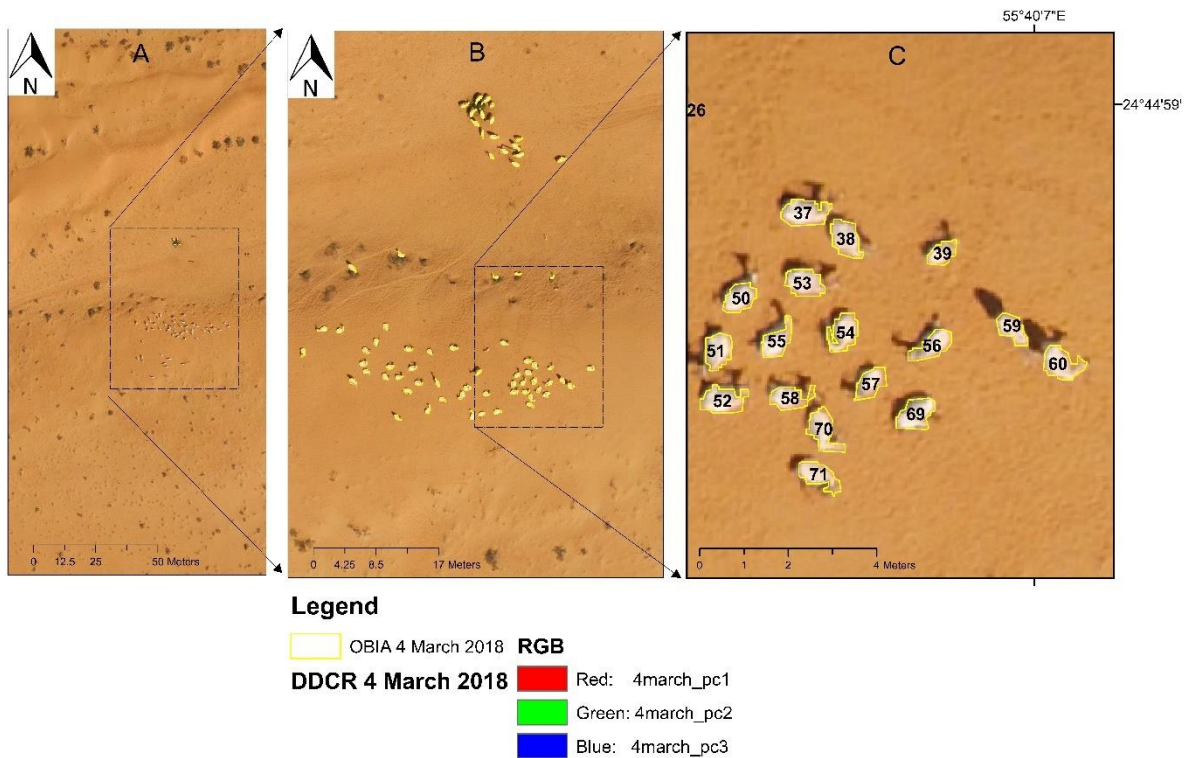
Figure 13: The resulting output of the OBIA ruleset run on the UAV acquired data set of 4 March 2018. A: Show the processed imagery into an orthophoto mosaic. B: Shows the adult Arabian Oryx identified by OBIA (in yellow). C: Shows a closer view of the identified adult O. leucoryx with numbering labels.

The ruleset performed well in all three datasets that present different environmental conditions, and different times of the day and year. During visual result evaluation, the ruleset did not identify any *O. leucoryx* with the 'sandy' calf colour, as illustrated in Figure 13 *A&B - objects a*. However, there was one false negative in two of the datasets (Figure 13A- object B&C and 3B – object B).

The OBIA software groups pixels of similar values together to represent objects. The results of the object identified in the three datasets (*Table 5*) show the mean sRGB colour values. If there is no clearly defined boundary between objects of the same values specified in the ruleset, the objects will be grouped as a single object. This is observed in Figure 14A object C, where two animals are close to each other with a limited background to clearly define the boundary and therefore result in a single object classification.

Table 5: The mean sRGB values and standard deviation of the object identified by 'Arabian Oryx' OBIA ruleset.

Dataset Date	Mean Red	Standard Deviation	Mean Green	Standard Deviation	Mean Blue	Standard Deviation	Total Oryx Identified	Total Objects
4/04/2018	228.42	4.63	198.41	4.78	153.80	7.52	72	8561
18/04/2018	230.46	4.37	199.99	6.81	154.56	7.56	56	2435
14/10/2018	221.94	6.51	194.12	7.83	150.27	9.07	47	7131

In this case, although the OBIA ruleset identified the object, it failed to differentiate multiple

objects, and this shortcoming is a segmentation issue rather than a final classification process. The failure to distinguish between numerous objects within the identified object will affect the survey's overall accuracy, resulting in undercounting.
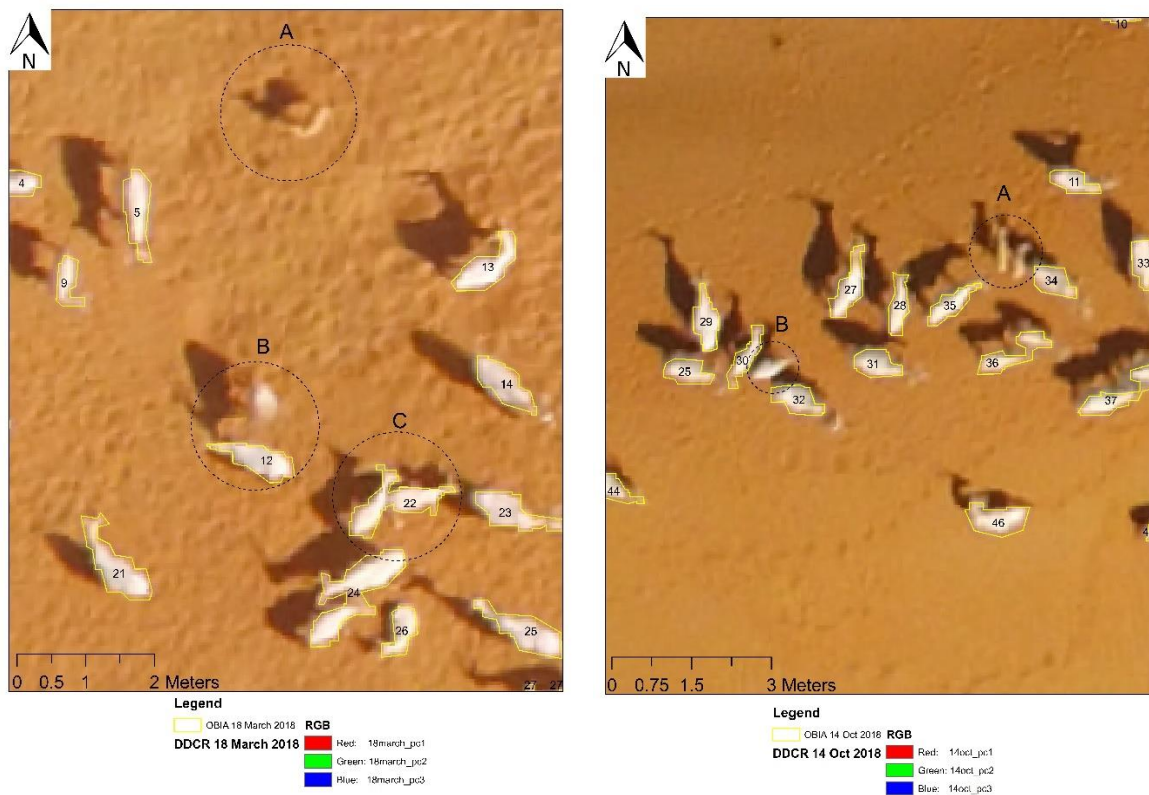
Figure 14: A: Identified adult O. leucoryx from the 18 March 2018 dataset. Object A- The O. leucoryx calves in their juvenile coat colour is not identified by the OBIA ruleset as an adult O. leucoryx. Object B- a 'ghost image of an O. leucoryx, where the shadow is visible; however, the animal itself moved during or between overlapping images resulting in the 'ghost' image. Object C- Multiple objects identified as a single object. B: Identified adult O. leucoryx from the 18 March 2018 dataset. Object A- The O. leucoryx calves still in their juvenile coat colour is not identified by the OBIA ruleset as an adult O. leucoryx.

Table 6: Result of identified Adult O. leucoryx applying the OBIA ruleset: 'Adult Arabian Oryx' on all three datasets, indicated as a confusion matrix.

	Yes	No
Yes	175	0
No	2	25083

4.3. Feature extraction

4.3.1 Morphometric data extraction and application

The accuracy was 98.41% with a Standard Error of the Mean (SEM) of 0.401 for the DP and 97.99% with an SEM of 0.345 between the fixed camera image and zoometric measurements from processed UAV imagery of the reference herd (*Table 7*).

Table 7: Accuracy assessment between baseline and UAV acquired imagery with the Standard Error for the Mean (SEM)

ID	Baseline measurements		UAV images		Accuracy in %	
	Drone print (cm^2)	Total length (cm)	Drone print (cm^2)	Total length (cm)	Drone print	Total length
2475	2797.99	124.49	2778	121.52	99.29	97.61
2007	2805.65	120.75	2792	118.96	99.51	98.52
2205	2973.67	121.4	3054	123.32	97.37	98.44
2390	3570.23	150.12	3609	147.2	98.93	98.05
1173	2496.85	117.3	2427.88	115.92	97.24	98.82
1964	2574.62	124.92	2525	120.54	98.07	96.49
				Average	**98.4**	**97.99**
				SEM	**0.4008**	**0.3446**

The candidate weight predictive models *(Appendix 5)* consisted of two linear models and two polynomial models to determine which models were best supported by the data (*Table 8*). The linear regression model predicted the weight of individual *O. leucoryx* using the DP predicted weight produced a relatively high model fit (R^2 0.799, overall comparison of AIC 923.49). However, based on the R^2 the model performed poorly, especially considering residuals, which included younger animals that were growing rapidly to adult body size. The model using NDP (*Figure 15)* resulted in an R^2 of 0.7969 and an AIC of 948.83. Of the polynomial models using DP and DP^2, and NDP and NDP^2, the first resulted in R^2 of 0.85 and AIC 919.68, while the NDP and NDP^2 model performed the best in predicted weight (R^2 0.85, AIC 912.38).

Table 8: Candidate predictive model comparison of fit. Weight (W), Drone Print (DP) and Normalised Drone Print (NDP)

Model	Predict	Inputs	R^2	AIC
Linear Regression	W	DP	0.8	923.49
Linear Regression	W	NDP	0.8	948.83
Polynomial	W	DP & DP^2	0.85	919.68
Polynomial	W	NDP & NDP^2	0.85	912.38
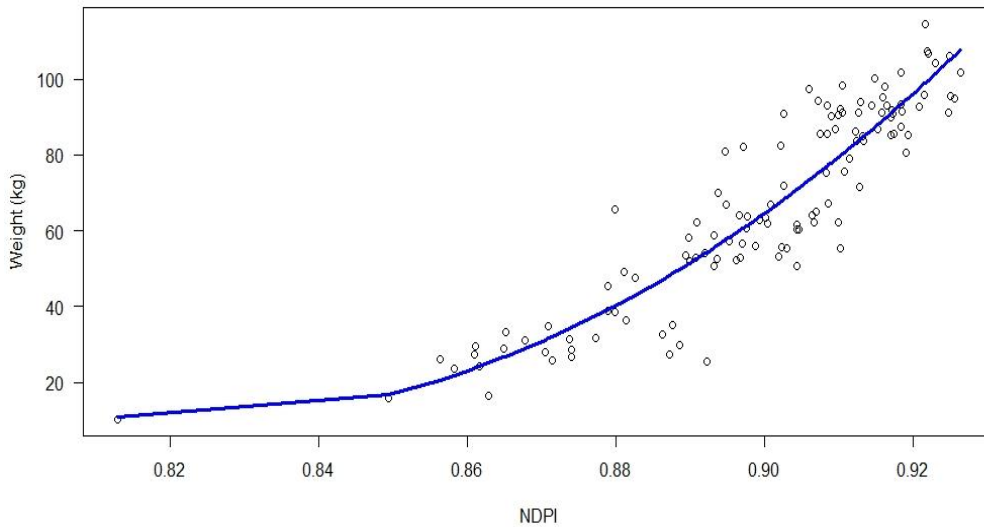
Figure 15: Oryx leucoryx normalised drone print index (NDPI) and weight (n=121) graph, with a fitted polynomial regression model, with NDPI and normalised drone print index squared (DNPI2).

The age predictive models using DP and NDP were not significant: the polynomial regression using DP to predict age (R^2 0.562, df 119, residual stander error of 35.17), and that using the NDP to predict age (R^2 0.525, df 119, residual standard error 36.61). The models' inability to predict the age with relatively high precision is influenced by the growth curve that flattens out when antelope reach adulthood. The bracketed index, when focusing on age, from birth to adulthood showed more potential, possibly related to the natural breaks in the data and general lack there off when the animals reach adult size.

The decision-tree models (*Appendix 6-9*) using the width to predict pregnancy and the model using the DP, NDP, TL and W had the same accuracy (0.917, p < 0.01). However, the model only using the width was preferred because of the simplicity and the fact that the accuracy and p-value were not affected. The decision tree model predicted that O. *leucoryx* with a measurement of > 37 cm on the widest part of the drone print was pregnant. The high accuracy made this model a reliable tool to predict pregnancy in an O. *leucoryx* herd from UAV based imagery.

The decision tree model predicted that O. *leucoryx* with a measurement of ≥ 33 cm on the widest part of the drone print, NDPI > 0.88 and total length > 115 cm, were males. The model fit test utilising 30 % of the data indicated a 72.2% accuracy (p = 0.58). The model's low accuracy, high *p* value and low representation of adult male O. *leucoryx* within the train and test dataset, negatively affected the usability of the predictive model.

Data with a high correlation with the DP allowed for predicted values using the NDPI to have a higher level of confidence. Data features like the age of the animals that had a lower correlation with the DP were predicted to perform poorly when the NDPI was used to predict age in a population.

Applying the bracketed range of the NDPI (*Table 9*) to the sample data results allowed the prediction of limited age group information, female pregnancy and weight ranges within the herd, with a high probability.

Table 9: Bracketed index of Oryx leucoryx features with probabilities

Index range	Feature indicated	Probability (%)
0.85–0.90	<16 months old	96%
≥0.915	Female pregnant	92%
≥0.915	Weight ≥80 kg	100%
≥0.922	Female	100%

The bracketed NDPI was applied to a UAV acquired and photogrammetry processed orthophoto mosaic of the reintroduced herd of *O. leucoryx* within the DDCR. The age bracket was applied to the reintroduced herd in the DDCR and showed 100% accuracy, as verified by trained rangers' researcher-led visual observations.

The weight bracket could not be verified; verification would require the capture and weight of these wild animals and this was not an ethical or practical option. The pregnancy bracket index showed that 24 individuals were identified as possibly pregnant from the 43 identified individuals identified by OBIA; possibly pregnant females are shown on the map as green triangles (*Figure 16*). The DDCR rangers' researcher-led observations of 21 females showed visible signs of pregnancy, resulting in an overall accuracy of the applied NDPI bracketed guideline for identifying the high probability of pregnancy in *O. leucoryx* of 87.5%. Lastly, the female-identified by the female bracketed index was 100% accurate.
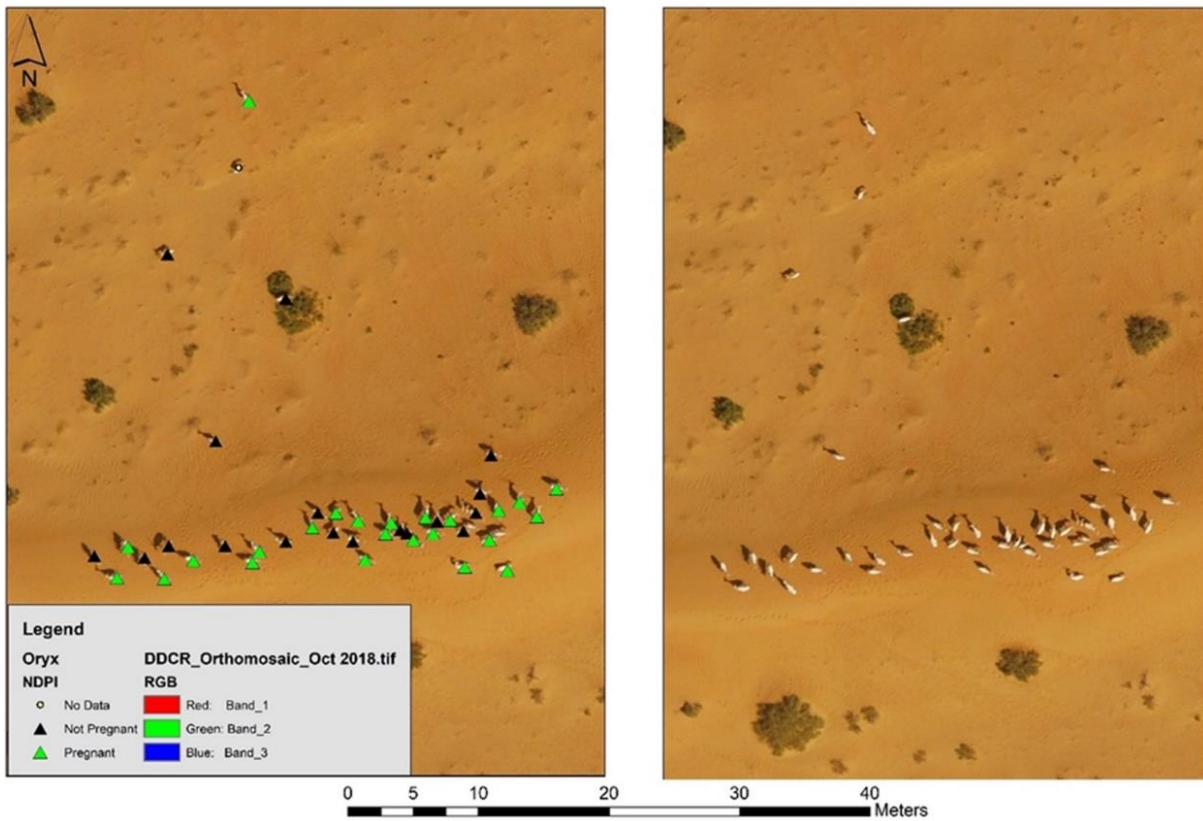
Figure 16: A - Applied NDPI bracketed guidelines for estimating possible pregnancy in O. leucoryx from one of the re-introduced(n=43) herds on DDCR. B - Orthophoto mosaic processed from UAS acquired imagery.

5. Discussion

5.1 Methods and ethical considerations for the monitoring of ungulates using UAVs: Systematic review

UAVs are an appropriate monitoring tool for ungulate population surveys if the UAV is launched far enough from the survey area and is kept above 60 m AGL. This also makes the platform ideal for many other ecological surveys, as even small UAVs provide resolutions at the sub 5cm/px GSD (Ground sampling distance, measured in centimetre per pixel) level at 60 m AGL.

Many filed biologists relying on traditional survey techniques may be overwhelmed by the ever-developing UAV monitoring industry, which can hinder the implementation of the technique. It is important not to overlook the advantages of this low-impact survey method, especially when compared to manned aerial surveys, which are orders of magnitude more costly and invasive, inducing flight responses at much greater altitudes (Christie et al. 2016). In context, UAV-based monitoring of ungulates is relatively new and has undergone limited research on the application of this method, its shortcomings and the effect on species and the environment compared to more traditional and established monitoring methods. Most off-the-shelf multi-rotors use lithium polymer (LiPo) batteries and the increase in the UAV size results in increased power needs. Therefore, generally speaking, the larger the electrical UAV the larger the battery and lithium content. Increased restrictions on the transport of LiPo batteries especially during air travel (Shen et al. 2020), may add additional complications during transportation. In addition, the full impact of battery waste on the environment is still unclear and may add complications during the recycling process and the containment of dangerous elements (Melchor-Martínez et al. 2021).

It is also important to consider the shortcomings of the UAV approach and to identify the specific requirements for implementing UAVs as a survey tool on various scales. For instance, it would be unfeasible to attempt a large reserve survey using a small multirotor. Conversely, a large fixed-wing UAV will increase disturbance levels if flights need to be conducted on small reserves at low altitudes for the monitoring of smaller species, especially considering the footprint of a fixed-wing UAV, which resembles a large raptor.

Multirotor UAVs were by far the most widely implemented platform for ungulate surveys, but they range considerably in size. Smaller UAVs, typically in the 1000-1500g range were widely implemented, and this may be due to a trade-off between efficiency and capital investment, as these platforms (mostly DJI Phantom's) are relatively low-cost, offering high-quality imaging sensors in an easy-to-use package. However, limitations like battery life and legal limitations on maximum flight operations limit off-the-shelf multi-rotors (e.g., DJI Phantom 4 Pro), to cover smaller areas (2.016 km^2) even with an energy optimisation setup and favourable environmental conditions (Pradeep et al. 2018).

Pre-flight planning is an important phase when developing census methodologies for any area, and this is reflected in the published literature, as most studies use automated flights that follow premeditated flight characteristics. This also highlights the need to be aware of a few factors before commencing with any survey-type flight over any ungulate species. Knowledge of the species, habits and habitat is required to identify the best resolution and flight path

characteristics that will ensure high detectability and efficiency. Additionally, ethical considerations need to include the effects on the target species, but also the environment in which the UAV will be operating. For instance, during some of our surveys (*Appendix 1*), the UAV did not induce a disturbance in Western Derby eland that we could identify visibly, but the presence of a large flying object induced vocal responses and fleeing in monkey populations (*Chlorocebus sabaeus*) within the study area. Not all UAV disturbances provoke visible behavioural response, physiological response was recorded with limited behavioural responses to UAVs (Ditmer et al. 2015). In other instances, no disturbance effects were observed on the Northern giraffe (*Giraffa camelopardalis*), Dorcas gazelle (*Gazella dorcas*), Dama Gazelle and Addax (*Addax nasomaculatus*). In rare cases, the UAV was actively pursued by black kites (*Milvus migans*) and forced an abandonment of the survey flights in that area. The framework of these flights (*Table 10*) is summarised and includes references to vegetation types, species monitored, UAV selection, mean average flight perimeters (AGL and flight time) and if visible reactions to UAV disturbance were observed.

Table 10: Summary of our research on UAV-based ungulate monitoring focuses on the vegetation type, UAV selection, flight perimeters and species monitored

Vegetation Type	Flights (n=121)	Type	Species	UAV Type	Area covered	Avr Flight time	Avr AGL (m)	Disturbance Detected
Semi-desert	38% (n=46)	Census 73% (n=34) Targeted 26% (n=12)	*Addax nasomaculatus* *Camelus dromedarius* *Giraffa camelopardalis* *Nanger dama* *Oryx dammah* *Gazella dorcas*	Fixed Wing 74% (n=34) Multi-Rotor 26% (n=12)	< 1km2 4% (n=2) 1 - 2km^2 26% (n=12) 2 - 5 km^2 20% (n=9) > 5 km^2 50% (n=23)	00:31:25	106.3	N 80% (n=37) Y 20% (n=9)
Senegalese savanna	32% (n=39)	Census 44% (n=17) Targeted 56% (n=22)	*Taurotragus derbianus derbianus* *Ceratotherium simum* *Oryx gazella* *Equus burchelli* *Nanger dama* *ragelaphus scriptus* *Giraffa camelopardalis* *Camelus dromedarius* *Gazella dorcas* *Phacochoerus africanus*	Multi-Rotor 100% (n=39)	< 1km^2 59% (n=23) 1 - 2km^2 36% (n=14) 2 - 5 km^2 5% (n=2)	00:09:11	72.56	N 87% (n=34) Y 13% (n=5)
Desert biome	23% (n=28)	Census 100% (n=28)	*Camelus dromedarius* *Nanger dama* *Oryx leucoryx* *Gazella marica*	Fixed Wing 3.6% (n=1) Multi-Rotor 96.4% (n=27)	< 1km^2 25% (n=7) 1 - 2km^2 71% (n=20) 2 - 5 km^2 3.6% (n=1)	00:14:34	89.11	N 100% (n=28)
Forest biome	5% (n=6)	Census 100% (n=6)	*Sus barbatus*	Multi-Rotor 100% (n=6)	< 1km^2 67% (n=4)	00:15:20	88.33	N 100% (n=6)

A current shortcoming of quantifying disturbance is linking the reaction of the animal directly to the presence of a UAV. The majority of UAV pilots are qualified under the visual line of sight

(VLOS) category, usually legally limited to a maximum of 500 m between pilot and UAV. Therefore, the pilot needs to be ≤ 500 m from the target and the presence of humans and human activity at this distance may be the cause or a contributing factor to the disturbance response. During ungulate monitoring in Chad, scimitar-horned oryx and *dorcas gazelle* showed a strong movement response and kept > 1 km between them and the UAV pilots (personal experience). When the method of piloting was changed to a first-person view (FPV) and the UAV was launched > 1 km away from the target species and where terrain restricts the visibility of the vehicles and people, we managed to monitor scimitar-horned oryx and *Dorcas gazelle* as close as 40 m, without inducing an evasive response.

This highlights the importance of site-specific assessments of possible disturbances that need to be considered to ensure that appropriate steps are in place to respond to any adverse conditions during surveys. A specialist on the species and habitat under survey would be best suited to evaluate the possible effects of a UAV survey.

A concerning factor is the lack of ethical considerations in many of the studies that were evaluated. Even though these studies may have included this as part of their ethical research approval, the novelty of the methods requires this to be reported, as the expertise to assess ethical flight considerations may not exist within the framework of many institutions. If no experts are available, a panel of reviewers, who are specialists in UAV surveys, could be consulted as part of the methodological development process and any alterations to reduce disturbance can be mentioned in survey reports. As a minimum, it would be beneficial for any census to preserve records of the flight plans/flight paths which can be evaluated/advanced or repeated in future applications. In the absence of this information, studies are not replicable, and the scientific method is void. Coupled with this, the rapid advance in UAV sensor technologies would require comparative data between survey flights, as population increases may only be the result of increased detectability, and flight parameters would be required when this type of data is reviewed.

5.2 Semi-automated detection of large ungulates

Our study demonstrates the effective use of animal coat reflective spectrometry data as an input to OBIA to identify specific species from UAV base imagery, with good performance on the datasets. However, more data from a range of heterogeneous landscapes are needed to test the overall robustness and performance of the OBIA ruleset. The extracted reflective spectral data produced a species spectral reflectance signature, this proof of concept has a range of practical applications where specific species can be targeted during the data analysis of UAV-based imagery.

If confounding factors like data quality are controlled the OBIA ruleset performs well, this can include the standardisation of the sensor and settings like white balance to name a few. There are, however, data inconsistencies that affect the overall efficiency of the OBIA ruleset to identify individual animals. The UAV-acquired imagery is processed by photogrammetry software, using multiple images taken during the survey, and turns it into a composite orthophoto mosaic. The combination of overlapping images in the photogrammetry process to produce a single ortho-rectified image presents complications with objects that move during or in-between images. This results in 'ghost' objects as seen in Figure 3A object B and in extreme cases, the moving object between images can result in multiple representations of the same animal or no representation

of the object in the final composite image. In addition, confounding factors can include a range of factors related to the UAV platform: stability, the selected flight plan; the sensor: sensor sensitivity, motion blur and the environment: vegetation cover, heterogeneous landscapes etc.

The significant differences in images representing *O. leucoryx* visible in *Table 4, Figure 4* and *Figure 3* show the influence of a non-standardised sampling technique where the sensor perimeters are automatically adjusted with limited supervised input. The influence of the variation of white balance settings between the survey data and the change in lighting conditions on the survey dates results in a range of challenges during colour comparisons. Most off-the-shelf UAVs and sensors are programmed to produce a 'beautiful photo' with limited manual programming of the sensor, however, the automated setting adjustments of the sensor are negatively influenced by the automated gamma correction and white balance adjustment. Standardisation of the survey sensor, including the white balance (Seyednasrollah et al., 2019) can improve colour comparisons between datasets.

Ethical UAV-based wildlife surveys are paramount; however, these ethical standards are absent. Wildlife populations can respond idiosyncratically to UAV wildlife surveys, depending on a variety of factors (Hodgson & Koh 2016). Although some countries did develop ethical protocols when using UAVs for wildlife surveys (Gonzalez & Johnson 2017), ethical UAV wildlife survey operation is the main responsibility of the UAV pilot.

Automated wildlife detection from UAV-based imagery as a survey tool is a relatively new research area with a range of data extractions and analyses to investigate. The automated extraction of animals from photogrammetric-processed datasets includes spatial and temporal data. Additional data extraction of UAV-based animal surveys focuses on imagery baseline top view measurements applied to UAS-acquired imagery. This has a range of practical applications, which will increase with the addition of multiple UAV data acquisitions over set intervals e.g. seasonal. These time-specific dataset comparisons may include calculations of survival rates of offspring, herd dynamics, and behavioural research.

5.3 Feature extraction

There was a remarkably strong relationship between zoometric measurements and the *O. leucoryx* pregnancy predictive models. The developed models have a range of practical applications in the field of conservation. A field biologist responsible for the management of reintroduced *O. leucoryx* can use the tool to extract individual animal data applicable to the decision-making process. Furthermore, when multiple seasonal UAV acquired datasets are used, these time-specific data comparisons may include calculations of the age structure, pregnancy and body condition scoring of the herd.
The combination of the pregnancy predictive model and the age bracket to identify *O. leucoryx* <16 months, when used in yearly data analysis of the herd can provide insight into the relationship between pregnancy and calf survival rates. The age predicting model may improve if the data were filtered into a subset in a specific age range, with a better fitted linear model.

However, there are limitations. This tool can only be used where the animals can be detected and extracted in a semi-automated or automated way with relatively high accuracy. Data from smaller animals will prove to be more challenging to extract and would be directly influenced by

the resolution of the surveyed imagery. Vegetation, mist and other environmental conditions limit image capture of the species of interest with traditional red, green and blue (RGB) sensors. Similarities in the relation between the animal coat colour and the environmental background may be challenging for the detection process, especially if the survey data are limited to RGB camera sensors. The errors may be influenced by a range of factors that can include the quality of the data, the overall accuracy of the images processed by photogrammetry software resulting in a geo-rectified orthophoto-mosaic, the cm/pixel size of the resulting orthophoto-mosaic, the sensor used, and movement of the animals during the aerial survey. Further research in the area of animal detectability, detection probability and limitations using OBIA, is needed.

Safe operation of the UAVs is the primary concern of drone pilots and meteorological conditions may limit the performance of the UAV and result in grounding of the plane. The survey area is usually limited to UAV operations and, in most cases, the flight time per battery (Zhang et al. 2016). Better sensors with increased resolution are a current trend. This results in a larger file size for each picture and therefore an increase in the data set size, putting more pressure on computer hardware and increasing the cost of data analysis (Casella et al. 2017).

UAV legislation (Luppicini & So 2016; Stöcker et al. 2017) has been created in some countries and developed in others over the last decade. In a range of countries, UAVs are limited to dedicated or shared airspace with formal legislation limiting altitude, area of operation, UAV type, and formal UAV pilot training; thus, making use of UAVs for field observations in conservation is a complicated task. Field ecologist skill sets may be limited for deploying this tool effectively; a combination of UAV operations, photogrammetry software, and GIS-based data analysis skills are currently required to mine UAV data effectively. Future challenges include the automation of the range of this process in an interface that is user-friendly with technical analysis running in the background as well as providing an answer for the end-user, usable results, and results of value for the field biologist managing endangered species.

Ground-based monitoring of *O. leucoryx* in protected areas is commonly used as an observation and survey technique at ground level, and UAV surveys provide an efficient aerial alternative to some of these traditional survey techniques. The mostly desert terrain in the historical range of the species is relatively difficult to navigate; UAV surveys and the ability to extract additional animal-specific information may make this an attractive tool for future use.

6. Conclusions

Within the current legislative environment governing UAV flights, pre-flight assessments often require a tick-box approach where risks are considered subjectively and evaluated individually. This type of approach to wildlife surveys is problematic, as natural systems are dynamic and a "tick-box list" that considers all possible disturbance factors would be unfeasibly lengthy and complicated. For example, it would have to consider periods where there is an added environmental stress factor (Mulero-Pázmány et al. 2017) that may increase the sensitivity of the species e.g. droughts, and social dynamics like the breeding season or the species composition in the habitat under survey. We envision that future research on standardisation of UAV-based monitoring techniques is developed as a series of guidelines that need to be considered in context by a specialist in the habitat/system under survey, rather than a tick-box of parameters. Although the research indicates that ungulates could be monitored without inducing visible disturbance in the form of a moving response at an AGL of 60 m, we suggest that higher AGL, within the legal limits, should always be considered.

Creating an automated or semiautomated data extraction tool, in this case, an OBIA ruleset focus on the data extraction of adult *O. leucoryx* will assist field biologists during the technical data extraction process. Our study demonstrates that UAV-based monitoring combined with the OBIA ruleset to detect adult O. leucoryx can positively increase the accuracy of population estimates. The case study can be adapted to a range of species by extracting baseline coat reflection values and integrating the results in a similar process. The coat reflection data analysed to represent a specie's reflection signature can be added to the global species feature database. The ability to focus the automated detection to recognise species' reflection signatures can be a valuable tool in a range of wildlife studies. However, this method is a tool that performs well in optimal conditions for this toolset. The sampling of captive animals and applying the results to a free-living population allows for a non-invasive automated survey technique. The conditions may include meteorological, environmental, surveyed species, UAV sensor, flight plan, photogrammetric processing and the UAV pilot, which may all affect the data quality and performance of this toolset.

Islam et al. (2011) have suggested that historically, during post-release monitoring of *O. leucoryx*, the low-density distribution of these reintroduced animals results in a population size estimate with low accuracy. The DDCR with a single flagship species is dedicated in its efforts to protect *O. leucoryx*; however, there is a need to continuously monitor herd health, without the risk of adverse negative effects to the re-wilding strategy. UAV-acquired imagery proved to be an effective tool and can assist in providing critical information to reserve management in a non-invasive manner.

Future studies should aim to develop practical tools to support decision-making and focus on management-oriented results to assist in species and population management, especially in a delicate arid environment. Future studies on UAV-based zoometric data analysis are suggested to investigate more feature extraction like animal height, which has practical application in large mammal age classification. Furthermore, the height can be combined with the DP to calculate the volume and this may assist in individual animal body condition predictions from UAV imagery. This information will give protected area managers a better insight into the physical condition of individual animals and the overall herd especially during high-risk periods that may

include those after re-introductions, disease outbreaks and droughts. Moreover, the advantage of the imagery data is that it can be reprocessed and analysed in the future if needed, or if advances in analysis and software allow for more comprehensive data mining.

When a field biologist applies UAV-based imagery to conservation planning it requires the coming together of three skillsets: knowledge of the species in its environment, safe operations of drone hardware, and data interpretation. (De Kock & Gallacher 2016). In addition, ecological understanding of the species and the possible negative impact of this method are needed to select the optimum hardware, software and flight criteria to ensure high data quality and minimum environmental disturbance.

7. Supplementary Electronic Material

The data used in the research and R-markdown code is available at:
https://github.com/Meyerdk/Ungulate-UAV-monitoring
https://github.com/Meyerdk/Oryx_Reflective_Spectrometry

8. References

Allan BM, Nimmo DG, Ierodiaconou D, VanDerWal J, Koh LP, Ritchie EG. 2018. Futurecasting ecological research: the rise of technoecology. Ecosphere **9**:e02163.

Anderson K, Gaston KJ. 2013. Lightweight unmanned aerial vehicles will revolutionize spatial ecology. Frontiers in Ecology and the Environment **11**:138-146.

Andrews C. 2014. UAVs in the wild. Engineering & Technology **9**:33-35.

Beaver JT, Baldwin RW, Messinger M, Newbolt CH, Ditchkoff SS, Silman MR. 2020. Evaluating the Use of Drones Equipped with Thermal Sensors as an Effective Method for Estimating Wildlife. Wildlife Society Bulletin **44**:434-443.

Bennitt E, Bartlam-Brooks HL, Hubel TY, Wilson AM. 2019. Terrestrial mammalian wildlife responses to Unmanned Aerial Systems approaches. Scientific Reports **9**:1-10.

Berger-Wolf TY, Rubenstein DI, Stewart CV, Holmberg JA, Parham J, Menon S, Crall J, Van Oast J, Kiciman E, Joppa L. 2017. Wildbook: Crowdsourcing, computer vision, and data science for conservation. arXiv preprint arXiv:1710.08880.

Bertelsen MF, Mohammed O, Wang T, Manger PR, Scantlebury DM, Ismael K, Bennett NC, Alagaili A. 2017. The hairy lizard: heterothermia affects anaesthetic requirements in the Arabian oryx (Oryx leucoryx). Veterinary Anaesthesia and Analgesia.

Berteška T, Ruzgienė B. 2013. Photogrammetric mapping based on UAV imagery. Geodesy and Cartography **39**:158-163.

Bezryadin S, Bourov P, Ilinih D. 2007. Brightness calculation in digital image processing. Pages 10-15. International symposium on technologies for digital photo fulfillment. Society for Imaging Science and Technology.

Blaschke T. 2010. Object based image analysis for remote sensing. ISPRS Journal of Photogrammetry and Remote Sensing **65**:2-16.

Brambilla A, Brivio F. 2018. Assessing the effects of helicopter disturbance in a mountain ungulate on different time scales. Mammalian Biology **90**:30-37.

Burnett JD, Lemos L, Barlow D, Wing MG, Chandler T, Torres LG. 2018. Estimating morphometric attributes of baleen whales with photogrammetry from small UASs: A case study with blue and gray whales. Marine Mammal Science.

Buters TM, Bateman PW, Robinson T, Belton D, Dixon KW, Cross AT. 2019. Methodological ambiguity and inconsistency constrain unmanned aerial vehicles as a silver bullet for monitoring ecological restoration. Remote Sensing **11**:1180.

Butler J, Lane S, Chandler J. 1998. Assessment of DEM quality for characterizing surface roughness using close range digital photogrammetry. The Photogrammetric Record **16**:271-291.

Cai S, Liu D. 2013. A comparison of object-based and contextual pixel-based classifications using high and medium spatial resolution images. Remote Sensing Letters **4**:998-1007.

Casella E, Collin A, Harris D, Ferse S, Bejarano S, Parravicini V, Hench JL, Rovere A. 2017. Mapping coral reefs using consumer-grade drones and structure from motion photogrammetry techniques. Coral Reefs **36**:269-275.

Castellanos-Galindo GA, Casella E, Mejía-Rentería JC, Rovere A. 2019. Habitat mapping of remote coasts: Evaluating the usefulness of lightweight unmanned aerial vehicles for conservation and monitoring. Biological Conservation **239**:108282.

Chabot D. 2009. Systematic evaluation of a stock unmanned aerial vehicle (UAV) system for small-scale wildlife survey applications. McGill University.

Chretien LP, Theau J, Menard P. 2016. Visible and thermal infrared remote sensing for the detection of white-tailed deer using an unmanned aerial system. Wildlife Society Bulletin **40**:181-191.

Christiansen F, Vivier F, Charlton C, Ward R, Amerson A, Burnell S, Bejder L. 2018. Maternal body size and condition determine calf growth rates in southern right whales. Marine Ecology Progress Series **592**:267-281.

Christie KS, Gilbert SL, Brown CL, Hatfield M, Hanson L. 2016. Unmanned aircraft systems in wildlife research: current and future applications of a transformative technology. Frontiers in Ecology and the Environment **14**:241-251.

Colomina I, Molina P. 2014. Unmanned aerial systems for photogrammetry and remote sensing: A review. ISPRS Journal of Photogrammetry and Remote Sensing **92**:79-97.

Corcoran E, Winsen M, Sudholz A, Hamilton G. 2021. Automated detection of wildlife using drones: Synthesis, opportunities and constraints. Methods in Ecology and Evolution **12**:1103-1114.

Covidence. 2022. Covidence systematic review software.

Cukor J, Bartoska J, Rohla J, Sova J, Machalek A. 2019. Use of aerial thermography to reduce mortality of roe deer fawns before harvest. Peerj **7**.

Daly RH. 1988. The early stages of re-introduction of the Arabian oryx in Oman. Conservation and Biology of Desert Antelopes:14-17.

De Kock M, Al Qarqaz, M., Burns, K., Al Faqeer, M., Chege, S., Lloyd, C.,Gilbert, T., Alzahlawi, N., Al Kharusi, Y.H., Chuven, J., Javed, S., and Al Dhaheri, S. . 2018. Arabian Oryx Housing & Husbandry Guidelines. Environment Agency- Abu Dhabi (EAD), Abu Dhabi. **V.01**

De Kock ME. 2015. Using remote sensing data and weighted object-based image analysis to determine animal distribution. (Master's thesis, University of Salzburb - UNIGIS).

De Kock ME, Gallacher D. 2016. From drone data to decisions: Turning images into ecological answers. Innovation Arabia 2016.

de Kock ME, O'Donovan D, Khafaga T, Hejcmanova P. 2021a. Zoometric data extraction from drone imagery: the Arabian oryx (Oryx leucoryx). Environmental Conservation **48**:295-300.

de Kock ME, O'Donovan D, Khafaga T, Hejcmanová P. 2021b. Zoometric data extraction from drone imagery: the Arabian oryx (Oryx leucoryx). Environmental Conservation:1-6.

Dennis C. Duro SEF, Monique G. Dubé. 2012. A comparison of pixel-based and object-based image analysis with selected machine learning algorithms for the classification of agricultural landscapes using SPOT-5 HRG imagery. Remote Sensing of Environment **118**:259–272.

Dingle Robertson L, King DJ. 2011. Comparison of pixel-and object-based classification in land cover change mapping. International Journal of Remote Sensing **32**:1505-1529.

Ditmer MA, Vincent JB, Werden LK, Tanner JC, Laske TG, Iaizzo PA, Garshelis DL, Fieberg JR. 2015. Bears show a physiological but limited behavioral response to unmanned aerial vehicles. Current Biology **25**:2278-2283.

Duro DC, Coops NC, Wulder MA, Han T. 2007. Development of a large area biodiversity monitoring system driven by remote sensing. Progress in Physical Geography **31**:235-260.

El Alqamy H, Kiwan K, Al Daherie A. 2008. Arabian Oryx Project-UAE: One Year of Post Release Monitoring. Ninth AnnualSahelo-Saharan Interest Group meeting:3 - 19.

Fabris M, Pesci A. 2005. Automated DEM extraction in digital aerial photogrammetry: precisions and validation for mass movement monitoring. Annals of Geophysics.

Frid A, Dill L. 2002. Human-caused disturbance stimuli as a form of predation risk. Conservation ecology **6**.

Fritsch CJ, Downs CT. 2020. Evaluation of low-cost consumer-grade UAVs for conducting comprehensive high-frequency population censuses of hippopotamus populations. Conservation Science and Practice **2**.

Fritsch CJ, Hanekom C, Downs CT. 2021. Hippopotamus population trends in Ndumo Game Reserve, South Africa, from 1951 to 2021. Global Ecology and Conservation **32**.

Gonzalez F, Johnson S. 2017. Standard operating procedures for UAV or drone based monitoring of wildlife. Proceedings of UAS4RS 2017 (Unmanned Aircraft Systems for Remote Sensing).

Gonzalez LF, Montes GA, Puig E, Johnson S, Mengersen K, Gaston KJ. 2016. Unmanned Aerial Vehicles (UAVs) and artificial intelligence revolutionizing wildlife monitoring and conservation. Sensors **16**:97.

Groom G, Stjernholm M, Nielsen RD, Fleetwood A, Petersen IK. 2013. Remote sensing image data and automated analysis to describe marine bird distributions and abundances. Ecological Informatics **14**:2-8.

Gu H, Lyu X, Li Z, Shen S, Zhang F. 2017. Development and experimental verification of a hybrid vertical take-off and landing (VTOL) unmanned aerial vehicle (UAV). Pages 160-169. 2017 International Conference on Unmanned Aircraft Systems (ICUAS). IEEE.

Hahn N, Mwakatobe A, Konuche J, de Souza N, Keyyu J, Goss M, Chang'a A, Palminteri S, Dinerstein E, Olson D. 2017. Unmanned aerial vehicles mitigate human-elephant conflict on the borders of Tanzanian Parks: a case study. Oryx **51**:513-516.

Harrison DL, Bates PJJ 1991. The mammals of Arabia. Harrison Zoological Museum.

Hartmann WL, Fishlock V, Leslie A. 2021. First guidelines and suggested best protocol for surveying African elephants (Loxodonta africana) using a drone. Koedoe **63**.

Hatwood M. 2017. Arabian oryx , back from the brink, thanks to zoos. AZA, Antelope and Giraffe TAG.

Henderson D. 1974. Were they the last Arabian oryx? Oryx **12**:347-350.

Herold M, Roberts DA, Gardner ME, Dennison PE. 2004. Spectrometry for urban area remote sensing—Development and analysis of a spectral library from 350 to 2400 nm. Remote sensing of environment **91**:304-319.

Hodgson JC, Baylis SM, Mott R, Herrod A, Clarke RH. 2016. Precision wildlife monitoring using unmanned aerial vehicles. Scientific reports **6**:22574.

Hodgson JC, Koh LP. 2016. Best practice for minimising unmanned aerial vehicle disturbance to wildlife in biological field research. Current Biology **26**:R404-R405.

Horton TW, Hauser N, Cassel S, Klaus KF, Fettermann T, Key N. 2019. Doctor drone: Non-invasive measurement of humpback whale vital signs using unoccupied aerial system infrared thermography. Frontiers in Marine Science **6**:466.

Hu JB, Wu XM, Dai MX. 2020. Estimating the population size of migrating Tibetan antelopes Pantholops hodgsonii with unmanned aerial vehicles. Oryx **54**:101-109.

Ihaka R, Murrell P, Hornik K, Fisher J. 2019. 'colorspace' : A Toolbox for Manipulating and Assessing Colors and Palettes.

Inoue S, Yamamoto S, Ringhofer M, Mendonca RS, Pereira C, Hirata S. 2019. Spatial positioning of individuals in a group of feral horses: a case study using drone technology. Mammal Research **64**:249-259.

Islam MZ-u, Ismail K, Boug A. 2011. Restoration of the endangered Arabian Oryx Oryx leucoryx, Pallas 1766 in Saudi Arabia lessons learnt from the twenty years of re-introduction in

arid fenced and unfenced protected areas: (Mammalia: Artiodactyla). Zoology in the Middle East **54**:125-140.

Islam MZU, & Knutson, C. 2008. A plan to reduce the risk of mass mortalities of reintroduced animals in the Mahazat as-Sayd Protected Area in Saudi Arabia.

Ito TY, Miyazaki A, Koyama LA, Kamada K, Nagamatsu D. 2022. Antler detection from the sky: deer sex ratio monitoring using drone-mounted thermal infrared sensors. Wildlife Biology.

IUCN. 2021. The IUCN Red List of Threatened Species. Version 2021-3. https://www.iucnredlist.org. Accessed on [21 April 2022].

Jewell ZOE. 2013. Effect of Monitoring Technique on Quality of Conservation Science. Conservation Biology **27**:501-508.

JONES IV GP, Pearlstine LG, Percival HF. 2006. An assessment of small unmanned aerial vehicles for wildlife research. Wildlife Society Bulletin **34**:750-758.

Kellenberger B, Volpi M, Tuia D. 2017. Fast animal detection in UAV images using convolutional neural networks. Pages 866-869. 2017 IEEE international geoscience and remote sensing symposium (IGARSS). IEEE.

Kim M, Chung OS, Lee JK. 2021. A Manual for Monitoring Wild Boars (Sus scrofa) Using Thermal Infrared Cameras Mounted on an Unmanned Aerial Vehicle (UAV). Remote Sensing **13**.

Koski W, Rugh D, Punt A, Zeh J. 2006. An approach to minimise bias in estimation of the length-frequency distribution of bowhead whales (Balaena mysticetus) from aerial photogrammetric data. Journal of Cetacean Research and Management **8**:45.

Krause DJ, Hinke JT, Perryman WL, Goebel ME, LeRoi DJ. 2017. An accurate and adaptable photogrammetric approach for estimating the mass and body condition of pinnipeds using an unmanned aerial system. PloS one **12**:e0187465.

Kuhn M. 2019. The CARET Package.

Laliberte AS, Herrick JE, Rango A, Winters C. 2010. Acquisition, Orthorectification, and Object-based Classification of Unmanned Aerial Vehicle (UAV) Imagery for Rangeland Monitoring. Photogrammetric Engineering & Remote Sensing **76**:661-672.

LeCun Y, Bengio Y, Hinton G. 2015. Deep learning. nature **521**:436.

Leyequien E, Verrelst J, Slot M, Schaepman-Strub G, Heitkönig IMA, Skidmore A. 2007. Capturing the fugitive: Applying remote sensing to terrestrial animal distribution and diversity. International Journal of Applied Earth Observation and Geoinformation **9**:1-20.

Lhoest S, Linchant J, Quevauvillers S, Vermeulen C, Lejeune P, Wg Iii 2 Point Cloud Proc WGVIIITDI, Sensors WGVIISRI. 2015. HOW MANY HIPPOS (HOMHIP): ALGORITHM FOR AUTOMATIC COUNTS OF ANIMALS WITH INFRA-RED THERMAL IMAGERY FROM UAV. ISPRS Geospatial Week **40-3**:355-362.

Liang YJ, Kuo H, Giordano AJ, Pei KJC. 2020. Seasonal variation in herd composition of the Formosan sika deer (Cervus nippon taiouanus) in a forest-grassland mosaic habitat of southern Taiwan. Global Ecology and Conservation **24**.

Linchant J, Lhoest S, Quevauvillers S, Lejeune P, Vermeulen C, Ngabinzeke JS, Belanganayi BL, Delvingt W, Bouche P. 2018a. UAS imagery reveals new survey opportunities for counting hippos. Plos One **13**.

Linchant J, Lhoest S, Quevauvillers S, Lejeune P, Vermeulen C, Semeki Ngabinzeke J, Luse Belanganayi B, Delvingt W, Bouché P. 2018b. UAS imagery reveals new survey opportunities for counting hippos. PLoS One **13**:e0206413.

Linchant J, Lhoest S, Quevauvillers S, Semeki J, Lejeune P, Vermeulen C, Wg Iii 2 Point Cloud Proc WGVIIITDI, Sensors WGVIISRI. 2015a. WIMUAS: DEVELOPING A TOOL TO REVIEW WILDLIFE DATA FROM VARIOUS UAS FLIGHT PLANS. ISPRS Geospatial Week **40-3**:379-384.

Linchant J, Lisein J, Semeki J, Lejeune P, Vermeulen C. 2015b. Are unmanned aircraft systems (UAS s) the future of wildlife monitoring? A review of accomplishments and challenges. Mammal Review **45**:239-252.

Linchant J, Lisein J, Semeki J, Lejeune P, Vermeulen C. 2015c. Are unmanned aircraft systems (UASs) the future of wildlife monitoring? A review of accomplishments and challenges. Mammal Review **45**:239-252.

Luppicini R, So A. 2016. A technoethical review of commercial drone use in the context of governance, ethics, and privacy. Technology in Society **46**:109-119.

Maeda T, Sueur C, Hirata S, Yamamoto S. 2021. Behavioural synchronization in a multilevel society of feral horses. Plos One **16**.

Maire F, Alvarez LM, Hodgson A. 2015. Automating marine mammal detection in aerial images captured during wildlife surveys: a deep learning approach. Pages 379-385. Australasian Joint Conference on Artificial Intelligence. Springer.

Mallon DP, Price MRS. 2013. The fall of the wild. Oryx **47**:467-468.

Malo JE, Acebes P, Traba J. 2011. Measuring ungulate tolerance to human with flight distance: a reliable visitor management tool? Biodiversity and Conservation **20**:3477-3488.

Mangewa LJ, Ndakidemi PA, Munishi LK. 2019. Integrating UAV technology in an ecological monitoring system for community wildlife management areas in Tanzania. Sustainability **11**:6116.

Mathworks. 2020. Convert CIE 1976 L*a*b* to RGB. User Guide (R2019a) **Retrieved March 27, 2020 from: https://uk.mathworks.com/help/images/ref/lab2rgb.html**.

McMahon MC, Ditmer MA, Isaac EJ, Moore SA, Forester JD. 2021. Evaluating Unmanned Aerial Systems for the Detection and Monitoring of Moose in Northeastern Minnesota. Wildlife Society Bulletin **45**:312-324.

Melchor-Martínez EM, Macias-Garbett R, Malacara-Becerra A, Iqbal HM, Sosa-Hernández JE, Parra-Saldívar R. 2021. Environmental impact of emerging contaminants from battery waste: A mini review. Case Studies in Chemical and Environmental Engineering **3**:100104.

Mulero-Pazmany M, Barasona JA, Acevedo P, Vicente J, Negro JJ. 2015. Unmanned Aircraft Systems complement biologging in spatial ecology studies. Ecology and Evolution **5**:4808-4818.

Mulero-Pázmány M, Jenni-Eiermann S, Strebel N, Sattler T, Negro JJ, Tablado Z. 2017. Unmanned aircraft systems as a new source of disturbance for wildlife: A systematic review. PloS one **12**:e0178448.

Mulero-Pazmany M, Stolper R, van Essen LD, Negro JJ, Sassen T. 2014. Remotely Piloted Aircraft Systems as a Rhinoceros Anti-Poaching Tool in Africa. Plos One **9**.

Myburgh A, Botha H, Downs CT, Woodborne S. 2021a. The application and limitations of a low-cost UAV platform and open-source software combination for ecological mapping and monitoring. African Journal of Wildlife Research **51**:166-177.

Myburgh A, Botha H, Downs CT, Woodborne SM. 2021b. The application and limitations of a low-cost UAV platform and open-source software combination for ecological mapping and monitoring. African Journal of Wildlife Research **51**:166-177.

Natick M. 2019. MATLAB R2019a Update 2 (9.6.0.1114505). The MathWorks Inc.

O'Donovan D, Bailey T. 2006. Restraint of Arabian oryx (Oryx leucoryx) in Dubai, United Arab Emirates using a mobile raceway. Conference of the International Congress of Zookeepers: Gold Coast, Australia. **2**.

Obermoller TR, Norton AS, Michel ES, Haroldson BS. 2021. Use of Drones With Thermal Infrared to Locate White-tailed Deer Neonates for Capture. Wildlife Society Bulletin **45**:682-689.

Ostrowski S, Bedin E, Lenain DM, Abuzinada AH. 1998. Ten years of Arabian oryx conservation breeding in Saudi Arabia–achievements and regional perspectives. Oryx **32**:209-222.

Pathak AR, Pandey M, Rautaray S. 2018. Application of deep learning for object detection. Procedia computer science **132**:1706-1717.

Petso T, Jamisola RS, Mpoeleng D, Bennitt E, Mmereki W. 2021. Automatic animal identification from drone camera based on point pattern analysis of herd behaviour. Ecological Informatics **66**.

Pradeep P, Park SG, Wei P. 2018. Trajectory optimization of multirotor agricultural UAVs. Pages 1-7. 2018 IEEE Aerospace Conference. IEEE.

Preston TM, Wildhaber ML, Green NS, Albers JL, Debenedetto GP. 2021. Enumerating White-Tailed Deer Using Unmanned Aerial Vehicles. Wildlife Society Bulletin **45**:97-108.

Price MRS 1989. Animal reintroductions: the Arabian oryx in Oman. Cambridge University Press.

R_Core_Team. 2013. R: A language and environment for statistical computing. Foundation for Statistical Computing , Vienna, Austria.

Rahman DA, Sitorus ABY, Condro AA. 2022. From Coastal to Montane Forest Ecosystems, Using Drones for Multi-Species Research in the Tropics. Drones **6**.

Rebolo-Ifrán N, Grilli MG, Lambertucci SA. 2019. Drones as a threat to wildlife: YouTube complements science in providing evidence about their effect. Environmental Conservation **46**:205-210.

Reinhard E, Stark M, Shirley P, Ferwerda J. 2002. Photographic tone reproduction for digital images. Pages 267-276. Proceedings of the 29th annual conference on Computer graphics and interactive techniques.

Rey N, Volpi M, Joost S, Tuia D. 2017. Detecting animals in African Savanna with UAVs and the crowds. Remote Sensing of Environment **200**:341-351.

Riede K. 2000. Conservation and modern information technologies: the global register of migratory species (GROMS).

Roberts B, Neal M, Snooke N, Labrosse F, Curteis T, Fraser M. 2020. A bespoke low-cost system for radio tracking animals using multi-rotor and fixed-wing unmanned aerial vehicles. Methods in Ecology and Evolution **11**:1427-1433.

Ryu B, Kim K, Ha Y, Bae J, Lee S, Song J, Lee K, Lee J, Kim K, Kim H. 2014. New RGB primary for various multimedia systems. Journal of Information Display **15**:65-70.

Schiffman R. 2014. WILDLIFE CONSERVATION Drones Flying High as New Tool For Field Biologists. Science **344**:459-459.

Schroeder NM, Panebianco A. 2021. Sociability strongly affects the behavioural responses of wild guanacos to drones. Scientific Reports **11**.

Seddon PJ, Ismail K, Shobrak M, Ostrowski S, Magin C. 2003. A comparison of derived population estimate, mark-resighting and distance sampling methods to determine the population size of a desert ungulate, the Arabian oryx. Oryx **37**:286-294.

Shen H, Zhang Y, Wu Y. 2020. A comparative study on air transport safety of lithium-ion batteries with different SOCs. Applied Thermal Engineering **179**:115679.

Simkins G. 2007. Re-introduction of Arabian Oryx into the Dubai Desert Conservation Reserve, Dubai, UAE Dubai Desert Conservation Reserve.

Singleton PH, Lehmkuhl JF, Gaines WL, Graham SA. 2010. Barred Owl Space Use and Habitat Selection in the Eastern Cascades, Washington. The Journal of Wildlife Management **74**:285-294.

Spalton JA, Lawerence M, Brend S. 1999. Arabian oryx reintroduction in Oman: successes and setbacks. Oryx **33**:168-175.

Stankowich T. 2008. Ungulate flight responses to human disturbance: a review and meta-analysis. Biological conservation **141**:2159-2173.

Stöcker C, Bennett R, Nex F, Gerke M, Zevenbergen J. 2017. Review of the current state of UAV regulations. Remote sensing **9**:459.

Stokes M. 1996. A standard default color space for the internet-srgb. http://www. color. org/contrib/sRGB. html.

Su X, Dong S, Liu S, Cracknell AP, Zhang Y, Wang X, Liu G. 2018a. Using an unmanned aerial vehicle (UAV) to study wild yak in the highest desert in the world. International Journal of Remote Sensing:1-14.

Su XK, Dong SK, Liu SL, Cracknell AP, Zhang Y, Wang XX, Liu GH. 2018b. Using an unmanned aerial vehicle (UAV) to study wild yak in the highest desert in the world. International Journal of Remote Sensing **39**:5490-5503.

Süsstrunk S, Buckley R, Swen S. 1999. Standard RGB color spaces. Pages 127-134. Color and Imaging Conference. Society for Imaging Science and Technology.

Tarakini T, Mundy P, Tarakini T-UCB, Crosmary W-G-UCB, Fritz H-UCB, Crosmary W-G. 2014. Flight behavioural responses to sport hunting by two African herbivores. South African Journal of Wildlife Research-24-month delayed open access **44**:76-83.

Tear TH, Mosley JC, Ables ED. 1997. Landscape-scale foraging decisions by reintroduced Arabian oryx. The Journal of wildlife management:1142-1154.

Torres LG, Nieukirk SL, Lemos L, Chandler TE. 2018. Drone up! Quantifying whale behavior from a new perspective improves observational capacity. Frontiers in Marine Science **5**:319.

Tuia D, Kellenberger B, Beery S, Costelloe BR, Zuffi S, Risse B, Mathis A, Mathis MW, van Langevelde F, Burghardt T. 2022. Perspectives in machine learning for wildlife conservation. Nature communications **13**:1-15.

Watts AC, Perry JH, Smith SE, Burgess MA, Wilkinson BE, Szantoi Z, Ifju PG, Percival HF. 2010. Small unmanned aircraft systems for low-altitude aerial surveys. Journal of Wildlife Management **74**:1614-1619.

Weller H. 2019. colordistance: Distance Metrics for Image Color Similarity.

Wickham H. 2016. ggplot2: Elegant Graphics for Data Analysis. Springer-Verlag New York.

Wilson A, Price MS. 1994. Reintroduction as a reason for captive breeding. Pages 243-264. Creative conservation. Springer.

Witczuk J, Pagacz S, Zmarz A, Cypel M. 2018. Exploring the feasibility of unmanned aerial vehicles and thermal imaging for ungulate surveys in forests - preliminary results. International Journal of Remote Sensing **39**:5504-5521.

Yamashita T, Gaynor KM, Kioko J, Brashares J, Kiffner C. 2018. Antipredator behaviour of African ungulates around human settlements. African Journal of Ecology **56**:528-536.

Yu Q, Gong P, Clinton N, Biging G, Kelly M, Schirokauer D. 2006. Object-based detailed vegetation classification with airborne high spatial resolution remote sensing imagery. Photogrammetric Engineering & Remote Sensing **72**:799-811.

Zafar-Ul Islam M, Ismail, K., & Boug, A. . 2011. Restoration of the endangered Arabian Oryx Oryx leucoryx. Pallas **1766**:125-140.

Zhang J, Hu J, Lian J, Fan Z, Ouyang X, Ye W. 2016. Seeing the forest from drones: Testing the potential of lightweight drones as a tool for long-term forest monitoring. Biological Conservation **198**:60-69.

Zheng X, Kellenberger B, Gong R, Hajnsek I, Tuia D. 2021. Self-Supervised Pretraining and Controlled Augmentation Improve Rare Wildlife Recognition in UAV Images. Pages 732-741. Proceedings of the IEEE/CVF International Conference on Computer Vision.

Zhou ML, Elmore JA, Samiappan S, Evans KO, Pfeiffer MB, Blackwell BF, Iglay RB. 2021. Improving Animal Monitoring Using Small Unmanned Aircraft Systems (sUAS) and Deep Learning Networks. Sensors **21**.

9. Appendixes

Appendix 1 Supplementary Table 4: UAV-based ungulate monitoring, which included 121 flights in eight countries and 17 ungulate species

Date	Country	Type	Species_2	UAV	UAV_size	Area	Flight_time	Alt_Max	Speed	Disturbance
20/01/2020	Africa	Census	*Bos taurus*	Multi Rotor	>1500g	1 - 2km2	16.21	60	20	N
26/07/2018	Middle East	Census	*Camelus dromedarius*	Fixed Wing	>1500g	2 - 5 km2	21.43	80	26	N
01/08/2018	Africa	Census	*Nanger dama*	Fixed Wing	>1500g	> 5 km2	51.7	120	26	N
30/06/2019	Africa	Census	*Oryx dammah*	Fixed Wing	>1500g	2 - 5 km2	27.31	120	26	N
30/06/2019	Africa	Census	*Oryx dammah*	Fixed Wing	>1500g	2 - 5 km2	18.41	120	26	N
30/07/2019	Africa	Census	*Oryx dammah, Gazella dorcas*	Fixed Wing	>1500g	> 5 km2	31.45	120	26	N
01/07/2019	Africa	Census	*Oryx dammah, Gazella dorcas*	Fixed Wing	>1500g	> 5 km2	30.03	120	26	N
01/07/2019	Africa	Census	*Oryx dammah, Gazella dorcas*	Fixed Wing	>1500g	> 5 km2	45.22	120	26	N
01/07/2019	Africa	Census	*Oryx dammah, Gazella dorcas*	Fixed Wing	>1500g	> 5 km2	31.33	120	26	N
01/07/2019	Africa	Census	*Oryx dammah, Gazella dorcas*	Fixed Wing	>1500g	1 - 2km2	16.19	120	26	N
02/07/2019	Africa	Census	*Oryx dammah, Gazella dorcas*	Fixed Wing	>1500g	1 - 2km2	12.51	120	26	N
02/07/2019	Africa	Census	*Oryx dammah, Gazella dorcas*	Fixed Wing	>1500g	2 - 5 km2	29.16	120	26	N
02/07/2019	Africa	Census	*Oryx dammah, Gazella dorcas*	Fixed Wing	>1500g	2 - 5 km2	34.2	120	26	N
02/07/2019	Africa	Census	*Oryx dammah, Gazella dorcas*	Fixed Wing	>1500g	2 - 5 km2	27.52	120	26	N
03/07/2019	Africa	Census	*Oryx dammah, Gazella dorcas*	Fixed Wing	>1500g	2 - 5 km2	31.44	120	26	N
03/07/2019	Africa	Census	*Oryx dammah, Gazella dorcas*	Fixed Wing	>1500g	2 - 5 km2	32.2	120	26	N
03/07/2019	Africa	Census	*Oryx dammah, Gazella dorcas*	Fixed Wing	>1500g	2 - 5 km2	23.57	120	26	N
28/01/2018	Middle East	Census	*Oryx leucoryx*	Multi Rotor	>1500g	1 - 2km2	12.38	75	16	N
01/08/2018	Africa	Census	*Camelus dromedarius, Gazella dorcas, Nanger dama*	Fixed Wing	>1500g	> 5 km2	36.38	120	26	N
02/08/2018	Africa	Census	*Camelus dromedarius, Gazella dorcas, Nanger dama*	Fixed Wing	>1500g	> 5 km2	52.01	120	26	N
02/08/2018	Africa	Census	*Camelus dromedarius, Gazella dorcas, Nanger dama*	Fixed Wing	>1500g	> 5 km2	37.16	120	26	N

02/08/2018	Africa	Census	*Camelus dromedarius, Gazella dorcas, Nanger dama*	Fixed Wing	>1500g	> 5 km2	40.25	120	26	N
02/08/2018	Africa	Census	*Camelus dromedarius, Gazella dorcas, Nanger dama*	Fixed Wing	>1500g	> 5 km2	60.22	120	26	N
02/08/2018	Africa	Census	*Camelus dromedarius, Gazella dorcas, Nanger dama*	Fixed Wing	>1500g	> 5 km2	47.43	120	26	N
04/08/2018	Africa	Census	*Camelus dromedarius, Gazella dorcas, Nanger dama*	Fixed Wing	>1500g	> 5 km2	51.11	120	26	N
04/08/2018	Africa	Census	*Camelus dromedarius, Gazella dorcas, Nanger dama*	Fixed Wing	>1500g	> 5 km2	46.18	120	26	N
04/08/2018	Africa	Census	*Camelus dromedarius, Gazella dorcas, Nanger dama*	Fixed Wing	>1500g	> 5 km2	31.41	120	26	N
04/08/2018	Africa	Census	*Camelus dromedarius, Gazella dorcas, Nanger dama*	Fixed Wing	>1500g	> 5 km2	44.54	120	26	N
07/08/2018	Africa	Census	*Camelus dromedarius, Gazella dorcas*	Fixed Wing	>1500g	> 5 km2	44.58	120	26	N
07/08/2018	Africa	Census	*Camelus dromedarius, Gazella dorcas*	Fixed Wing	>1500g	> 5 km2	45.17	120	26	N
07/08/2018	Africa	Census	*Camelus dromedarius, Gazella dorcas*	Fixed Wing	>1500g	> 5 km2	44.36	120	26	N
07/08/2018	Africa	Census	*Camelus dromedarius, Gazella dorcas*	Fixed Wing	>1500g	> 5 km2	40.56	120	26	N
08/08/2018	Africa	Census	*Camelus dromedarius, Gazella dorcas*	Fixed Wing	>1500g	> 5 km2	55.32	120	26	N
08/08/2018	Africa	Census	*Camelus dromedarius, Gazella dorcas*	Fixed Wing	>1500g	> 5 km2	39.28	120	26	N
08/08/2018	Africa	Census	*Camelus dromedarius, Gazella dorcas*	Fixed Wing	>1500g	> 5 km2	45.55	120	26	N
08/08/2018	Africa	Census	*Camelus dromedarius, Gazella dorcas*	Fixed Wing	>1500g	> 5 km2	43.03	120	26	N
08/08/2018	Africa	Census	*Camelus dromedarius, Gazella dorcas*	Fixed Wing	>1500g	2 - 5 km2	33.04	120	26	N
28/01/2018	Middle East	Targeted	*Oryx leucoryx*	Multi Rotor	>1500g	< 1km2	6.56	100	16	N
09/12/2017	Africa	Census	*Taurotragus derbianus derbianus*	Multi Rotor	1000g - 1500g	2 - 5 km2	25.11	100	22	N
09/12/2017	Africa	Census	*Taurotragus derbianus derbianus*	Multi Rotor	1000g - 1500g	< 1km2	4.22	100	22	N
09/12/2017	Africa	Census	*Taurotragus derbianus derbianus*	Multi Rotor	1000g - 1500g	2 - 5 km2	27.05	100	22	N
09/12/2017	Africa	Census	*Taurotragus derbianus derbianus*	Multi Rotor	1000g - 1500g	1 - 2km2	24.5	100	22	N

Date	Region	Type	Species	Aircraft	Weight / Area		Val1	Val2	Val3	Flag
09/12/2017	Africa	Census	*Taurotragus derbianus derbianus*	Multi Rotor	1000g - 1500g	1 - 2km2	14.18	100	22	N
10/12/2017	Africa	Census	*Taurotragus derbianus derbianus*	Multi Rotor	1000g - 1500g	1 - 2km2	22.14	100	12	N
10/12/2017	Africa	Census	*Taurotragus derbianus derbianus*	Multi Rotor	1000g - 1500g	1 - 2km2	17.39	100	12	N
10/12/2017	Africa	Census	*Ceratotherium simum*	Multi Rotor	1000g - 1500g	1 - 2km2	20.55	100	12	N
12/12/2017	Africa	Census	*Taurotragus derbianus derbianus*	Multi Rotor	1000g - 1500g	1 - 2km2	18.31	100	20	N
29/05/2019	Africa	Census	*Oryx gazella*	Multi Rotor	1000g - 1500g	1 - 2km2	14.17	115	22	N
08/06/2019	Africa	Census	*Oryx gazella, Equus burchelli*	Multi Rotor	1000g - 1500g	1 - 2km2	17.2	120	22	N
05/09/2016	Asia	Census	*Sus barbatus*	Multi Rotor	1000g - 1500g	1 - 2km2	23.07	100	22	N
05/09/2016	Asia	Census	*Sus barbatus*	Multi Rotor	1000g - 1500g	1 - 2km2	17.19	100	22	N
06/09/2016	Asia	Census	*Sus barbatus*	Multi Rotor	1000g - 1500g	1 - 2km2	21.53	100	22	N
06/09/2016	Asia	Census	*Sus barbatus*	Multi Rotor	1000g - 1500g	< 1km2	4.22	100	22	N
07/09/2016	Asia	Census	*Rusa unicolor*	Multi Rotor	1000g - 1500g	1 - 2km2	18.08	80	22	N
07/09/2016	Asia	Census	*Rusa unicolor*	Multi Rotor	1000g - 1500g	< 1km2	7.11	50	22	N
20/09/2016	Middle East	Census	*Oryx leucoryx*	Multi Rotor	1000g - 1500g	1 - 2km2	13.36	110	20	N
15/02/2017	Middle East	Census	*Oryx leucoryx*	Multi Rotor	1000g - 1500g	1 - 2km2	20.22	100	20	N
04/03/2017	Middle East	Census	*Oryx leucoryx, Gazella marica*	Multi Rotor	1000g - 1500g	1 - 2km2	21.2	90	20	N
28/05/2017	Middle East	Census	*Oryx leucoryx*	Multi Rotor	1000g - 1500g	1 - 2km2	22.05	95	20	N
28/05/2017	Middle East	Census	*Oryx leucoryx*	Multi Rotor	1000g - 1500g	1 - 2km2	28.01	95	20	N
04/10/2017	Middle East	Census	*A Oryx, Mountain Gazelle*	Multi Rotor	1000g - 1500g	1 - 2km2	23.16	100	20	N
13/11/2017	Middle East	Census	*Oryx leucoryx*	Multi Rotor	1000g - 1500g	1 - 2km2	17.14	100	20	N
10/01/2018	Middle East	Census	*Oryx leucoryx*	Multi Rotor	1000g - 1500g	1 - 2km2	15.08	100	20	N
11/01/2018	Middle East	Census	*Oryx leucoryx*	Multi Rotor	1000g - 1500g	1 - 2km2	13.49	100	20	N
04/03/2018	Middle East	Census	*Oryx leucoryx*	Multi Rotor	1000g - 1500g	1 - 2km2	11.38	100	20	N
04/03/2018	Middle East	Census	*Oryx leucoryx*	Multi Rotor	1000g - 1500g	< 1km2	2.58	90	20	N
04/03/2018	Middle East	Census	*Oryx leucoryx*	Multi Rotor	1000g - 1500g	< 1km2	3.11	90	20	N
04/03/2018	Middle East	Census	*Oryx leucoryx*	Multi Rotor	1000g - 1500g	< 1km2	3.24	90	20	N
18/03/2018	Middle East	Census	*Oryx leucoryx*	Multi Rotor	1000g - 1500g	1 - 2km2	18.06	95	20	N
18/03/2018	Middle East	Census	*Oryx leucoryx*	Multi Rotor	1000g - 1500g	1 - 2km2	10.25	75	20	N
18/03/2018	Middle East	Census	*Oryx leucoryx*	Multi Rotor	1000g - 1500g	1 - 2km2	12.36	75	20	N
10/09/2018	Middle East	Census	*Oryx leucoryx, Gazella marica*	Multi Rotor	1000g - 1500g	1 - 2km2	22.14	100	20	N
11/09/2018	Middle East	Census	*Oryx leucoryx, Gazella marica*	Multi Rotor	1000g - 1500g	1 - 2km2	13.42	100	20	N

14/10/2018	Middle East	Census	*Oryx leucoryx, Gazella marica*	Multi Rotor	1000g - 1500g	1 - 2km2	22.58	95	20	N
21/10/2018	Middle East	Census	*Oryx leucoryx, Gazella marica*	Multi Rotor	1000g - 1500g	1 - 2km2	16.12	95	20	N
04/11/2018	Middle East	Census	*Oryx leucoryx, Gazella marica*	Multi Rotor	1000g - 1500g	1 - 2km2	22.45	100	20	N
11/11/2018	Middle East	Census	*Oryx leucoryx*	Multi Rotor	1000g - 1500g	1 - 2km2	13.2	95	20	N
13/02/2019	Africa	Census	*Nanger dama*	Multi Rotor	250g - 1000g	1 - 2km2	20.02	100	23	N
08/11/2021	Africa	Census	*Nanger dama*	Multi Rotor	250g - 1000g	1 - 2km2	21.08	100	23	N
17/11/2020	Africa	Census	*Camelus dromedarius, Gazella dorcas, Phacochoerus africanus*	Multi Rotor	250g - 1000g	1 - 2km2	14.19	80	23	N
17/11/2021	Africa	Census	*Camelus dromedarius, Gazella dorcas, Phacochoerus africanus*	Multi Rotor	250g - 1000g	1 - 2km2	16.44	90	23	N
18/11/2022	Africa	Census	*Camelus dromedarius, Gazella dorcas, Phacochoerus africanus*	Multi Rotor	250g - 1000g	1 - 2km2	15.21	80	20	N
18/11/2023	Africa	Census	*Camelus dromedarius, Gazella dorcas, Phacochoerus africanus*	Multi Rotor	250g - 1000g	1 - 2km2	20.47	100	22	N
18/06/2020	Africa	Targeted	*Oreotragus oreotragus, Philantomba monticola, Choeropsis liberiensis*	Multi Rotor	>1500g	1 - 2km2	23.45	50	12	N
12/12/2017	Africa	Targeted	*Taurotragus derbianus derbianus*	Multi Rotor	1000g - 1500g	< 1km2	5.18	50	12	Y
13/12/2017	Africa	Targeted	*Taurotragus derbianus derbianus*	Multi Rotor	1000g - 1500g	< 1km2	6.25	75	12	N
16/02/2018	Africa	Targeted	*Taurotragus derbianus derbianus*	Multi Rotor	1000g - 1500g	< 1km2	1.04	50	10	N
16/02/2018	Africa	Targeted	*Taurotragus derbianus derbianus*	Multi Rotor	1000g - 1500g	< 1km2	3.28	50	5	Y
17/02/2018	Africa	Targeted	*ragelaphus scriptus*	Multi Rotor	1000g - 1500g	< 1km2	2.23	50	10	N
17/02/2018	Africa	Targeted	*Giraffa camelopardalis*	Multi Rotor	1000g - 1500g	< 1km2	1.45	50	10	N
18/02/2018	Africa	Targeted	*Taurotragus derbianus derbianus*	Multi Rotor	1000g - 1500g	< 1km2	1.49	45	11	N
18/02/2018	Africa	Targeted	*Taurotragus derbianus derbianus*	Multi Rotor	1000g - 1500g	< 1km2	3.01	45	10	N
18/02/2018	Africa	Targeted	*Taurotragus derbianus derbianus*	Multi Rotor	1000g - 1500g	< 1km2	0.33	45	10	N
18/02/2018	Africa	Targeted	*Taurotragus derbianus derbianus*	Multi Rotor	1000g - 1500g	< 1km2	3.22	60	10	N
18/02/2018	Africa	Targeted	*Taurotragus derbianus derbianus*	Multi Rotor	1000g - 1500g	< 1km2	1.01	45	10	N
18/02/2018	Africa	Targeted	*Taurotragus derbianus derbianus*	Multi Rotor	1000g - 1500g	< 1km2	2	45	14	N

Date	Region	Type	Species	Drone	Weight	Area				
18/02/2018	Africa	Targeted	*Taurotragus derbianus derbianus*	Multi Rotor	1000g - 1500g	< 1km2	9.21	60	16	N
18/02/2018	Africa	Targeted	*Taurotragus derbianus derbianus*	Multi Rotor	1000g - 1500g	< 1km2	0.54	60	18	N
19/02/2018	Africa	Targeted	*Taurotragus derbianus derbianus*	Multi Rotor	1000g - 1500g	< 1km2	7.28	60	16	N
19/02/2018	Africa	Targeted	*Taurotragus derbianus derbianus*	Multi Rotor	1000g - 1500g	< 1km2	1.42	60	14	N
19/02/2018	Africa	Targeted	*Taurotragus derbianus derbianus*	Multi Rotor	1000g - 1500g	< 1km2	1.11	50	16	Y
19/02/2018	Africa	Targeted	*Taurotragus derbianus derbianus*	Multi Rotor	1000g - 1500g	< 1km2	0.47	50	16	Y
19/02/2018	Africa	Targeted	*Taurotragus derbianus derbianus*	Multi Rotor	1000g - 1500g	< 1km2	1.42	50	16	Y
19/02/2018	Africa	Targeted	*Taurotragus derbianus derbianus*	Multi Rotor	1000g - 1500g	< 1km2	0.54	50	16	N
19/02/2018	Africa	Targeted	*Taurotragus derbianus derbianus*	Multi Rotor	1000g - 1500g	< 1km2	1.11	50	12	N
19/02/2018	Africa	Targeted	*Taurotragus derbianus derbianus, Giraffa camelopardalis*	Multi Rotor	1000g - 1500g	< 1km2	2.02	45	12	N
04/03/2018	Middle East	Targeted	*Oryx leucoryx*	Multi Rotor	1000g - 1500g	< 1km2	6.18	50	8	N
09/06/2018	Middle East	Targeted	*Nanger dama*	Multi Rotor	1000g - 1500g	< 1km2	5.45	40	12	N
10/06/2018	Middle East	Targeted	*Nanger dama*	Multi Rotor	1000g - 1500g	< 1km2	6.54	60	12	N
22/07/2018	Africa	Census	*Nanger dama*	Multi Rotor	250g - 1000g	1 - 2km2	15.17	60	15	Y
22/07/2018	Africa	Census	*Nanger dama*	Multi Rotor	250g - 1000g	1 - 2km2	21.11	80	18	N
11/03/2019	Africa	Census	*Giraffa camelopardalis*	Multi Rotor	250g - 1000g	1 - 2km2	9.56	60	15	Y
13/04/2019	Africa	Census	*Giraffa camelopardalis*	Multi Rotor	250g - 1000g	1 - 2km2	14.32	80	15	Y
03/08/2019	Africa	Census	*Giraffa camelopardalis*	Multi Rotor	250g - 1000g	1 - 2km2	12.28	60	15	Y
07/09/2019	Africa	Census	*Nanger dama*	Multi Rotor	250g - 1000g	1 - 2km2	20.45	100	23	N
02/06/2021	Africa	Census	*Addax nasomaculatus*	Multi Rotor	250g - 1000g	< 1km2	6.05	60	15	Y
15/03/2022	Africa	Census	*Giraffa camelopardalis*	Multi Rotor	250g - 1000g	1 - 2km2	20.47	50	15	Y
15/03/2022	Africa	Census	*Giraffa camelopardalis*	Multi Rotor	250g - 1000g	< 1km2	6.09	60	15	Y
09/11/2021	Africa	Census	*Nanger dama*	Multi Rotor	250g - 1000g	1 - 2km2	12.19	60	15	Y
12/11/2021	Africa	Census	*Oryx dammah*	Multi Rotor	250g - 1000g	1 - 2km2	15.27	80	18	N
13/11/2021	Africa	Census	*Gazella dorcas*	Multi Rotor	250g - 1000g	1 - 2km2	19.47	60	18	Y

Appendix 2   Supplementary Table 2: Data extracted from the reviewed articles (n=36)

Study ID	Country	Type	UAV	UAV_size	Alt_MIN	Alt_Max	Speed_Max	Launch	Disturbance	Ethical_considerations
Hu 2020	Asia	Census	Fixed Wing	>1500g	150	200	22.22		N	Not mentioned
Linchant 2015	Africa	Census	Fixed Wing	>1500g	100	100	13.88			Not mentioned
Linchant 2018	Africa	Census	Fixed Wing	>1500g	20	140	13.88		Y	Not mentioned
Mulero-Pazmany 2015	EU	Census	Fixed Wing	>1500g	100	100	11		N	Not mentioned
Basu 2019	Africa	Other	Multi Rotor	1000g - 1500g				>50 m	Y	Multiple species considered
deKock 2021	Middle East	Feature extraction	Multi Rotor	1000g - 1500g	100	100	15		N	Multiple species considered
Fritsch 2020	Africa	Census	Multi Rotor	1000g - 1500g	30	60	10		Y	Multiple species considered
Fritsch 2021	Africa	Census	Multi Rotor	1000g - 1500g	30	50	10			Multiple species considered
Hartmann 2021	Africa	Census	Multi Rotor	250g - 1000g	35	100	6	>50m	Y	Multiple species considered
Hirata 2022	EU	Behavior	Multi Rotor	250g - 1000g	180					Not mentioned
Inoue 2019	EU	Behavior	Multi Rotor	1000g - 1500g	25	80	10	> 50 m		Not mentioned
Liang 2020	Asia	Census	Multi Rotor	1000g - 1500g	10	50			N	Not mentioned
Maeda 2021	EU	Behavior	Multi Rotor	250g - 1000g	30	50				Not mentioned
Maeda 2021	EU	Behavior	Multi Rotor	250g - 1000g	30	50				Not mentioned
Mendonca 2021	EU	Behavior	Multi Rotor	1000g - 1500g	30	90		>10 m	N	Not mentioned
Petso 2021	Africa	Census	Multi Rotor	1000g - 1500g	15	130			N	Species of interst only
Schiffman 2014	Africa	Other	Multi Rotor	1000g - 1500g						Species of interst only
Schroeder 2021	Other	Behavior	Multi Rotor	1000g - 1500g	60	200	10	>100m	Y	Species of interst only
Bennitt 2019	Africa	Behavior	VTOL	>1500g	10	120	6.5	>100	Y	Multiple species considered

Study	Region	Type	Platform	Weight						Species
Mulero-Pazmany 2014	Africa	Other	Fixed Wing	>1500g	100	180			N	Not mentioned
Cukor 2019	EU	Census	Multi Rotor	>1500g	25	120	6			Multiple species considered
Kim 2021	Asia	Census	Multi Rotor	>1500g						Not mentioned
McMahon 2021	USA	Census	Multi Rotor	>1500g	71	122		>100m	N	Not mentioned
Obermoller 2021	USA	Other	Multi Rotor	>1500g	45	60	9		Y	Species of interst only
Preston 2021	USA	Census	Multi Rotor	1000g - 1500g	90	90	9		N	Species of interst only
Rahman 2021	Asia	Census	Multi Rotor	>1500g						Not mentioned
Zhou 2021	USA	Census	Multi Rotor	>1500g	60	60	9.7		N	Species of interst only
Chretien 2016	Canada	Census	VTOL	>1500g	55	60	6.11			Multiple species considered
Beaver 2020	USA	Census	Fixed Wing	>1500g	96.5	102.5	21	>50m		Multiple species considered
Lhoest 2015	Africa	Census	Fixed Wing	>1500g	38	155				Not mentioned
Witczuk 2018	EU	Census	Fixed Wing	>1500g	149	150	20		N	Species of interst only
Iwanoto 2020	Asia	Behavior	Multi Rotor	>1500g	50	50			N	Not mentioned
Takehiko 2022	Asia	Feature extraction	Multi Rotor	>1500g	40	120			N	Not mentioned
Schroeder 2021	Other	Behavior	Multi Rotor	1000g - 1500g	60	180	10	>100m	Y	Species of interst only
Hahn 2016	Africa	Other	Multi Rotor	1000g - 1500g					N	Multiple species considered
Roberts 2020	EU	Census	Fixed Wing	>1500g	100	100	18			Multiple species considered

Appendix 3 Supplementary Table 3: The digital zoometric measurement results of the O. leucoryx study herd.

ID	Sex	Transponder No.	DoB	DoP	Months	D_Print (cm²)	TotalLength	Width (cm)	Kg
85	female	00061F6770	14/07/2000	01/11/2017	207.75	3480.49	146.64	38.95	80.5
485	female	000621473B	11/04/2002	01/11/2017	186.84	3171.39	139.2	39.44	95.3
486	female	00061F605F	21/04/2002	01/11/2017	186.51	3068.98	130.56	41.58	101.7
547	female	00065DE1C1	01/09/2002	30/10/2017	182.07	3177.86	127.13	38.26	104.1
552	female	6136693	16/01/2003	01/11/2017	177.63	2745.75	121.41	39.39	86.8
643	female	00062155AF	09/03/2004	01/11/2017	163.89	3355.43	142.5	39.42	91.5
672	female	00062163C8	30/11/2003	01/11/2017	167.18	3232.55	144.45	42.04	92.9
726	female	000621440C	26/08/2004	01/11/2017	158.30	2969.16	130.53	39.44	91.2
1026	female	0006678F97	30/11/2005	01/11/2017	143.15	3283.63	127.83	41.15	95.5
1055	female	00066EE227D	01/02/2006	30/10/2017	141.01	2456.49	117.85	31.1	93
1093	female	0006696FD7	12/07/2006	01/11/2017	135.78	2693.77	126.17	36.44	91
1173	female	00066DC76E	26/12/2006	30/10/2017	130.22	2496.85	117.3	39.92	92.1
1177	female	00066DFDAB	11/04/2007	30/10/2017	126.74	2497.71	113.58	35.21	93.9
1270	female	00066E13EE	02/01/2007	30/10/2017	129.99	2832.12	129.87	35.62	86.2
1294	female	00066DE916	24/02/2008	30/10/2017	116.25	3012.25	128.11	38.84	93.2
1342	female	0006CA1339	11/09/2008	30/10/2017	109.68	2712.21	118.26	37.86	93
1344	female	0006CE4379	28/09/2008	30/10/2017	109.12	2717.1	128.03	35.15	90.5
1367	female	0006CA00B3	28/10/2008	30/10/2017	108.13	3369.63	138.89	37.26	92.7
1387	female	0006C9E79F	26/11/2008	01/11/2017	107.24	3008.35	130.16	37.28	85.3
1436	female	0006C9FA7D	25/11/2008	01/11/2017	107.28	3725.31	143.87	47.4	95
1473	female	0006CA07C4	20/06/2009	30/10/2017	100.41	2450	126.01	33.67	82.5
1481	female	0006CE2660	24/08/2008	30/10/2017	110.27	2766.63	126.23	37.05	91.1
1490	female	0006C9EAC8	26/07/2009	30/10/2017	99.22	2730.07	104.28	40.95	101.7
1506	female	0006C9E7D9	03/08/2009	01/11/2017	99.02	3458.12	134.85	41.18	106.1
1647	female	0006CA10D4	19/12/2009	30/10/2017	94.42	2100.01	113.8	33	82.1
1649	female	0006C9DB85	27/12/2009	30/10/2017	94.16	2561	126.25	37.82	97.3
1657	female	0006CA0CC2	14/01/2010	30/10/2017	93.57	2695	127.63	40.54	86.7
1912	female	0006CA01E2	28/04/2010	30/10/2017	90.15	2449.14	117.45	34.89	85.4
1915	female	000706D128	17/04/2010	30/10/2017	90.51	2452.56	111.17	35.35	84.9

1921	female	0006CE37D0	24/03/2010	30/10/2017	91.30	2665.1	127	35.7	90.2
1922	female	0006CE3E2D	22/03/2010	30/10/2017	91.36	2598.22	126.27	37.8	94.4
1964	female	956000001834132	20/11/2010	30/10/2017	83.38	2574.62	124.92	36.69	85.4
2007	female	0006CA116C	18/01/2011	30/10/2017	81.44	2805.65	120.75	35.78	85.5
2189	female	956000001824626	24/01/2011	30/10/2017	81.24	2676.25	125.29	37.83	98.2
2197	female	000708C08B	01/03/2011	30/10/2017	80.05	2595.9	111.97	37.85	90.9
2205	female	000708836F	19/12/2011	30/10/2017	70.42	2973.67	121.4	41.35	95.8
2222	female	000708B105	22/12/2011	30/10/2017	70.32	3185	129.45	42.02	107.3
2223	female	00070B4FA7	23/12/2011	30/10/2017	70.29	3199.17	136.01	42	101.7
2226	female	70883000000	17/01/2012	30/10/2017	69.47	2474.3	111.97	36.9	83.7
2230	female	0007074402	05/02/2012	30/10/2017	68.84	2682.91	122.95	38.47	83.6
2240	female	000708EC4A	11/04/2012	30/10/2017	66.67	2149.61	110	32.25	71.9
2262	female	00075B16E1	17/01/2012	01/11/2017	69.53	2762.04	107.87	40.95	91.3
2264	female	00070B75B0	08/10/2011	01/11/2017	72.85	2865.09	133.73	40.68	75.7
2267	female	0007088B7D	28/10/2011	01/11/2017	72.20	2450.19	113.45	35.69	78.9
2375	female	000708859F	22/06/2012	01/11/2017	64.37	2917.79	124.11	40.25	87.3
2390	female	000708B4B6	22/06/2012	01/11/2017	64.37	3570.23	150.12	41.47	85.3
2392	female	000708B87F	05/07/2012	01/11/2017	63.95	3225.12	130.81	43.94	106.6
2409	male	00070B180D	26/11/2012	30/10/2017	59.15	3377.25	137.59	39.25	114.6
2421	male	000708D906	01/01/2012	01/11/2017	70.06	2200.25	122.24	27.89	80.8
2456	female	000708D64F	06/02/2012	01/11/2017	68.88	3111.47	136.12	40.24	98
2466	female	00075B52FB	17/04/2013	01/11/2017	54.54	2351.7	120.39	34.43	90.9
2475	female	000708E4D2	18/01/2013	30/10/2017	57.40	2797.99	124.49	39.45	100.1
2483	female	00070890C3	16/02/2013	30/10/2017	56.45	2891.63	124.9	39.54	91.8
2776	female	00066C748C	07/01/2013	01/11/2017	57.83	3373.04	145.91	38.08	89.9
2847	female	000708CAC7	26/01/2014	30/10/2017	45.14	2338.76	112.36	38.52	75.2
3633	female	00075CC5E0	25/08/2016	30/10/2017	14.17	1895.72	110.6	27.86	58.1
3634	female	00075B44E4	25/08/2016	30/10/2017	14.17	2196.18	116.39	31.9	62.7
3635	male	00075B0DF8	24/08/2016	30/10/2017	14.20	2667.96	121.52	33.54	71.7
3641	female	00075CF5F2	16/08/2016	01/11/2017	14.53	1952.37	109.51	28.35	70.1
3643	female	00075D1C33	17/08/2016	01/11/2017	14.50	2655.64	127.09	34.14	67.3
3646	female	000708CAB6	22/08/2016	01/11/2017	14.33	2794.99	136.39	36.85	64.9
3650	female	00075B538C	30/08/2016	01/11/2017	14.07	2182.44	109.58	32.54	61.5

3651 male	00075D1DD6	30/08/2016	01/11/2017	14.07	2222.36	116.46	29.07	61.8
3652 female	00075D7D8D	09/09/2016	01/11/2017	13.74	1937.98	104.47	28.1	63.8
3654 male	00075B3BBF	11/09/2016	01/11/2017	13.68	2017.97	111.91	27.94	66.9
3658 male	00075CB347	05/09/2016	30/10/2017	13.81	1946.79	112.25	29.8	62.2
3659 male	00075B4D92	05/09/2016	30/10/2017	13.81	2234.81	116.6	31.96	67
3663 female	00075CC428	05/09/2016	30/10/2017	13.81	2180.76	118.93	33.58	64
3665 female	00075B4E24	06/09/2016	30/10/2017	13.78	2340.23	110.31	34.28	62.1
3666 male	0007074562	14/09/2016	30/10/2017	13.51	2159.62	105.61	29.2	62.3
3667 male	000706B20F	14/09/2016	30/10/2017	13.51	1572.79	100.45	25.21	65.6
3669 male	00075C79FA	14/09/2016	01/11/2017	13.58	2520.11	123.76	31.66	64
3674 female	000708C3E4	24/09/2016	30/10/2017	13.18	1813.13	99.23	28.13	52.4
3676 male	000708B878	28/09/2016	30/10/2017	13.05	1519.74	85.66	27.67	50.8
3677 male	00070743FC	01/10/2016	30/10/2017	12.95	2122	115.14	29.83	56.5
3683 male	00070B51DD	08/09/2016	30/10/2017	13.71	2060.87	108.34	32.34	63.4
3685 female	00075CD991	14/09/2016	01/11/2017	13.58	2292.41	114.81	32.76	60.5
3686 female	000708E5F1	10/09/2016	30/10/2017	13.64	1749.14	102.38	26.8	53.6
3687 male	000706B1F5	12/09/2016	30/10/2017	13.58	2140.37	107.44	31.3	60.4
3688 male	0007089CE1	02/01/2017	30/10/2017	9.90	2000.87	102	32.93	55.5
3695 female	000708D107	04/11/2016	30/10/2017	11.84	1637.05	105.53	27.61	45.4
3697 male	0007073738	05/11/2016	30/10/2017	11.80	1592.54	82.09	29.48	53.2
3699 female	000708EBD7	14/11/2016	30/10/2017	11.51	2259.93	122	31.68	60.7
3703 female	000708BDC3	29/11/2016	30/10/2017	11.01	2195.6	110.31	30.3	50.8
3704 male	00070B18E6	02/12/2016	30/10/2017	10.92	1767.2	102.92	29.67	52.1
3706 male	000708DDF5	03/12/2016	30/10/2017	10.88	1551.54	98.02	28.04	49.3
3714 female	0007089F2D	09/12/2016	30/10/2017	10.68	2270	120.93	33.7	55.9
3715 female	000706AEEC	11/12/2016	30/10/2017	10.62	1946.82	107.52	30.02	57.1
3719 male	000708EC3B	21/12/2016	30/10/2017	10.29	1914.66	98.35	28.3	55.6
3737 male	00070B41AA	02/01/2017	30/10/2017	9.90	2003.91	115.72	29.42	53
3750 female	00075B4FCF	05/11/2016	01/11/2017	11.87	1782.56	100.59	28.31	58.7
3751 male	0007088005	09/01/2017	30/10/2017	9.67	1591.62	99.255	27.34	47.7
3760 male	00075CC87D	07/02/2017	30/10/2017	8.71	1829.98	104.45	29.01	54
3768 female	00075D0C1B	13/11/2016	01/11/2017	11.61	2684.44	126.21	32.22	55.4
3769 male	00075B07DC	13/11/2016	01/11/2017	11.61	2087.83	113.61	30.21	52.8

3775	female	00075B0B96	27/02/2017	01/11/2017	8.12	1927.54	108.33	28.73	52.7
3778	male	00075B12E5	27/02/2017	30/10/2017	8.05	1389.24	87.61	26.98	36.4
3896	female	00075D239D	25/03/2017	30/10/2017	7.20	1486.11	95.74	26.85	39
3908	male	00075CCB89	22/03/2017	30/10/2017	7.30	1445.07	92.31	25.54	38.7
3909	female	0007087000	22/05/2017	30/10/2017	5.29	1200.87	82.83	23.57	34.8
3910	female	00070B1F66	30/05/2017	30/10/2017	5.03	1205.64	83.46	23.46	27.9
3911	female	0007087DA1	31/05/2017	30/10/2017	5.00	1236.34	80.77	22.69	31.7
3913	female	00075CC826	05/01/2017	30/10/2017	9.80	1199.83	86.7	22.81	33.4
3917	female	00075CC96D	12/01/2017	30/10/2017	9.57	1068.91	79.83	21.14	27.3
3930	male	00075B5B83	17/06/2017	30/10/2017	4.44	15982.39	96.42	23.97	32.6
3937	female	000708C01B	15/01/2017	01/11/2017	9.53	1542.07	103.85	24.39	31.5
3939	male	000708C524	17/06/2017	01/11/2017	4.50	1242.61	74.3	25.57	27.4
3940	female	00070B5058	18/01/2017	01/11/2017	9.44	1256.94	89.04	22.23	31.2
3942	male	00070B2274	25/01/2017	01/11/2017	9.21	1358.36	91.3	23.54	28.6
3943	male	000707358E	26/06/2017	01/11/2017	4.21	1532.52	87.28	25.62	25.6
3944	female	000707395B	27/06/2017	01/11/2017	4.18	1128.72	84.22	20.39	29.4
3950	male	00075CCD29	02/07/2017	30/10/2017	3.95	1706.65	100.71	28.59	30
3952	male	00075CF88B	05/07/2017	30/10/2017	3.85	1078.52	78.12	19.4	28.8
3955	female	00075B0CBF	10/07/2017	30/10/2017	3.68	915.05	70.86	18.78	26.2
3962	male	00075CC23D	26/07/2017	30/10/2017	3.16	1026.81	78.35	17.28	23.7
3967	male	00075B38E0	03/09/2017	30/10/2017	1.87	1052	77.44	19.02	16.4
3969	male	00075CC94C	15/08/2017	30/10/2017	2.50	1018.96	75.73	18.12	24.1
3971	female	000708AA5C	05/07/2017	01/11/2017	3.91	1733.9	103.19	26.16	35.1
3972	female	000708CD58	07/07/2017	01/11/2017	3.85	1049.35	72.06	15.5	25.9
3974	female	000708A40C	13/08/2017	01/11/2017	2.63	1549.19	104.12	24.75	26.7
3982	female	000708EFC9	03/09/2017	01/11/2017	1.94	1273.27	103.71	28.52	16
4012	female	000706B294	30/09/2017	01/11/2017	1.05	586.35	60.54	12.2	10.2

Appendix 4   R-markdown file: UAV_based_Ungulate_monitoring

Methods and ethical considerations for the monitoring of ungulates using UAVs: A systematic review and evaluation

Meyer E. De Kock, Albert Myburgh, Abdoul Razack Moussa, Karolína Brandlová, Pavla Hejcmanová

21/05/2022

Import Data-Sets

```
library(readxl)
Ungulate <- read_excel("C:/Users/meyer/Desktop/Ungulate review/Ungulate.xlsx")

## New names:
## * `` -> ...12
## * `` -> ...13
## * `` -> ...14

UngulateCluster <- read_excel("C:/Users/meyer/Desktop/Ungulate review/UngulateCluster.xlsx")
Flights <- read_excel("C:/Users/meyer/Desktop/Ungulate review/FlightType.xlsx")

## New names:
## * `` -> ...13

##mutate (Type = as_factor(Flights$Type)%>% fct_relevel("Automated", "Piloted))
View(UngulateCluster)
```

import Libraris

```
library(ggplot2)
library(mgcv, lib.loc = "C:/Program Files/R/R-4.0.2/library")

## Loading required package: nlme

## This is mgcv 1.8-31. For overview type 'help("mgcv-package")'.

library(nlme, lib.loc = "C:/Program Files/R/R-4.0.2/library")
library(dplyr)

##
## Attaching package: 'dplyr'

## The following object is masked from 'package:nlme':
##
##     collapse

## The following objects are masked from 'package:stats':
##
##     filter, lag

## The following objects are masked from 'package:base':
##
```

```
##     intersect, setdiff, setequal, union
library(tidyverse)

## -- Attaching packages ------------------------------------- tidyverse 1.3.1 --

## v tibble  3.1.6     v purrr   0.3.4
## v tidyr   1.1.4     v stringr 1.4.0
## v readr   2.1.0     v forcats 0.5.1

## -- Conflicts ---------------------------------------- tidyverse_conflicts() --
## x dplyr::collapse() masks nlme::collapse()
## x dplyr::filter()   masks stats::filter()
## x dplyr::lag()      masks stats::lag()
library(FactoMineR)
library(factoextra)

## Welcome! Want to learn more? See two factoextra-related books at https://goo.gl/ve3WBa
library(multcompView)
library(ggpubr)


which (!complete.cases(UngulateCluster))

## integer(0)

str(Flights)

## tibble [122 x 15] (S3: tbl_df/tbl/data.frame)
## $ 43260       : chr [1:122] "43149" "43149" "43149" "43149" ...
## $ UAE         : chr [1:122] "Senegal" "Senegal" "Senegal" "Senegal" ...
## $ SHJ         : chr [1:122] "Bandia" "Bandia" "Bandia" "Bandia" ...
## $ 1000g 1500g : chr [1:122] "1000g 1500g" "1000g 1500g" "1000g 1500g" "1000g - 1500g" ...

## $ 5.45        : chr [1:122] "1.49" "3.01" "0.33" "1.01" ...
## $ 40          : chr [1:122] "45" "45" "45" "45" ...
## $ 12          : chr [1:122] "11" "10" "10" "10" ...
## $ Dama        : chr [1:122] "Derby eland" "Derby eland" "Derby eland" "Derby eland" ...
## $ Targeted    : chr [1:122] "Targeted" "Targeted" "Targeted" "Targeted" ...
## $ Piloted     : chr [1:122] "Piloted" "Piloted" "Piloted" "Piloted" ...
## $ N           : chr [1:122] "N" "N" "N" "N" ...
## $ ...13       : chr [1:122] NA NA NA NA ...
## $ No Cover    : chr [1:122] "no cover" "Cover" "Cover" "Cover" ...
## $ Up wind     : chr [1:122] "Up wind" "Up wind" "Up wind" "Up wind" ...
```
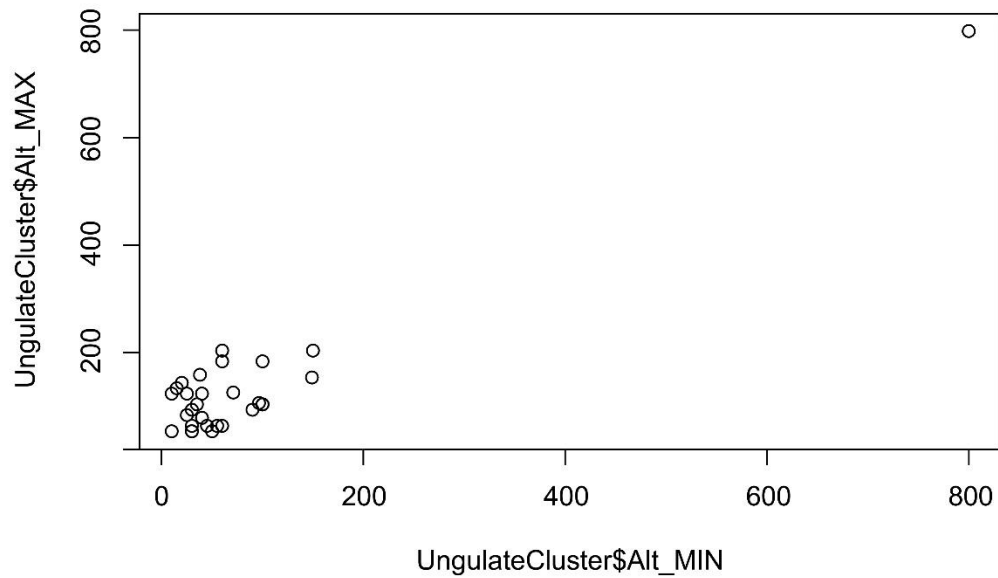
Plot Range

```
df <-UngulateCluster
plot(UngulateCluster$Alt_MIN, UngulateCluster$Alt_MAX)
```

```
kmeans(x = UngulateCluster, centers = 2)

## K-means clustering with 2 clusters of sizes 31, 1
##
## Cluster means:
##   Covidence #  Alt_MIN Alt_MAX
## 1    220.7419 57.8871 104.6613
## 2    367.0000 800.0000 800.0000
##
## Clustering vector:
##  [1] 1 1 2 1 1 1 1 1 1 1 1 1 1 1 1 1 1 1 1 1 1 1 1 1 1 1 1 1 1 1 1 1
##
## Within cluster sum of squares by cluster:
## [1] 422638.5     0.0
##  (between_SS / total_SS =  70.8 %)
##
## Available components:
##
## [1] "cluster"     "centers"     "totss"       "withinss"    "tot.withinss"
## [6] "betweenss"   "size"        "iter"        "ifault"
review <- read_excel("C:/Users/meyer/Desktop/Ungulate review/review.xlsx")

## New names:
## * Species -> Species...7
## * Species -> Species...9
```

74

```
ggplot(data = review, aes(x= Alt_MAX, y= Speed_Max , fill = UAV))+
geom_boxplot ()+ theme_classic2()+
scale_fill_manual(breaks=review$UAV,
                  values = c ("#f3f6f4", "#bcbcbc","#999999" ))+
  labs(x="Maximum AGL m", y="Maximum Air Speed m/s")
```

```
## Warning: Removed 6 rows containing missing values (stat_boxplot).
```

```
## Warning: Removed 11 rows containing non-finite values (stat_boxplot).
```



```
review <- read_excel("C:/Users/meyer/Desktop/Ungulate review/review.xlsx")
```
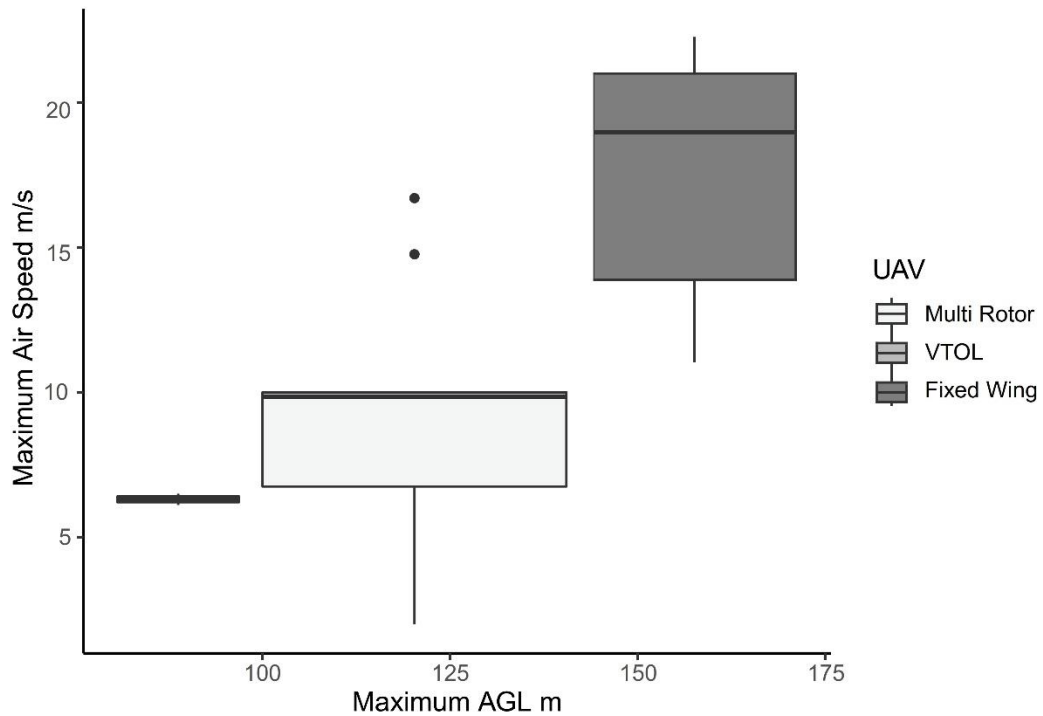
```
## New names:
## * Species -> Species...7
## * Species -> Species...9
```

```
par(mfrow=c(2,2))
ggplot(data = review, aes(x= Alt_MIN, y= Speed_Min , fill = UAV))+
geom_boxplot ()+ theme_classic2()+
scale_fill_manual(breaks=review$UAV,
                  values = c ("#f3f6f4", "#bcbcbc","#999999" ))+
  labs(x="Minimum AGL m", y=" Minimum Air Speed m/s")
```

```
## Warning: Removed 6 rows containing missing values (stat_boxplot).
```
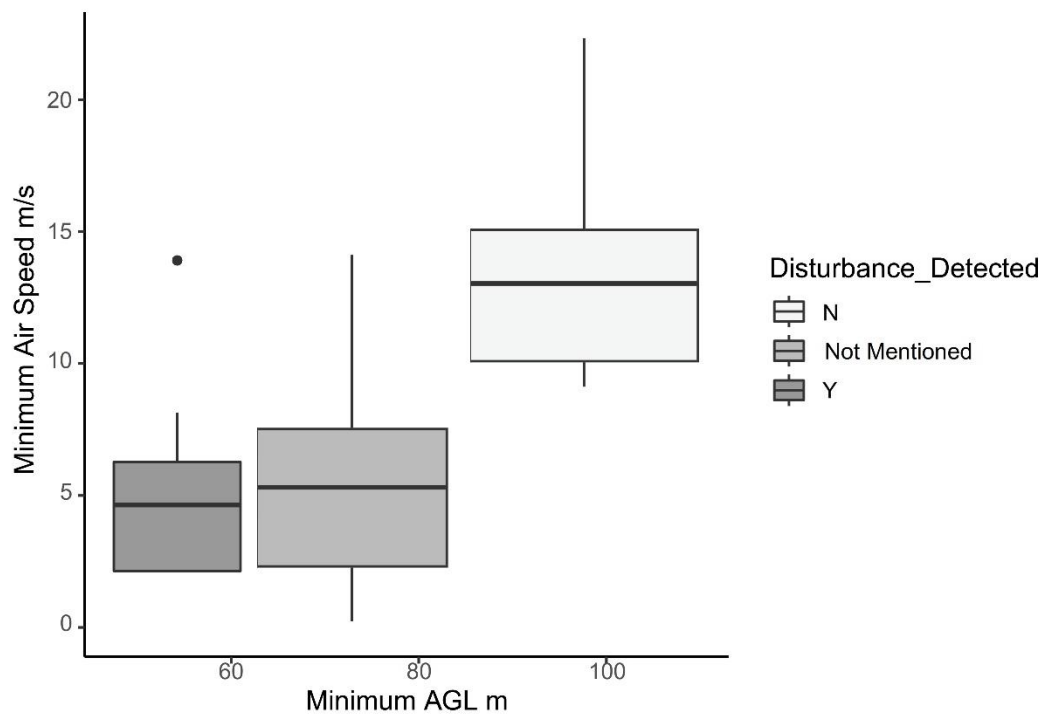
```
## Warning: Removed 11 rows containing non-finite values (stat_boxplot).
```
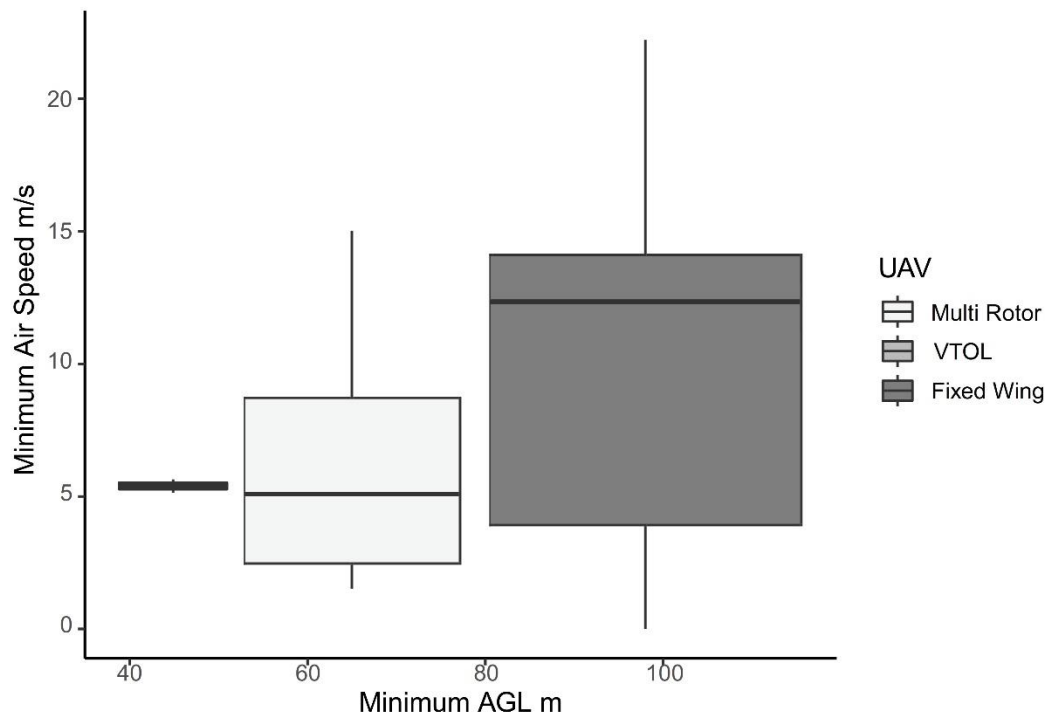
```
ggplot(data = review, aes(x= Alt_MIN, y= Speed_Min , fill =
Disturbance_Detected))+
geom_boxplot ()+ theme_classic2()+
scale_fill_manual(breaks=review$Disturbance_Detected,
                  values = c ("#f3f6f4", "#bcbcbc","#999999" ))+
  labs(x="Minimum AGL m", y=" Minimum Air Speed m/s")
```
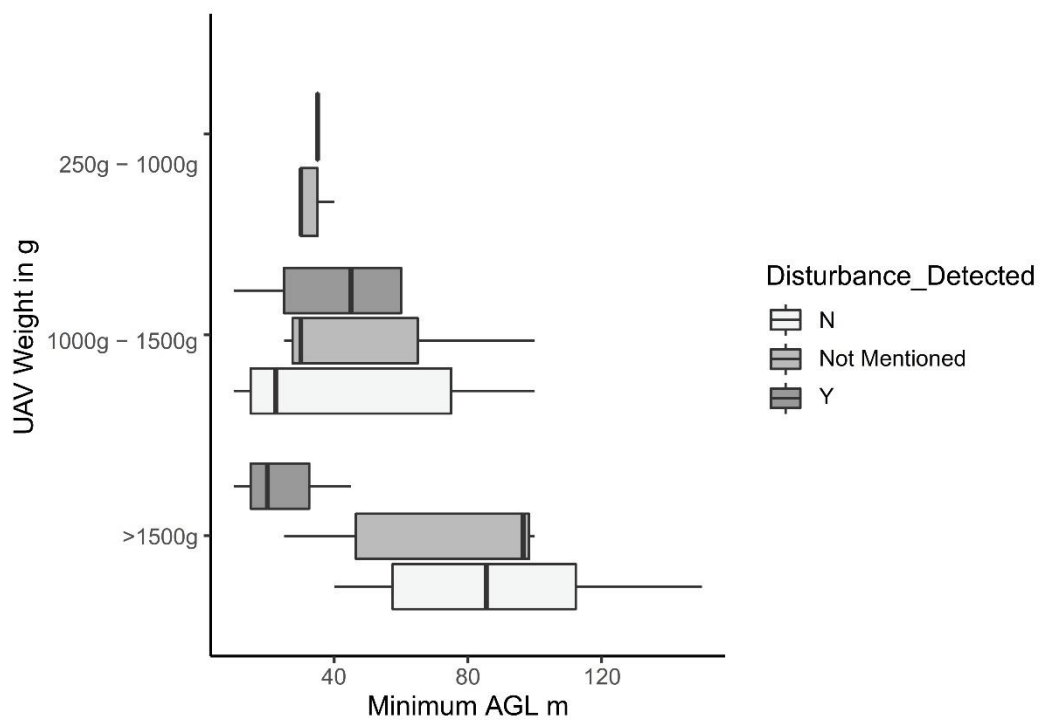
Warning: Removed 6 rows containing missing values (stat_boxplot).

Warning: Removed 11 rows containing non-finite values (stat_boxplot).

76

```r
ggplot(data = review, aes(x= Alt_MIN, y= UAV_size , fill = Disturbance_Detected))+
geom_boxplot ()+ theme_classic2()+
scale_fill_manual(breaks=review$Disturbance_Detected,
                  values = c ("#f3f6f4", "#bcbcbc","#999999" ))+
  labs(x="Minimum AGL m", y=" UAV Weight in g")
```

```
## Warning: Removed 6 rows containing non-finite values (stat_boxplot).
```

```
ggplot(data = review, aes(x= Alt_MIN, y= Ethical_considerations
, fill = Disturbance_Detected))+
geom_boxplot ()+
theme_classic2()+
scale_fill_manual(breaks=review$Disturbance_Detected,
                  values = c ("#f3f6f4", "#bcbcbc","#999999" ))+
  labs(x="Minimum AGL m", y=" Ethical Considerations")
```

```
## Warning: Removed 6 rows containing non-finite values (stat_boxplot).
```
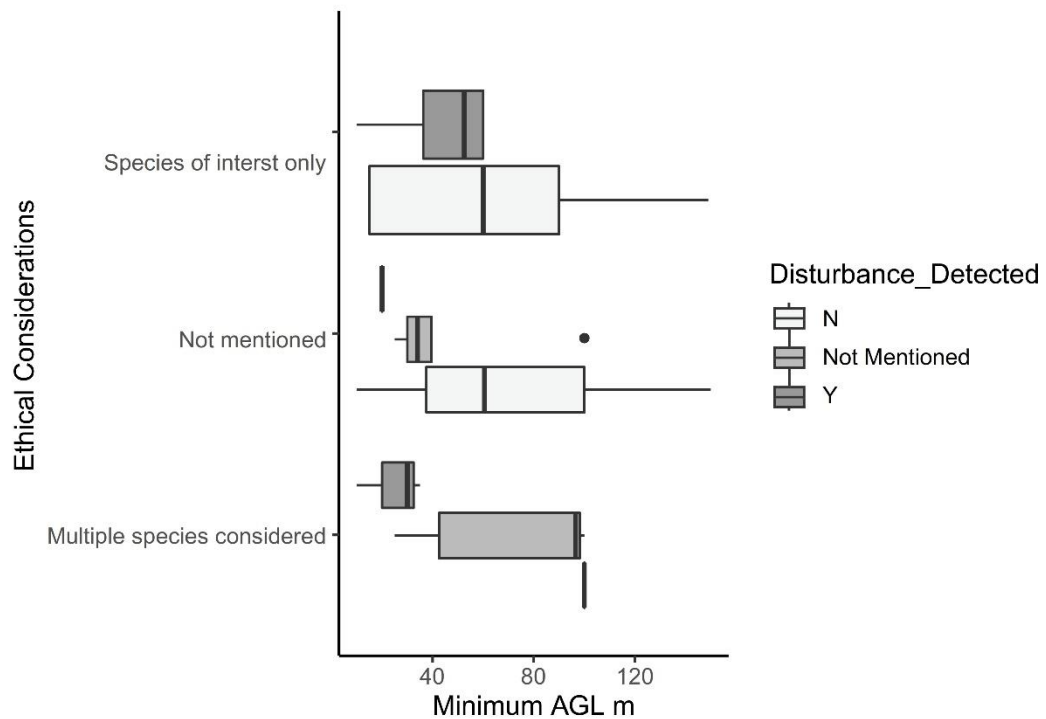
Review data collection

For the purpose of this review, we searched for scientific peer-reviewed papers using the Web of ScienceTM database on 2022/04/24. We used the timeframe from 2000/01/01 to 2022/04/24 and a topic search with the following Boolean operators: (((ALL=(Ungulates OR Wildlife OR Mammals)) AND ALL=(Drones OR UAV OR RPAS)) NOT ALL=(marine OR whale)) and only considered publications in the English language.

```
Flights <- read_excel("E:/Ungulate review/Ungulate.xlsx")

## New names:
## * Area -> Area...4
## * Species -> Species...5
## * Species -> Species...7
## * Area -> Area...15

  ggplot(data = Flights, aes(x= Alt_Max, , y= Speed, fill = UAV))+
  geom_boxplot ()+ theme_classic2()+
  scale_fill_manual(breaks=Flights$UAV,
                    values = c ("#f3f6f4", "#bcbcbc", "#999999" ))+
    labs(x="AGL m", y="Air Speed m/s")
```
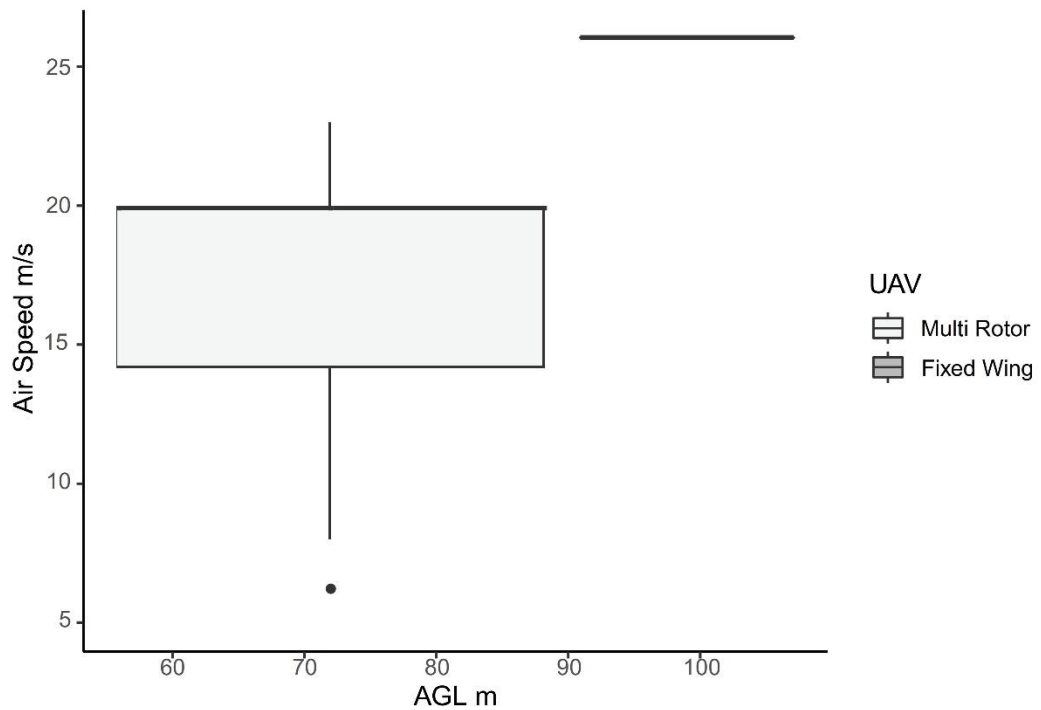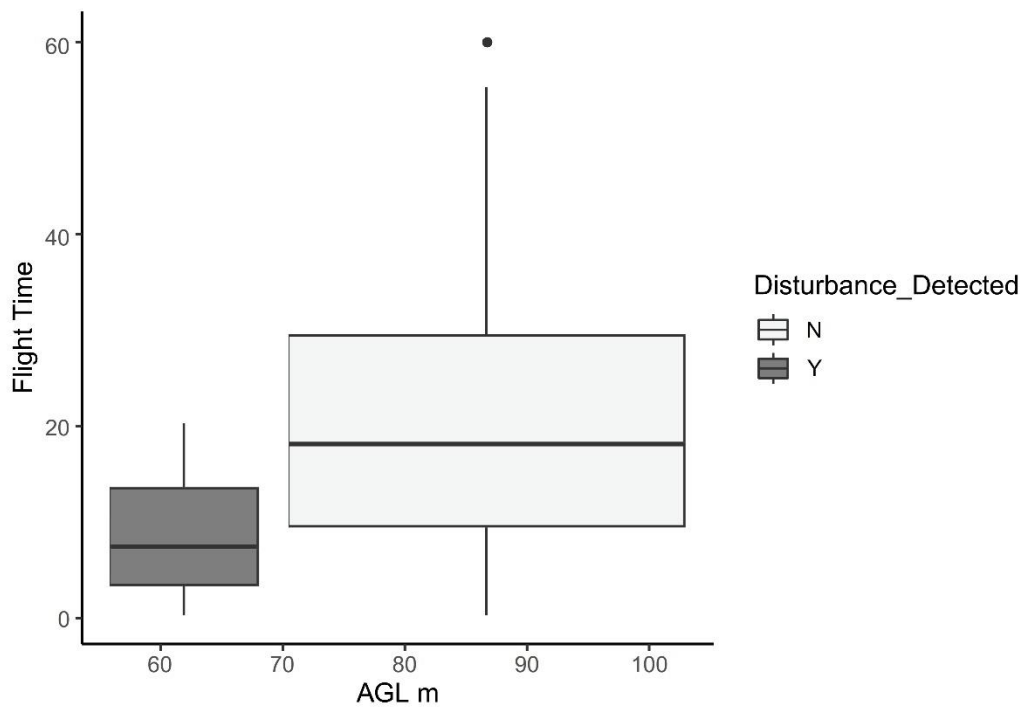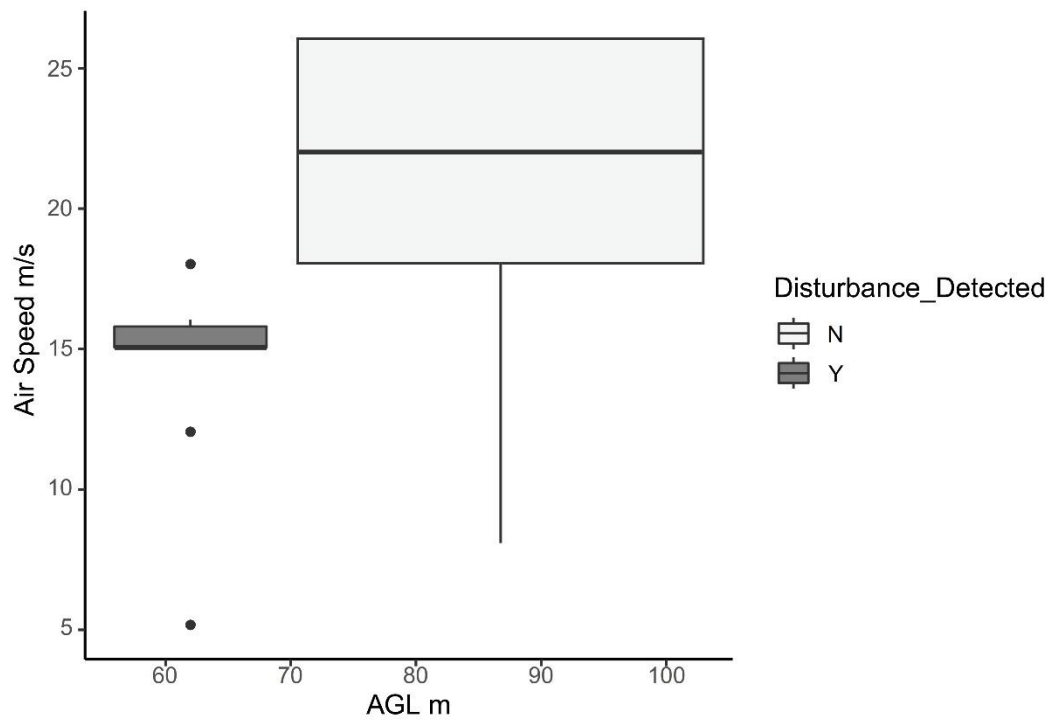
```
ggplot(data = Flights, aes(x= Alt_Max, , y= Flight_time, fill = Disturbance_Detected))+
  geom_boxplot ()+ theme_classic2()+
  scale_fill_manual(breaks=Flights$Disturbance_Detected,
                    values = c ("#f3f6f4", "#bcbcbc"))+
    labs(x="AGL m", y=" Flight Time")
```

```
ggplot(data = Flights, aes(x= Alt_Max, , y= Speed, fill = Disturbance_Detected))+
  geom_boxplot ()+ theme_classic2()+
  scale_fill_manual(breaks=Flights$Disturbance_Detected,
                    values = c ("#f3f6f4", "#bcbcbc"))+
    labs(x="AGL m", y=" Air Speed m/s")
```

```
ggplot(data = Flights, aes(x= Alt_Max, , y= UAV_size, fill = Disturbance_Detected))+
  geom_boxplot ()+ theme_classic2()+
  scale_fill_manual(breaks=Flights$Disturbance_Detected,
                 values = c ("#f3f6f4", "#bcbcbc"))+
  labs(x="AGL m", y=" UAV Weight in g")
```
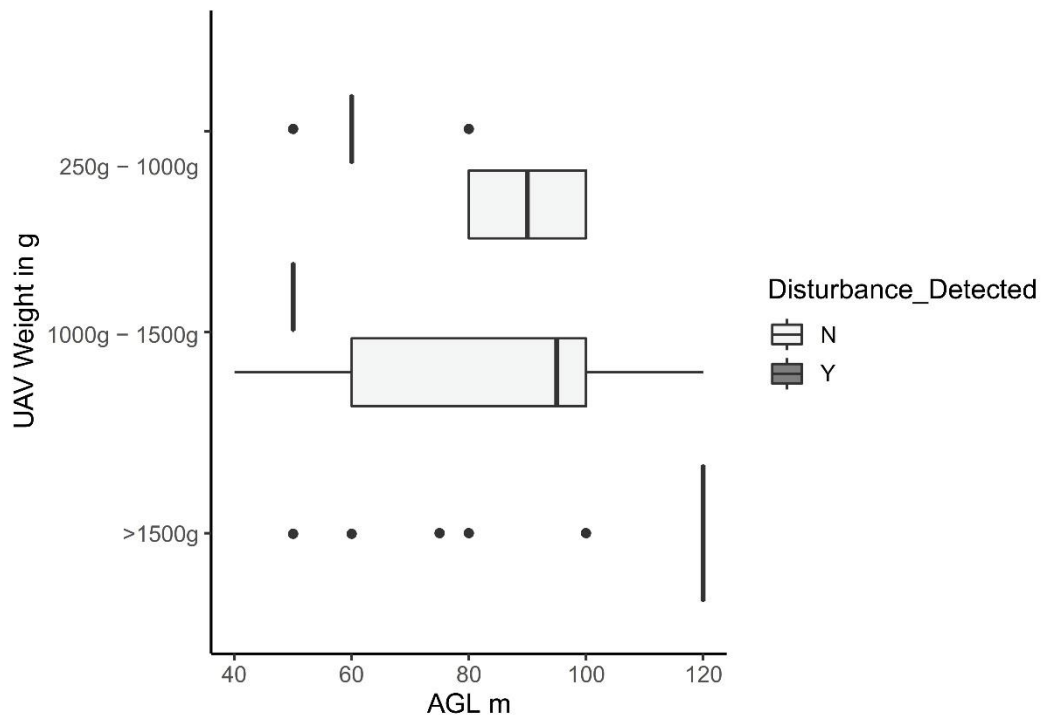
Quantifying disturbance: a case study on the Western Derby Eland (Taurotragus derbianus derbianus)

The disturbance study was done on the Western Derby Eland (Taurotragus derbianus derbianus) in Bandia Reserve (Senegal). We used two types of multi-rotor UAVs: DJI (Da-Jiang Innovations Science and Technology Co., Ltd.) Phantom 3 Pro and DJI Phantom 4 Pro. All flights were launched > 200m away from the target.

```
Disturb <- read_excel("C:/Users/meyer/Desktop/Ungulate review/Q_disturb.xlsx")
  ggplot(data = Disturb, aes(x= AGL, , y= Disturbance, fill = UAV))+
  geom_boxplot ()+
  theme_classic2()+
  scale_fill_manual(breaks=Disturb$UAV,
                    values = c ("#f3f6f4", "#bcbcbc"))+
    labs(x="AGL m", y="Disturbance Level")
```
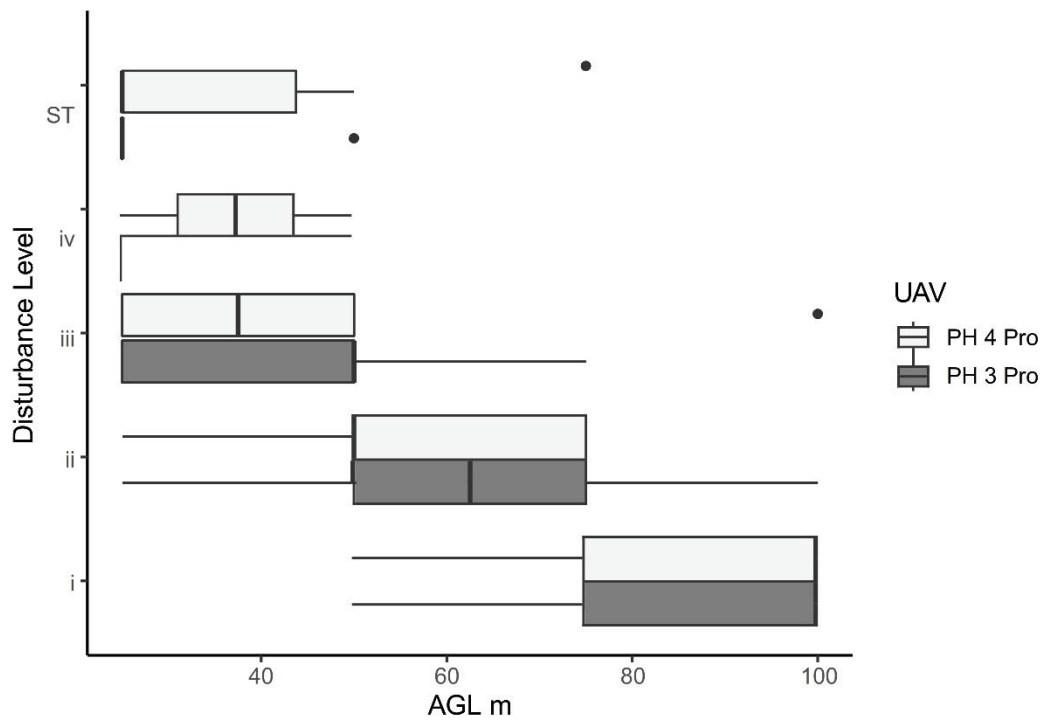
Note that the `echo = FALSE` parameter was added to the code chunk to prevent printing of the R code that generated the plot.

##Decision-tree Analysis

Import Libraries

```
library(FSelector)
library(rpart)
library(rpart.plot)
library(caret)
```

```
## Loading required package: lattice

##
## Attaching package: 'caret'

## The following object is masked from 'package:purrr':
##
##     lift
```

```
library(lattice)
library(dplyr)
library(xlsx)
library(data.tree)
library(data.table)
```

```
##
## Attaching package: 'data.table'
```

```
## The following object is masked from 'package:purrr':
##
##     transpose

## The following objects are masked from 'package:dplyr':
##
##     between, first, last
library(caTools)
```

Decision-tree Analysis

The decision-tree models use the minimum and maximum AGL altitude, and minimum and maximum speed to predict disturbance

```
review <- read_excel("E:/Ungulate review/review.xlsx")

## New names:
## * Species -> Species...6
## * Species -> Species...8
review <- select(review,Alt_Max, Alt_MIN, Speed_Min, Speed_Max, Disturbance_Detected)
str(review)

## tibble [36 x 5] (S3: tbl_df/tbl/data.frame)
##  $ Alt_Max            : num [1:36] 200 100 140 100 NA 100 60 50 100 NA ...
##  $ Alt_MIN            : num [1:36] 150 100 20 100 NA 100 30 30 35 180 ...
##  $ Speed_Min          : num [1:36] 22.2 13.9 13.9 11 NA ...
##  $ Speed_Max          : num [1:36] 22.2 13.9 13.9 11 NA ...
##  $ Disturbance_Detected: chr [1:36] "N" NA "Y" "N" ...

review$Disturbance_Detected <- factor(review$Disturbance_Detected)
str(review)

## tibble [36 x 5] (S3: tbl_df/tbl/data.frame)
##  $ Alt_Max            : num [1:36] 200 100 140 100 NA 100 60 50 100 NA ...
##  $ Alt_MIN            : num [1:36] 150 100 20 100 NA 100 30 30 35 180 ...
##  $ Speed_Min          : num [1:36] 22.2 13.9 13.9 11 NA ...
##  $ Speed_Max          : num [1:36] 22.2 13.9 13.9 11 NA ...
##  $ Disturbance_Detected: Factor w/ 2 levels "N","Y": 1 NA 2 1 2 1 2 NA 2 NA ...
```

Decision-tree Analysis

The decision tree model using minimum altitude and UAV size as an input to predict disturbance detected

```
set.seed(123)
sample = sample.split (review$Disturbance_Detected, SplitRatio = .70)
train = subset(review, sample == TRUE)
test= subset(review,sample== FALSE)
##Training the Decision tree Classifier To Predict Pregnacy tree <-
rpart(Disturbance_Detected~.,data=train) tree.Disturbance_Detected.predicted
<- predict (tree, test, type ='class')
confusionMatrix(tree.Disturbance_Detected.predicted,test$Disturbance_Detected)

## Confusion Matrix and Statistics
##
##           Reference
## Prediction N Y
```

```
##           N 4 2
##           Y 0 0
##
##                  Accuracy : 0.6667
##                    95% CI : (0.2228, 0.9567)
##       No Information Rate : 0.6667
##       P-Value [Acc > NIR] : 0.6804
##
##                     Kappa : 0
##
##    Mcnemar's Test P-Value : 0.4795
##
##               Sensitivity : 1.0000
##               Specificity : 0.0000
##            Pos Pred Value : 0.6667
##            Neg Pred Value :    NaN
##                Prevalence : 0.6667
##            Detection Rate : 0.6667
##      Detection Prevalence : 1.0000
##         Balanced Accuracy : 0.5000
##
##          'Positive' Class : N
##
```

```
prp(tree)
```

(N)

```
review <- read_excel("E:/Ungulate review/review.xlsx")

## New names:
## * Species -> Species...6
## * Species -> Species...8
review <- select(review, Alt_MIN, UAV_size, Disturbance_Detected)
str(review)

## tibble [36 x 3] (S3: tbl_df/tbl/data.frame)
##  $ Alt_MIN            : num [1:36] 150 100 20 100 NA 100 30 30 35 180 ...
##  $ UAV_size           : chr [1:36] ">1500g" ">1500g" ">1500g" ">1500g" ...
##  $ Disturbance_Detected: chr [1:36] "N" NA "Y" "N" ...

review$Disturbance_Detected <- factor(review$Disturbance_Detected)
str(review)

## tibble [36 x 3] (S3: tbl_df/tbl/data.frame)
##  $ Alt_MIN            : num [1:36] 150 100 20 100 NA 100 30 30 35 180 ...
##  $ UAV_size           : chr [1:36] ">1500g" ">1500g" ">1500g" ">1500g" ...
##  $ Disturbance_Detected: Factor w/ 2 levels "N","Y": 1 NA 2 1 2 1 2 NA 2 NA ...

set.seed(123)
sample = sample.split (review$Disturbance_Detected, SplitRatio = .70)
train = subset(review, sample == TRUE)
test= subset(review,sample== FALSE)
##Training the Decision tree Classifier To Predict Pregnacy tree <-
rpart(Disturbance_Detected~.,data=train) tree.Disturbance_Detected.predicted
<- predict (tree, test, type ='class')
confusionMatrix(tree.Disturbance_Detected.predicted,test$Disturbance_Detected)

## Confusion Matrix and Statistics
##
##           Reference
## Prediction N Y
##         N 4 2
##         Y 0 0
##
##                Accuracy : 0.6667
##                  95% CI : (0.2228, 0.9567)
##     No Information Rate : 0.6667
##     P-Value [Acc > NIR] : 0.6804
##
##                   Kappa : 0
##
##  Mcnemar's Test P-Value : 0.4795
##
##             Sensitivity : 1.0000
##             Specificity : 0.0000
##          Pos Pred Value : 0.6667
##          Neg Pred Value :    NaN
##              Prevalence : 0.6667
##          Detection Rate : 0.6667
##    Detection Prevalence : 1.0000
##       Balanced Accuracy : 0.5000
##
```

```
##          'Positive' Class : N
##
```
```r
prp(tree)
```

Ⓝ

```r
UngulateB <- read_excel("E:/Ungulate review/Ungulate.xlsx")
```
```
## New names:
## * Area -> Area...4
## * Species -> Species...5
## * Species -> Species...7
## * Area -> Area...15
```
```r
UngulateB <- select(UngulateB, Alt_Max, Flight_time, UAV)
str(UngulateB)
```
```
## tibble [121 x 3] (S3: tbl_df/tbl/data.frame)
##  $ Alt_Max    : num [1:121] 60 80 120 120 120 120 120 120 120 120 ...
##  $ Flight_time: num [1:121] 16.2 21.4 51.7 27.3 18.4 ...
##  $ UAV        : chr [1:121] "Multi Rotor" "Fixed Wing" "Fixed Wing" "Fixed Wing" ...
```
```r
UngulateB$UAV <- factor(UngulateB$UAV)
str(UngulateB)
```
```
## tibble [121 x 3] (S3: tbl_df/tbl/data.frame)
##  $ Alt_Max    : num [1:121] 60 80 120 120 120 120 120 120 120 120 ...
##  $ Flight_time: num [1:121] 16.2 21.4 51.7 27.3 18.4 ...
##  $ UAV        : Factor w/ 2 levels "Fixed Wing","Multi Rotor": 2 1 1 1 1 1 1 1 1 1 ...
```

```
set.seed(123)
sample = sample.split (UngulateB$UAV, SplitRatio = .70)
train = subset(UngulateB, sample == TRUE)
test= subset(UngulateB,sample== FALSE)
##Training the Decision tree Classifier To Predict Pregnacy
tree <- rpart(UAV~.,data=train)
tree.UAV.predicted <- predict (tree, test, type ='class')
confusionMatrix(tree.UAV.predicted,test$UAV)
```

```
## Confusion Matrix and Statistics
##
##                Reference
## Prediction   Fixed Wing Multi Rotor
##   Fixed Wing          10          0
##   Multi Rotor          1         26
##
##                Accuracy : 0.973
##                  95% CI : (0.8584, 0.9993)
##     No Information Rate : 0.7027
##     P-Value [Acc > NIR] : 3.565e-05
##
##                   Kappa : 0.9336
##
##  Mcnemar's Test P-Value : 1
##
##             Sensitivity : 0.9091
##             Specificity : 1.0000
##          Pos Pred Value : 1.0000
##          Neg Pred Value : 0.9630
##              Prevalence : 0.2973
##          Detection Rate : 0.2703
##    Detection Prevalence : 0.2703
##       Balanced Accuracy : 0.9545
##
##        'Positive' Class : Fixed Wing
##
```

```
prp(tree)
```

Alt_Max >= 118　*yes*　*no*

Fixed Wi　Multi Ro
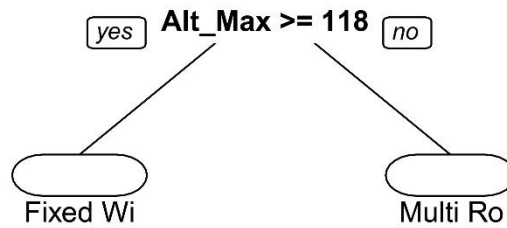
```r
disturb1 <- read_excel("E:/Ungulate review/disturb.xlsx")
disturb1 <- select(disturb1, AGL, Disturbance, UAV)
str(disturb1)

## tibble [80 x 3] (S3: tbl_df/tbl/data.frame)
##  $ AGL        : num [1:80] 100 75 50 25 100 75 50 25 100 75 ...
##  $ Disturbance: chr [1:80] "i" "i" "ii" "iii" ...
##  $ UAV        : chr [1:80] "PH 4 Pro" "PH 4 Pro" "PH 4 Pro" "PH 4 Pro" ...

disturb1$UAV <- factor(disturb1$UAV)
str(disturb1)

## tibble [80 x 3] (S3: tbl_df/tbl/data.frame)
##  $ AGL        : num [1:80] 100 75 50 25 100 75 50 25 100 75 ...
##  $ Disturbance: chr [1:80] "i" "i" "ii" "iii" ...
##  $ UAV        : Factor w/ 2 levels "PH 3 Pro","PH 4 Pro": 2 2 2 2 2 2 2 2 2 2 ...

set.seed(123)
sample = sample.split (disturb1$UAV, SplitRatio = .70)
train = subset(disturb1, sample == TRUE)
test= subset(disturb1,sample== FALSE)
##Training the Decision tree
tree <- rpart(UAV~.,data=train)
tree.UAV.predicted <- predict (tree, test, type ='class')
confusionMatrix(tree.UAV.predicted,test$UAV)

## Confusion Matrix and Statistics
##
```

```
##            Reference
## Prediction PH 3 Pro PH 4 Pro
##   PH 3 Pro        5        9
##   PH 4 Pro        7        3
##
##                 Accuracy : 0.3333
##                   95% CI : (0.1563, 0.5532)
##      No Information Rate : 0.5
##      P-Value [Acc > NIR] : 0.9680
##
##                    Kappa : -0.3333
##
##  Mcnemar's Test P-Value : 0.8026
##
##              Sensitivity : 0.4167
##              Specificity : 0.2500
##           Pos Pred Value : 0.3571
##           Neg Pred Value : 0.3000
##               Prevalence : 0.5000
##           Detection Rate : 0.2083
##     Detection Prevalence : 0.5833
##        Balanced Accuracy : 0.3333
##
##         'Positive' Class : PH 3 Pro
##
```
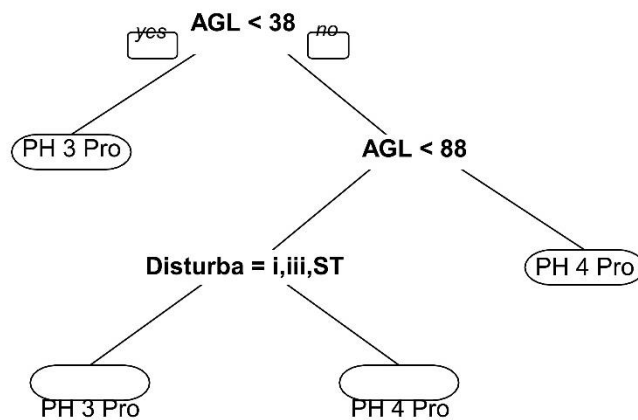
```
prp(tree)
```

Appendix 5 R-markdown file A_Oryx_weight_predictor

A_Oryx Weight Predicting Models

Meyer E de Kock

08/02/2021

Arabian Oryx Mesurements

```
library(readxl)
OryxDrone <- read_excel("C:/Users/meyer/Desktop/Oryx morphometrics/OryxDrone.xlsx")
View(OryxDrone)
```

load Libraries

```
library(ggplot2)
library(mgcv, lib.loc = "C:/Program Files/R/R-4.0.2/library")
```

```
## Loading required package: nlme
```

```
## This is mgcv 1.8-31. For overview type 'help("mgcv-package")'.
```

```
library(nlme, lib.loc = "C:/Program Files/R/R-4.0.2/library")
library(dplyr)
```

```
##
## Attaching package: 'dplyr'
```

```
## The following object is masked from 'package:nlme':
##
##     collapse
```

```
## The following objects are masked from 'package:stats':
##
##     filter, lag
```

```
## The following objects are masked from 'package:base':
##
##     intersect, setdiff, setequal, union
```

Polynomial Regression
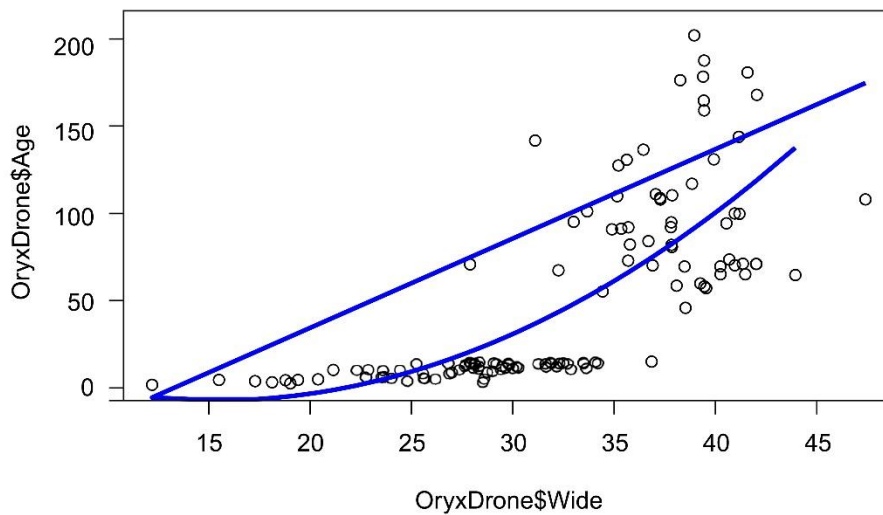## Using the S_drone Print to predict weight

```
Model1 <- lm(OryxDrone$Age ~ OryxDrone$Wide + I(OryxDrone$Wide^2))
summary(Model1)
```

```
##
## Call:
## lm(formula = OryxDrone$Age ~ OryxDrone$Wide + I(OryxDrone$Wide^2))
##
## Residuals:
```

```
##     Min      1Q  Median      3Q     Max
## -72.940 -23.000  -6.619  11.251 116.936
##
## Coefficients:
##                   Estimate Std. Error t value Pr(>|t|)
## (Intercept)       33.41736   53.08730   0.629  0.53024
## OryxDrone$Wide    -5.40492    3.50491  -1.542  0.12570
## I(OryxDrone$Wide^2) 0.17660    0.05633   3.135  0.00217 **
## ---
## Signif. codes: 0 '***' 0.001 '**' 0.01 '*' 0.05 '.' 0.1 ' ' 1
##
## Residual standard error: 36.09 on 119 degrees of freedom
## Multiple R-squared:  0.5465, Adjusted R-squared:  0.5388
## F-statistic: 71.69 on 2 and 119 DF,  p-value: < 2.2e-16
```

```r
plot(OryxDrone$Wide, OryxDrone$Age, main="Polynomal Regression",las=1)
lines(smooth.spline(OryxDrone$Wide, predict(Model1)), col="blue", lwd=3)
```

Polynomial Regression

Polynomial Regression ## Using the drone Print to predict weight

```r
Model2 <- lm(OryxDrone$Weight ~ OryxDrone$DronePrint + I(OryxDrone$DronePrint^2))
summary(Model2)
```

```
##
## Call:
## lm(formula = OryxDrone$Weight ~ OryxDrone$DronePrint + I(OryxDrone$DronePrint^2))
##
##
## Residuals:
```

```
##      Min      1Q  Median      3Q     Max
## -27.9090 -6.2700  0.8868  5.9790 20.5446
##
## Coefficients:
##                            Estimate Std. Error t value Pr(>|t|)
## (Intercept)              -3.511e+01  7.929e+00  -4.428 2.13e-05 ***
## OryxDrone$DronePrint      6.067e-02  7.515e-03   8.074 6.24e-13 ***
## I(OryxDrone$DronePrint^2) -6.169e-06  1.679e-06  -3.673 0.00036 ***
## ---
## Signif. codes: 0 '***' 0.001 '**' 0.01 '*' 0.05 '.' 0.1 ' ' 1
##
## Residual standard error: 9.974 on 119 degrees of freedom
## Multiple R-squared:  0.853, Adjusted R-squared:  0.8505
## F-statistic: 345.3 on 2 and 119 DF,  p-value: < 2.2e-16
```

```r
plot(OryxDrone$DronePrint, OryxDrone$Weight, main="Polynomal Regression",las=1)
lines(smooth.spline(OryxDrone$DronePrint, predict(Model2)), col="blue", lwd=3)
```

Polynomial Regression
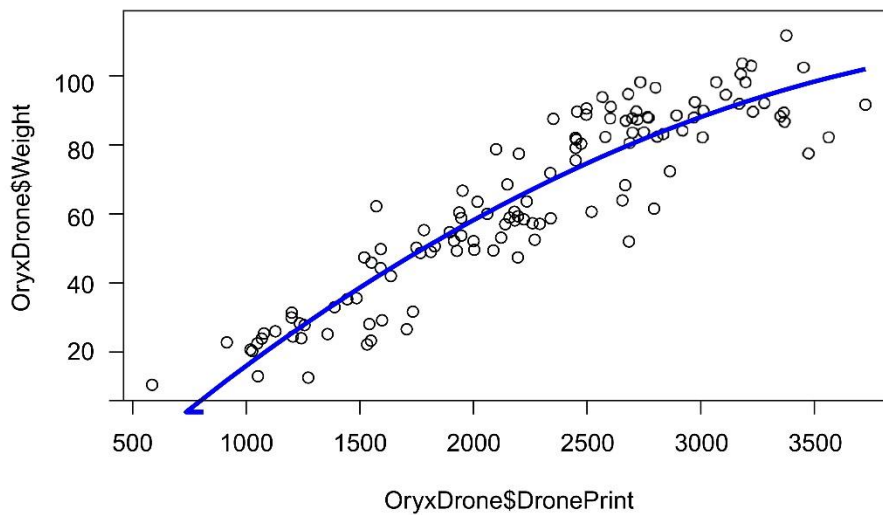
Model Evauation

```r
Model3 <- lm(OryxDrone$Weight ~ OryxDrone$S_DronePrint + I(OryxDrone$S_DronePrint^2))
summary(Model3)
```

```
##
## Call:
## lm(formula = OryxDrone$Weight ~ OryxDrone$S_DronePrint + I(OryxDrone$S_DronePrint^2))
```

```
##
## Residuals:
```

94

```
## -28.6773 -6.0997 -0.1263  6.4930 25.4267
##
## Coefficients:
##                               Estimate Std. Error t value Pr(>|t|)
## (Intercept)                       6033       1194   5.055 1.58e-06 ***
## OryxDrone$S_DronePrint          -14657       2690  -5.448 2.79e-07 ***
## I(OryxDrone$S_DronePrint^2)       8918       1516   5.883 3.78e-08 ***
## ---
## Signif. codes: 0 '***' 0.001 '**' 0.01 '*' 0.05 '.' 0.1 ' ' 1
##
## Residual standard error: 10.28 on 119 degrees of freedom
## Multiple R-squared:  0.844, Adjusted R-squared:  0.8413
## F-statistic: 321.8 on 2 and 119 DF,  p-value: < 2.2e-16
```

```
plot(OryxDrone$S_DronePrint, OryxDrone$Weight, main="Polynomal Regression",las=1)
lines(smooth.spline(OryxDrone$S_DronePrint, predict(Model3)), col="blue", lwd=3)
```
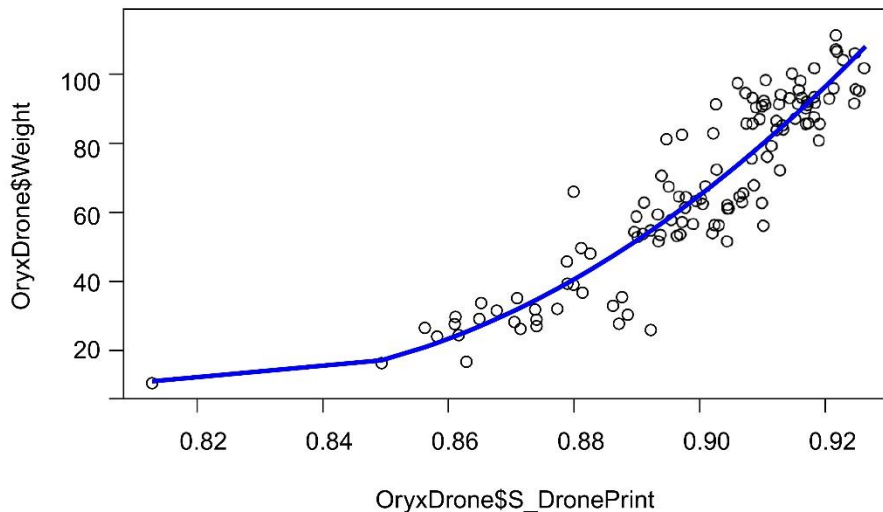
Polynomial Regression


```
library(stats, lib.loc = "C:/Program Files/R/R-4.0.2/library")
AIC (Model1)
```

```
## [1] 1226.152
```

```
AIC (Model2)
```

```
## [1] 912.3843
```

```
AIC (Model3)
```

S_drone adutl oryx Pregnacy

Meyer E de Kock

02/09/2020

Using morphometric measurements of ADULT Arabian Oryx from UAV imagery to predict positive pregnancy.Using S_Drone Print and Total Length

Data Import

```
library(readxl)
OryxDroneAD <- read_excel("C:/Users/meyer/Desktop/Oryx morphometrics/OryxDroneAD.xlsx")
View(OryxDroneAD)
```

Load Library

```
library(ggplot2)
library(FSelector)
library(rpart)
library(rpart.plot)
library(caret)
```

```
## Loading required package: lattice
```

```
library(lattice)
library(dplyr)
```

```
##
## Attaching package: 'dplyr'

## The following objects are masked from 'package:stats':
##
##     filter, lag

## The following objects are masked from 'package:base':
##
##     intersect, setdiff, setequal, union
```

```
library(xlsx)
library(data.tree)
library(data.table)
```

```
##
## Attaching package: 'data.table'

## The following objects are masked from 'package:dplyr':
##
##     between, first, last
```

```
library(caTools)
```

Data Prep

```
df3<-OryxDroneAD

df3 <- select(df3,S_DronePrint, TLenth, DronePrint, Wide, Pregnant)
str(df3)
```

```
## tibble [55 x 5] (S3: tbl_df/tbl/data.frame)
##  $ S_DronePrint: num [1:55] 0.908 0.903 0.917 0.915 0.917 ...
##  $ TLenth      : num [1:55] 112 120 125 124 146 ...
##  $ DronePrint  : num [1:55] 2339 2352 2892 2798 3373 ...
##  $ Wide        : num [1:55] 38.5 34.4 39.5 39.5 38.1 ...
##  $ Pregnant    : logi [1:55] FALSE TRUE TRUE TRUE TRUE FALSE ...
```

```
df3$Pregnant <- factor(df3$Pregnant)
str(df3)
```

```
## tibble [55 x 5] (S3: tbl_df/tbl/data.frame)
##  $ S_DronePrint: num [1:55] 0.908 0.903 0.917 0.915 0.917 ...
##  $ TLenth      : num [1:55] 112 120 125 124 146 ...
##  $ DronePrint  : num [1:55] 2339 2352 2892 2798 3373 ...
##  $ Wide        : num [1:55] 38.5 34.4 39.5 39.5 38.1 ...
##  $ Pregnant    : Factor w/ 2 levels "FALSE","TRUE": 1 2 2 2 2 1 2 2 2 1 ...
```

Decision tree to predict pregnancy

```
set.seed(123)
sample = sample.split (df3$Pregnant, SplitRatio = .70)
train = subset(df3, sample == TRUE)
test= subset(df3,sample== FALSE)
```

##Training the Decision tree Classifier To Predict Pregnancy

```
tree <- rpart(Pregnant~.,data=train)
tree.Pregnant.predicted <- predict (tree, test, type ='class')
confusionMatrix(tree.Pregnant.predicted,test$Pregnant)
```

```
## Confusion Matrix and Statistics
##
##           Reference
## Prediction FALSE TRUE
##      FALSE     2    2
##      TRUE      3    9
##
##                Accuracy : 0.6875
##                  95% CI : (0.4134, 0.8898)
##     No Information Rate : 0.6875
##     P-Value [Acc > NIR] : 0.618
##
##                   Kappa : 0.2308
##
##  Mcnemar's Test P-Value : 1.000
##
```

```
##             Sensitivity : 0.4000
##             Specificity : 0.8182
##          Pos Pred Value : 0.5000
##          Neg Pred Value : 0.7500
##              Prevalence : 0.3125
##          Detection Rate : 0.1250
##    Detection Prevalence : 0.2500
##       Balanced Accuracy : 0.6091
##
##        'Positive' Class : FALSE
##
```

Visualization

```
prp(tree)
```

Appendix 7   R-markdown file: A_Oryx_Sex_predicton
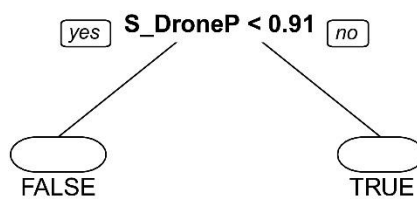
SEX_Predict_A_Oryx

Meyer E de Kock

02/09/2020

Import data

```r
#import Oryx.drone.xml file
library(readxl)
OryxDrone <- read_excel("C:/Users/meyer/Desktop/Oryx morphometrics/OryxDrone.xlsx")
View(OryxDrone)
```

'## Import Libraries

```r
library(ggplot2)
library(FSelector)
library(rpart)
library(rpart.plot)
library(caret)
```

```
## Loading required package: lattice
```

```r
library(lattice)
library(dplyr)
```

```
##
## Attaching package: 'dplyr'

## The following objects are masked from 'package:stats':
##
##     filter, lag

## The following objects are masked from 'package:base':
##
##     intersect, setdiff, setequal, union
```

```r
library(xlsx)
library(data.tree)
library(data.table)
```

```
##
## Attaching package: 'data.table'

## The following objects are masked from 'package:dplyr':
##
##     between, first, last
```

```r
library(caTools)
```

99

Data Prep

```
df4<-OryxDrone
df4 <- select(df4,Sex,DronePrint,TLenth,Wide,S_DronePrint)
str(df4)
```

```
## tibble [122 x 5] (S3: tbl_df/tbl/data.frame)
## $ Sex         : chr [1:122] "Female" "Female" "Male" "Male" ...
## $ DronePrint  : num [1:122] 586 915 1019 1027 1049 ...
## $ TLenth      : num [1:122] 60.5 70.9 75.7 78.3 72.1 ...
## $ Wide        : num [1:122] 12.2 18.8 18.1 17.3 15.5 ...
## $ S_DronePrint: num [1:122] 0.813 0.856 0.862 0.858 0.871 ...
```

```
df4$Sex <- factor(df4$Sex)
View(df4)
```

Train and Test Data Split

```
set.seed(123)
sample = sample.split (df4$Sex, SplitRatio = .70)
train = subset(df4, sample == TRUE)
test= subset(df4,sample== FALSE)
```

##Training the Decision tree Classifier To Predict Sex

```
tree <- rpart(Sex~.,data=train)
tree.Sex.predicted <- predict (tree, test, type ='class')
confusionMatrix(tree.Sex.predicted,test$Sex)
```

```
## Confusion Matrix and Statistics
##
##           Reference
## Prediction Female Male
##     Female    24     8
##     Male       2     2
##
##                Accuracy : 0.7222
##                  95% CI : (0.5481, 0.858)
##     No Information Rate : 0.7222
##     P-Value [Acc > NIR] : 0.5841
##
##                   Kappa : 0.1509
##
##  Mcnemar's Test P-Value : 0.1138
##
##             Sensitivity : 0.9231
##             Specificity : 0.2000
##          Pos Pred Value : 0.7500
##          Neg Pred Value : 0.5000
##              Prevalence : 0.7222
##          Detection Rate : 0.6667
##    Detection Prevalence : 0.8889
##       Balanced Accuracy : 0.5615
##
##        'Positive' Class : Female
```

Visualize the Decision-Tree

```
prp(tree)
```
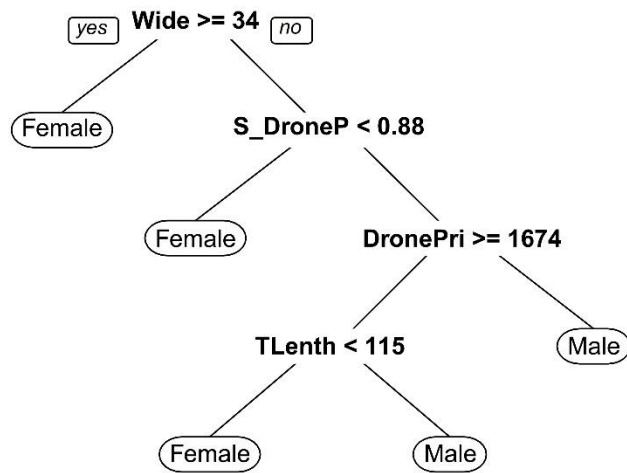
Oryx Pregnancy Predictor:-Decision tree

Meyer E de Kock

02/09/2020

Using morphometric measurements of Arabian Oryx from UAV imagery to predict positive pregnancy.

Data Import

```
library(readxl)
OryxDrone <- read_excel("C:/Users/meyer/Desktop/Oryx morphometrics/OryxDrone.xlsx")
View(OryxDrone)
```

Load Library

```
library(ggplot2)
library(FSelector)
library(rpart)
library(rpart.plot)
library(caret)
```

```
## Loading required package: lattice
```

```
library(lattice)
library(dplyr)
```

```
##
## Attaching package: 'dplyr'

## The following objects are masked from 'package:stats':
##
##     filter, lag

## The following objects are masked from 'package:base':
##
##     intersect, setdiff, setequal, union
```

```
library(xlsx)
library(data.tree)
library(data.table)
```

```
##
## Attaching package: 'data.table'

## The following objects are masked from 'package:dplyr':
##
##     between, first, last
```

```
library(caTools)
```

Data Prep

```
df1<-OryxDrone
subset(df1, Age>18)
```

```
## # A tibble: 55 x 15
##       ID Sex   Chip  DoB                 DoP                      Age DronePrint
##    <dbl> <chr> <chr> <dttm>              <dttm>                 <dbl>      <dbl>
## 1   1647 Fema~ 0006~ 2009-12-19 00:00:00 2017-10-30 00:00:00    94.4      2100.
## 2   2240 Fema~ 0007~ 2012-04-11 00:00:00 2017-10-30 00:00:00    66.7      2150.
## 3   2421 Male  0007~ 2012-01-01 00:00:00 2017-11-01 00:00:00    70.1      2200.
## 4   2847 Fema~ 0007~ 2014-01-26 00:00:00 2017-10-30 00:00:00    45.1      2339.
## 5   2466 Fema~ 0007~ 2013-04-17 00:00:00 2017-11-01 00:00:00    54.5      2352.
## 6   1912 Fema~ 0006~ 2010-04-28 00:00:00 2017-10-30 00:00:00    90.1      2449.
## 7   1473 Fema~ 0006~ 2009-06-20 00:00:00 2017-10-30 00:00:00   100.       2450
## 8   2267 Fema~ 0007~ 2011-10-28 00:00:00 2017-11-01 00:00:00    72.2      2450.
## 9   1915 Fema~ 0007~ 2010-04-17 00:00:00 2017-10-30 00:00:00    90.5      2453.
## 10  1055 Fema~ 0006~ 2006-02-01 00:00:00 2017-10-30 00:00:00   141.       2456.
## # ... with 45 more rows, and 8 more variables: TLenth <dbl>,
## #   S_DronePrint <dbl>, Wide <dbl>, Weight <dbl>, Pregnant <lgl>,
## #   IdOther <chr>, `2nd_mesure` <dbl>, Accuracy <dbl>
```

```
df1 <- select(df1,DronePrint, S_DronePrint, TLenth, Wide, Pregnant)
str(df1)
```

```
## tibble [122 x 5] (S3: tbl_df/tbl/data.frame)
##  $ DronePrint  : num [1:122] 586 915 1019 1027 1049 ...
##  $ S_DronePrint: num [1:122] 0.813 0.856 0.862 0.858 0.871 ...
##  $ TLenth      : num [1:122] 60.5 70.9 75.7 78.3 72.1 ...
##  $ Wide        : num [1:122] 12.2 18.8 18.1 17.3 15.5 ...
##  $ Pregnant    : logi [1:122] FALSE FALSE FALSE FALSE FALSE FALSE ...
```

```
df1$Pregnant <- factor(df1$Pregnant)
str(df1)
```

```
## tibble [122 x 5] (S3: tbl_df/tbl/data.frame)
##  $ DronePrint  : num [1:122] 586 915 1019 1027 1049 ...
##  $ S_DronePrint: num [1:122] 0.813 0.856 0.862 0.858 0.871 ...
##  $ TLenth      : num [1:122] 60.5 70.9 75.7 78.3 72.1 ...
##  $ Wide        : num [1:122] 12.2 18.8 18.1 17.3 15.5 ...
##  $ Pregnant    : Factor w/ 2 levels "FALSE","TRUE": 1 1 1 1 1 1 1 1 1 1 ...
```

Decision tree to predict pregnancy

```
set.seed(123)
sample = sample.split (df1$Pregnant, SplitRatio = .70)
train = subset(df1, sample == TRUE)
test= subset(df1,sample== FALSE)
```

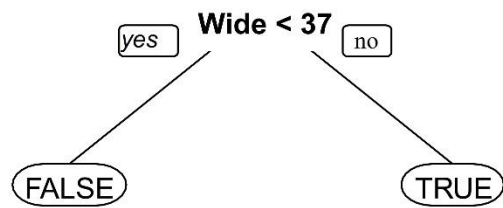##Training the Decision tree Classifier To Predict Pregnancy

```
tree <- rpart(Pregnant~.,data=train)
tree.Pregnant.predicted <- predict (tree, test, type ='class')
confusionMatrix(tree.Pregnant.predicted,test$Pregnant)
```

```
## Confusion Matrix and Statistics
##
##           Reference                ##
## Prediction FALSE TRUE              ##          Accuracy : 0.9167
##      FALSE    23    1              ##            95% CI : (0.7753,      0.9825)
##      TRUE      2   10              ##    No Information Rate : 0.6944
```

```
##      P-Value [Acc > NIR]  0.001487 no
##
##                   Kappa : 0.8085
##
##  Mcnemar's Test P-Value  1.000000
##
##             Sensitivity  0.9200
##             Specificity  0.9091
##          Pos Pred Value  0.9583
##          Neg Pred Value  0.8333
##              Prevalence  0.6944
##          Detection Rate  0.6389
##    Detection Prevalence  0.6667
##       Balanced Accuracy  0.9145
##
##        'Positive' Class  FALSE
##
```

Visualization of the Decision-Tree

prp(tree)

Appendix 9   R-markdown file: S

S_DronePrint_pregnancy_predictor

Using morphometric measurements of Arabian Oryx from UAV imagery to predict positive pregnancy.Using S_Drone Print and Total Lenth

Data Import

```
library(readxl)
OryxDrone <- read_excel("C:/Users/meyer/Desktop/Oryx morphometrics/OryxDrone.xlsx")
View(OryxDrone)
```

Load Library

```
library(ggplot2)
library(FSelector)
library(rpart)
library(rpart.plot)
library(caret)
```

```
## Loading required package: lattice
```

```
library(lattice)
library(dplyr)
```

```
##
## Attaching package: 'dplyr'
```

```
## The following objects are masked from 'package:stats':
##
##     filter, lag
```

```
## The following objects are masked from 'package:base':
##
##     intersect, setdiff, setequal, union
```

```
library(xlsx)
library(data.tree)
library(data.table)
```

```
##
## Attaching package: 'data.table'
```

```
## The following objects are masked from 'package:dplyr':
##
##     between, first, last
```

```
library(caTools)
```

Data Prep

```
df2<-OryxDrone
```

1

```
df2 <- select(df2,DronePrint, TLenth, Pregnant)
str(df2)
```

```
## tibble [122 x 3] (S3: tbl_df/tbl/data.frame)
##  $ DronePrint: num [1:122] 586 915 1019 1027 1049 ...
##  $ TLenth    : num [1:122] 60.5 70.9 75.7 78.3 72.1 ...
##  $ Pregnant : logi [1:122] FALSE FALSE FALSE FALSE FALSE FALSE ...
```

```
df2$Pregnant <- factor(df2$Pregnant)
str(df2)
```

```
## tibble [122 x 3] (S3: tbl_df/tbl/data.frame)
##  $ DronePrint: num [1:122] 586 915 1019 1027 1049 ...
##  $ TLenth    : num [1:122] 60.5 70.9 75.7 78.3 72.1 ...
##  $ Pregnant : Factor w/ 2 levels "FALSE","TRUE": 1 1 1 1 1 1 1 1 1 1 ...
```

Decision tree to predict pregnancy

```
set.seed(123)
sample = sample.split (df2$Pregnant, SplitRatio = .70)
train = subset(df2, sample == TRUE)
test= subset(df2,sample== FALSE)
```

##Training the Decision tree Classifier To Predict Pregnancy

```
tree <- rpart(Pregnant~.,data=train)
tree.Pregnant.predicted <- predict (tree, test, type ='class')
confusionMatrix(tree.Pregnant.predicted,test$Pregnant)
```

```
## Confusion Matrix and Statistics
##
##           Reference
## Prediction FALSE TRUE
##      FALSE   23    1
##      TRUE     2   10
##
##                Accuracy : 0.9167
##                  95% CI : (0.7753, 0.9825)
##     No Information Rate : 0.6944
##     P-Value [Acc > NIR] : 0.001487
##
##                   Kappa : 0.8085
##
##  Mcnemar's Test P-Value : 1.000000
##
##             Sensitivity : 0.9200
##             Specificity : 0.9091
##          Pos Pred Value : 0.9583
##          Neg Pred Value : 0.8333
##              Prevalence : 0.6944
##          Detection Rate : 0.6389
##    Detection Prevalence : 0.6667
##       Balanced Accuracy : 0.9145
##
##        'Positive' Class : FALSE
```

2

##

Visualization of the Decision-Tree

```
prp(tree)
```
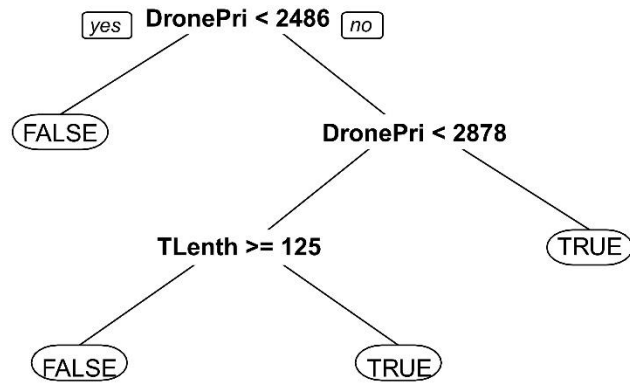
10. Curriculum Vitae

Meyer Etienne de Kock
House 1, Hans Hoheisen Wildlife Research Station, Orpen Gate Road, BushBuck Ridge, RSA
Mobile: 0027797451990
Dekock.meyer@up.ac.za
LinkedIn Profile: https://www.linkedin.com/in/meyer-e-de-kock-0515a243/

EDUCATION

Z_GIS, Salzburg University (Austria)
MSc (GIS)
Conservation GIS: Using remote sensing data and weighted Object-Based image analysis to determine animal distribution. (Arabian Oryx distribution)
2011 - 2015

Sparsholt College (UK)
Diploma in the Management of Zoo Animals (Pass with merit) BIAZA Award for the best international student 2015
2013 - 2015

University of the Free State (South Africa)
Project Management for Development Practitioners
2005

University of Technology (South Africa)
N.D. Nature Conservation
1995 – 1999

University of Technology (South Africa)
Certificate in Environmental Biology
1994 – 1995

WORK HISTORY

Free State (South Africa) Department of Environmental Affairs
Nature Conservation Officer/ Senior Nature Conservation Officer
Environmental awareness: Community Conservation
1996-2005

Al Bustan Zoological Centre, United Arab Emirates.
Assistant Manager & Antelope Curator
2005 –2009
Al Bustan Zoological Centre, United Arab Emirates.
General Manager
2009-2019a

Environmental Conservation Consultancy (ECC)
Director
2019-2020

The University of Pretoria, Hans Hoheisen Wildlife Research Station
Station Manager
2021-

LANGUAGES

Afrikaans - Native language
English – Excellent

RECENT PRESENTATIONS

African penguin Health	Cape town, RSA	2021
Automated Detection of		
Large Ungulates from UAV Acquired Imagery	Germany, Berlin	2020
PAAZA conference	South Africa	2019
Global Biodiversity Conservation Conference	Prague	2018
Facilitator Arabian Oryx, Data management Workshop	UAE	2017
Introduction to ABZC Giraffe, Antelope and Hippo	Prague,	2017
Ungulate Nutrition ABZC	Dubai, UAE	2017
Drone training, Rangers	Indonesia, Medan	2016
Conservation actions ABZC, AZAA,	UAE	2016
Drones for aerial imagery, building Innovator,	Abu Dhabi, UAE	2016
Conservation based, database management ICWAB,	SHJ, UAE	2015
Non-invasive data capture AZAA,	UAE	2014
Eastern bongo conservation framework	Dubai, UAE	2013

PUBLICATION CONTRIBUTIONS:

de Kock, M. E., O'Donovan, D., Khafaga, T., & Hejcmanová, P. (2021). Zoometric data extraction from drone imagery: the Arabian oryx (Oryx leucoryx). *Environmental Conservation*, *48*(4), 295-300.

de Kock, M.E., Al Qarqaz, M., Burns, K., Al Faqeer M, Chege, S., Lloyd, C. (2018). Arabian Oryx Housing & Husbandry Guidelines. Abu Dhabi, UAE: Environment Agency – Abu Dhabi (EAD). https://www.arabianoryx.org/En/Downloads/ORYX%20Housing%20and%20Husbandry%20Guidelines%20SINGLE%20PAGE.pdf

Al Dhaheri, S., Soorae, P. S., de Kock, M.E., Mehmood, A., Gouws, A., Burns, K., Al Zaabi, R. (2017). Conservation introduction of the Arabian Tahr to Sir Bani Yas Island, Abu Dhabi Emirate, UAE: challenges and lessons learnt. *Journal of Zoo and Aquarium Research*, *5*(3), 137-141.

Mallon, D., Al Dhaheri, S., de Kock, M. E., S., Soorae (2017). UAE National Forum for the Arabian Tahr: 1st Strategic Framework for the UAE; Al Bustan Zoological Centre Conference Report

de Kock, M.E., Gallacher, D. (2016). From drone data to decisions: turning images into ecological answers. Presented at: *Innovation Arabia 2016*, Dubai, UAE, 7–9 March

CONSERVATION REPORTS:

Barari Forest Management & Al Bustan Zoological Centre (2014). Arabian Tahr Conservation Introduction on Sir Bani Yas Island (UAE) June 2014 – Workshop. Al Bustan Zoological Centre, Sharjah, UAE.

Environmental Agency Abu Dhabi, Barari Forest Management, Al Bustan Zoological Centre; TDIC (2014). Arabian Tahr Conservation Introduction on Sir Bani Yas Island (UAE), Site selection.

Al Bustan Zoological Centre (2014). First Interregional Eastern Bongo Collection Workshop, Dubai (UAE) May 2013 – Workshop. Al Bustan Zoological Centre, Sharjah, UAE. Available from: http://www.easternbongo.org/public/default/frontend/custom/pdf/Bongo%20REPORT_ABZC.pdf

REFERENCES:

Mrs Amy Robbins, Director: Sumatran Ranger Project, New Zealand, www.sumatranrangerproject.com sumatranrangers@gmail.com

Dr Thomas Rabeil Chief Executive Officer, WILD AFRICA CONSERVATION (WAC). http://wac-niger.com/thomas.rabeil@gmail.com

Dr David Gallacher Research Associate, The University of Sydney. d.gallacher@sydney.edu.au

Mr Duart Hugo Free State Department of Environmental Affairs, Conservancy Services duarthugo99@gmail.com